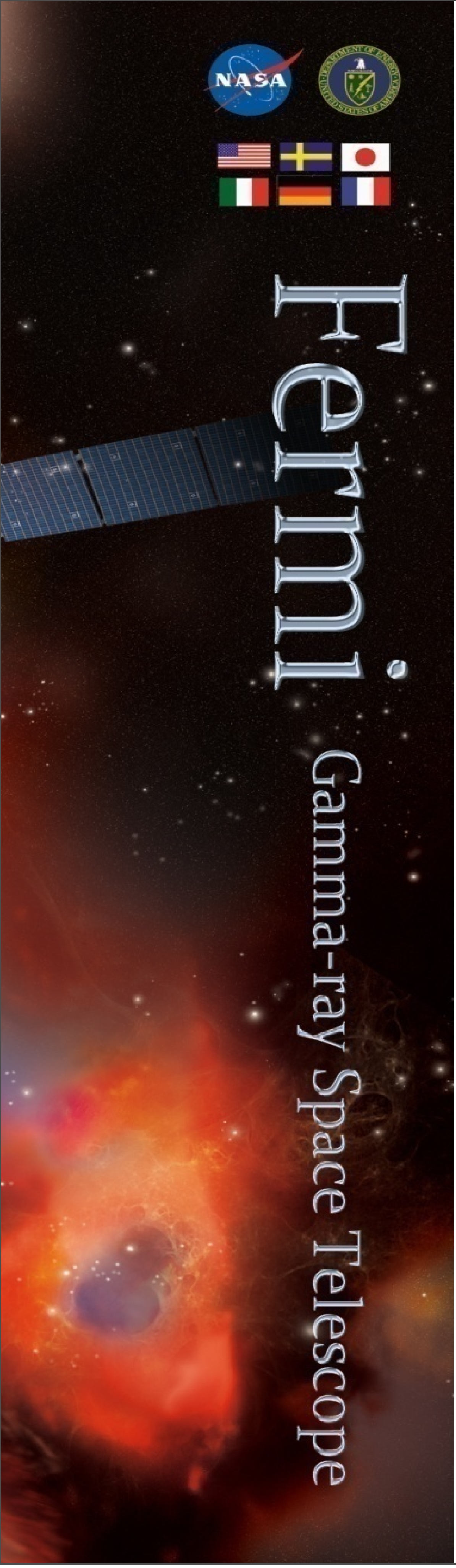

Observational signatures of the GRB photosphere

Felix Ryde
KTH Royal Institute of Technology
Stockholm

On behalf of the Fermi GBM and LAT teams

Ioffe Workshop on GRBs and other transient sources:
20 Years of Konus-Wind Experiment

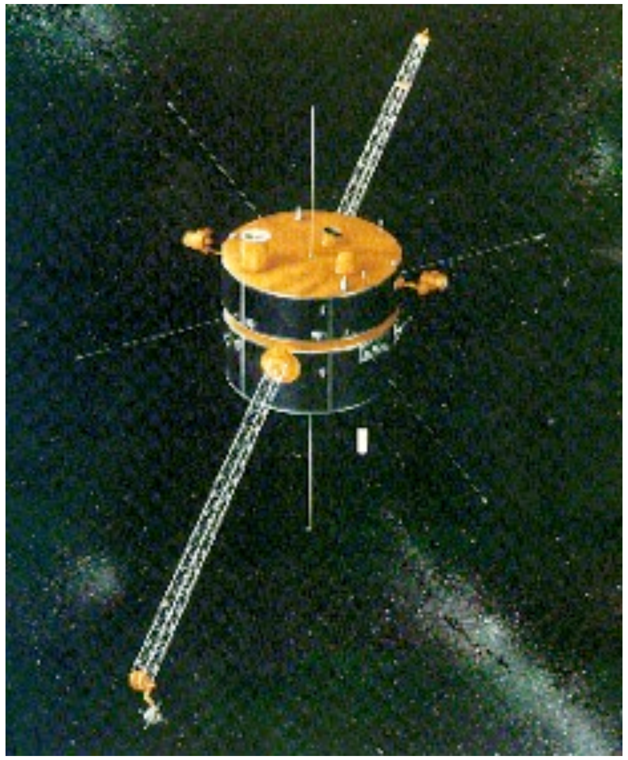

Konus-Wind 20 years
Congratulations!

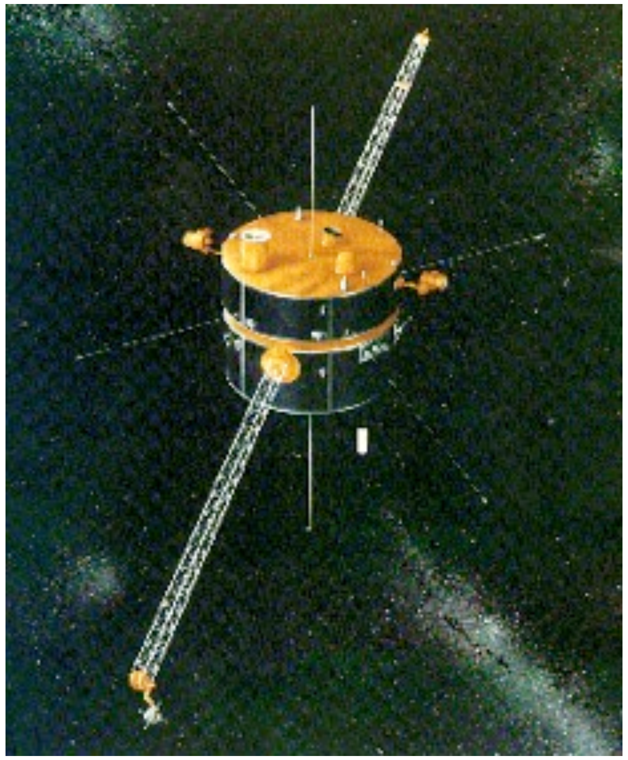

Konus-Wind 20 years Congratulations!

Ioffe Physical Technical Institute

The hardness intensity correlation 30 years

luminosity, flux

Thermal Bremsstrahlung fits

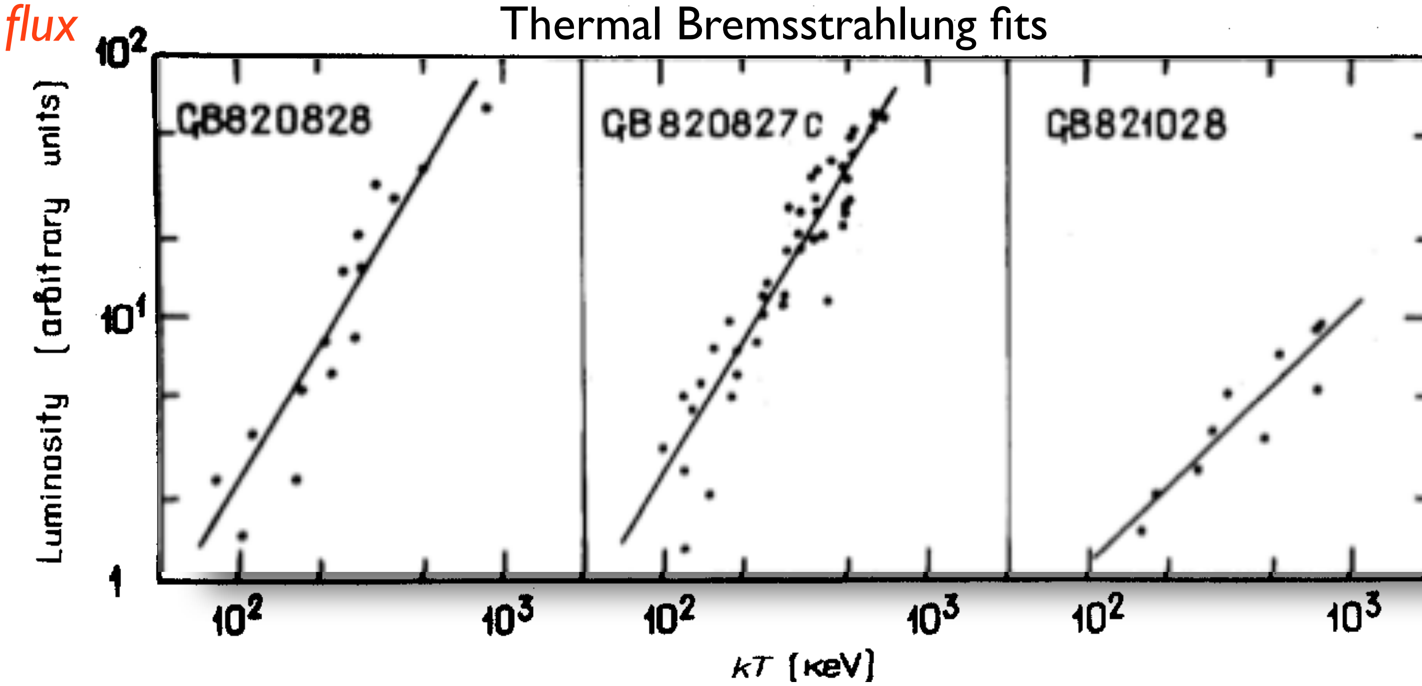

Konus Venera

Spectral peak energy

Ioffe Physical Technical Institute

Golenetskii et al. (1983)

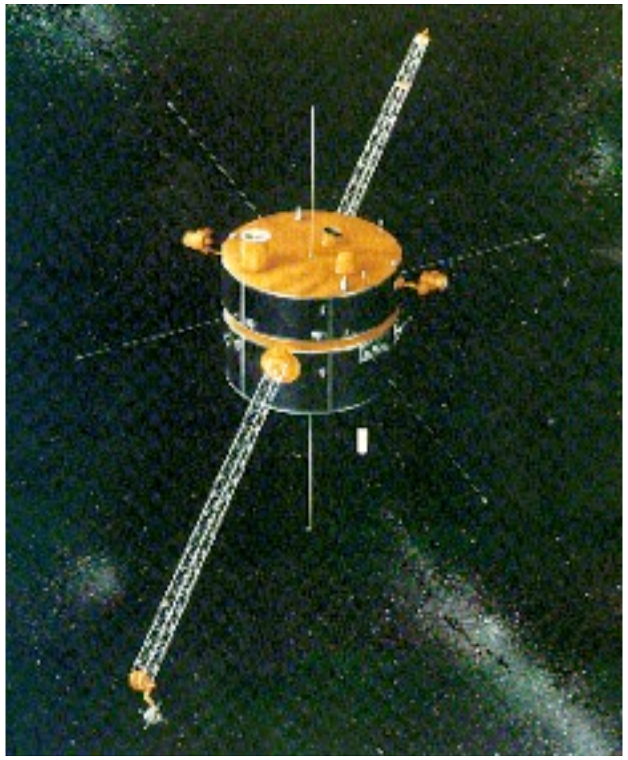

Konus-Wind 20 years Congratulations!

Ioffe Physical Technical Institute

The hardness intensity correlation 30 years

luminosity, flux

Thermal Bremsstrahlung fits

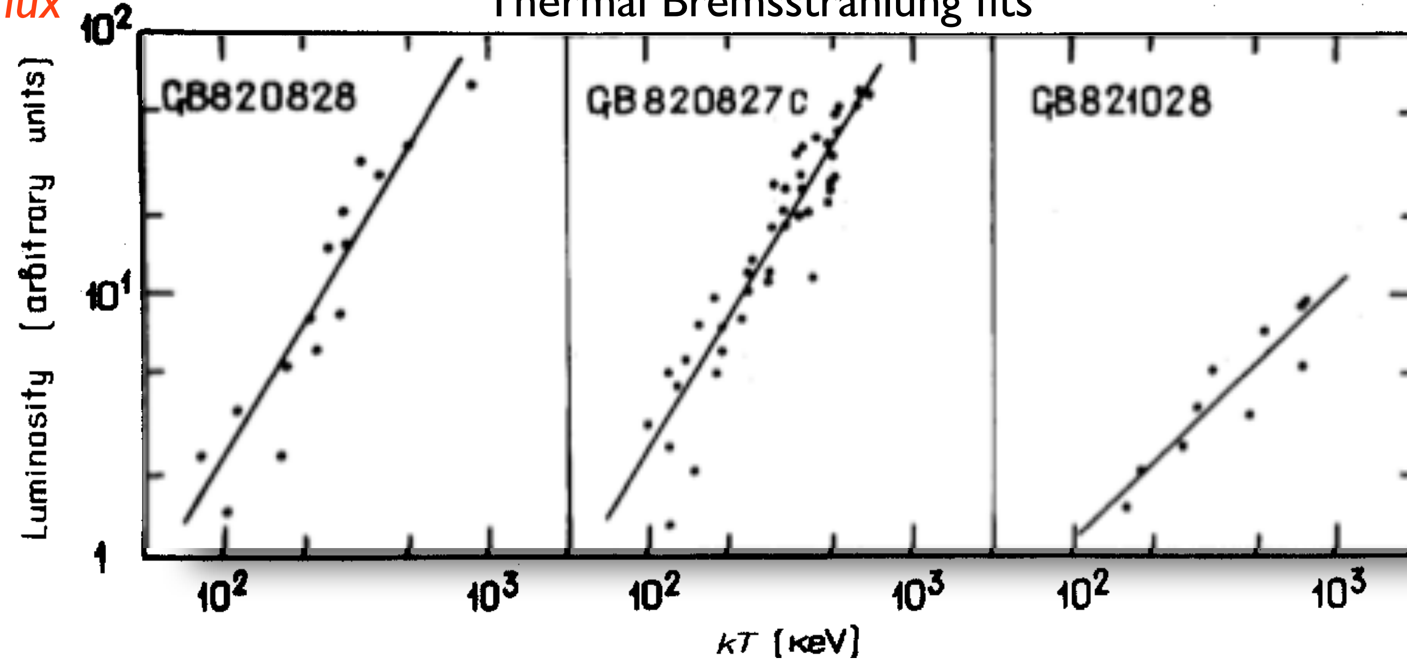

Konus Venera

Spectral peak energy

Ioffe Physical Technical Institute

Golenetskii et al. (1983)

Kargatis+94, Borgonovo & Ryde 02, Kocevski+10, Ghirlanda+12

Basic framework: the fireball model

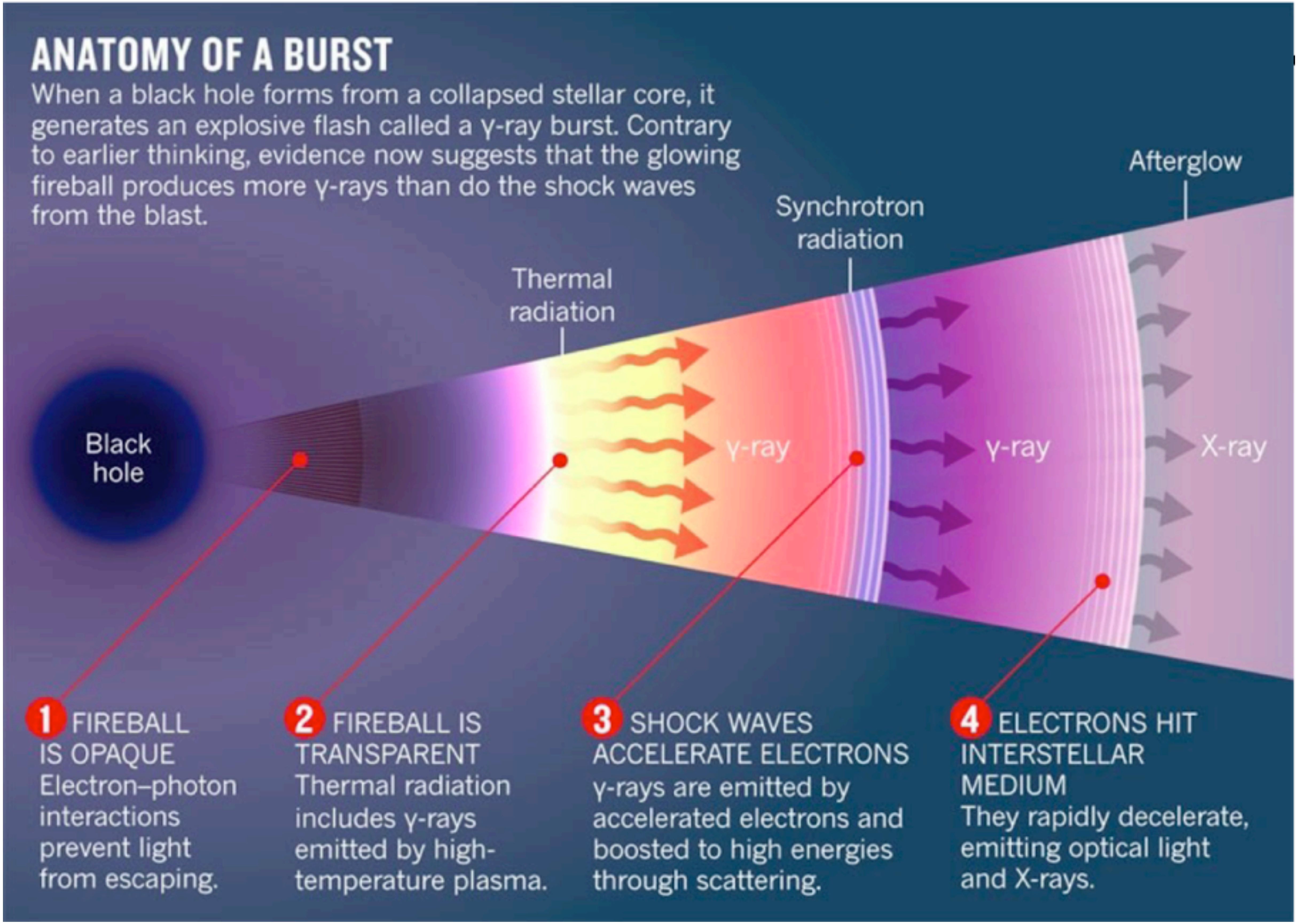

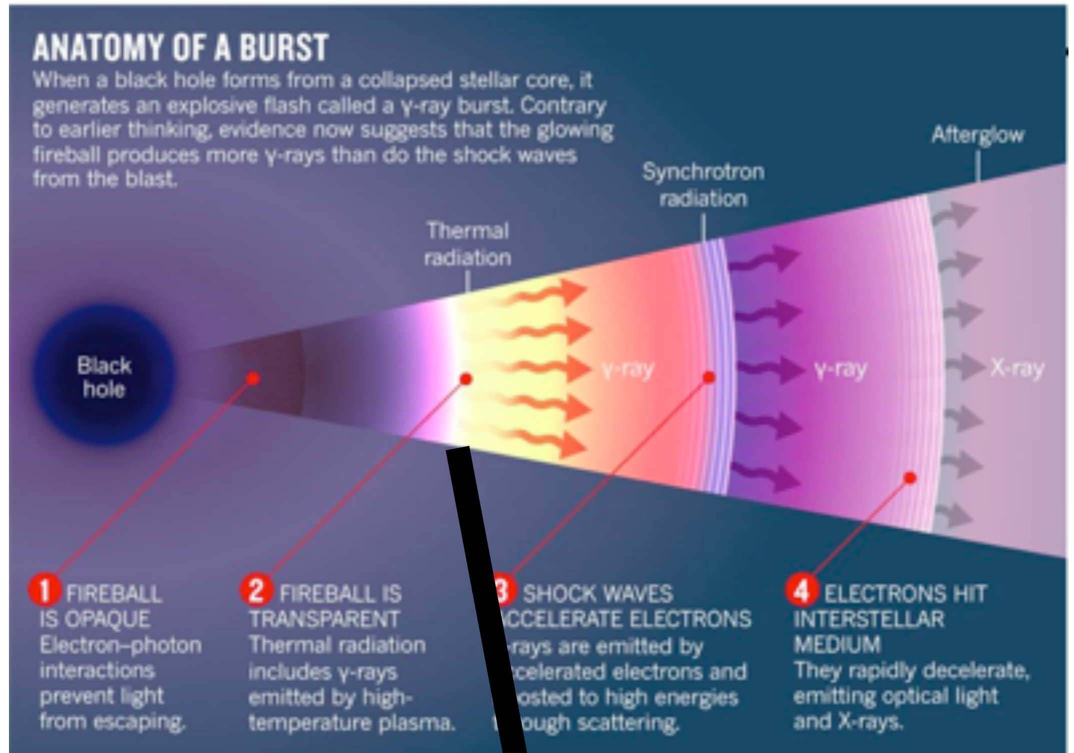

Paczyński 1986:

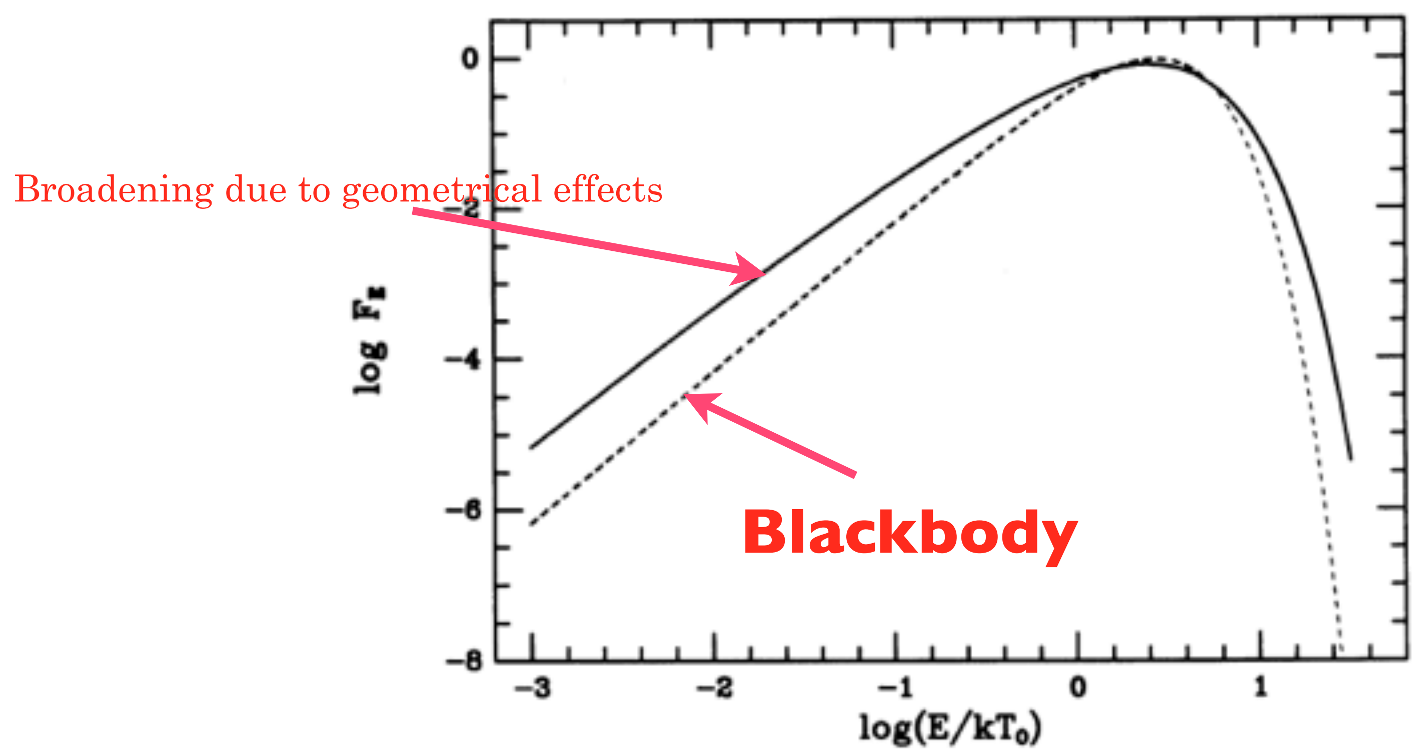

FIG. 1.—*Solid line*: energy distribution of the flux received by a distant observer at rest with respect to the center of mass of the fluid. The vertical scale is in arbitrary units. (*Dashed line*): corresponding distribution for a blackbody at the initial temperature of the fluid.

Paczyński 1986, ApJL, 308, 47

Single Planck function bursts

Compton Gamma-Ray Observatory

GRB930214

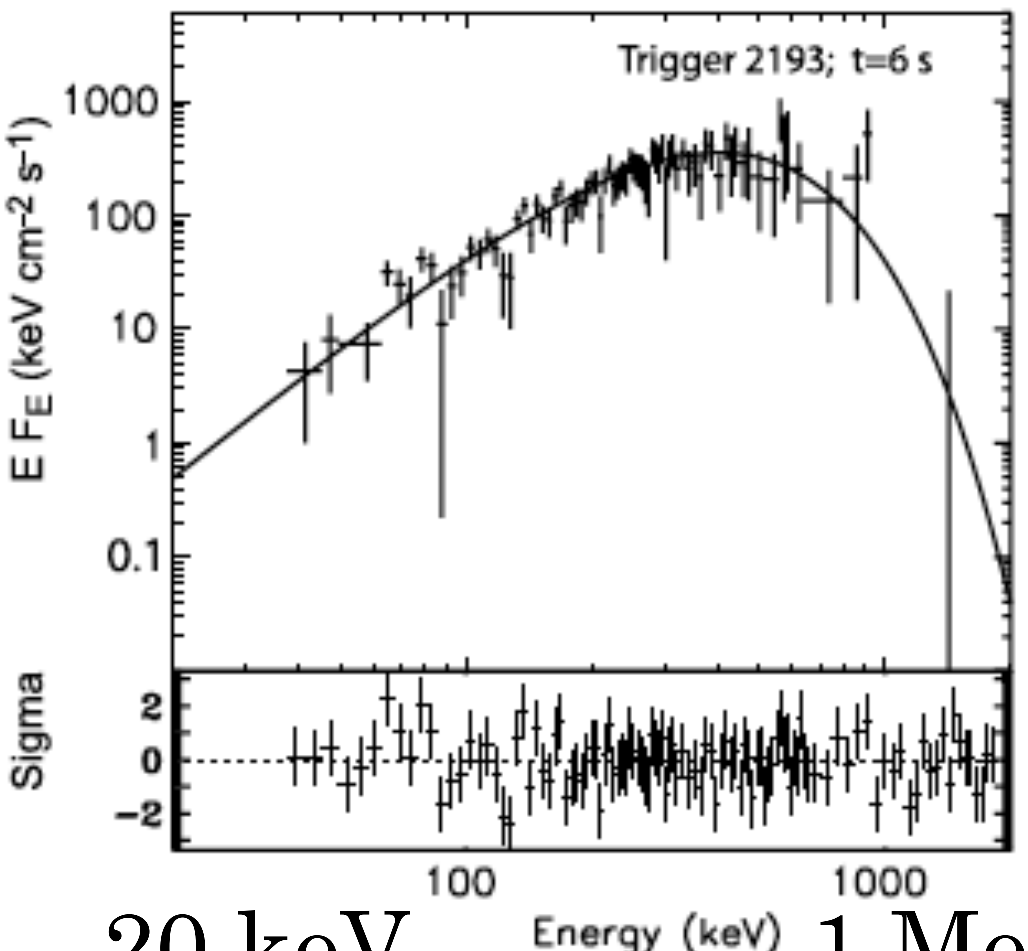

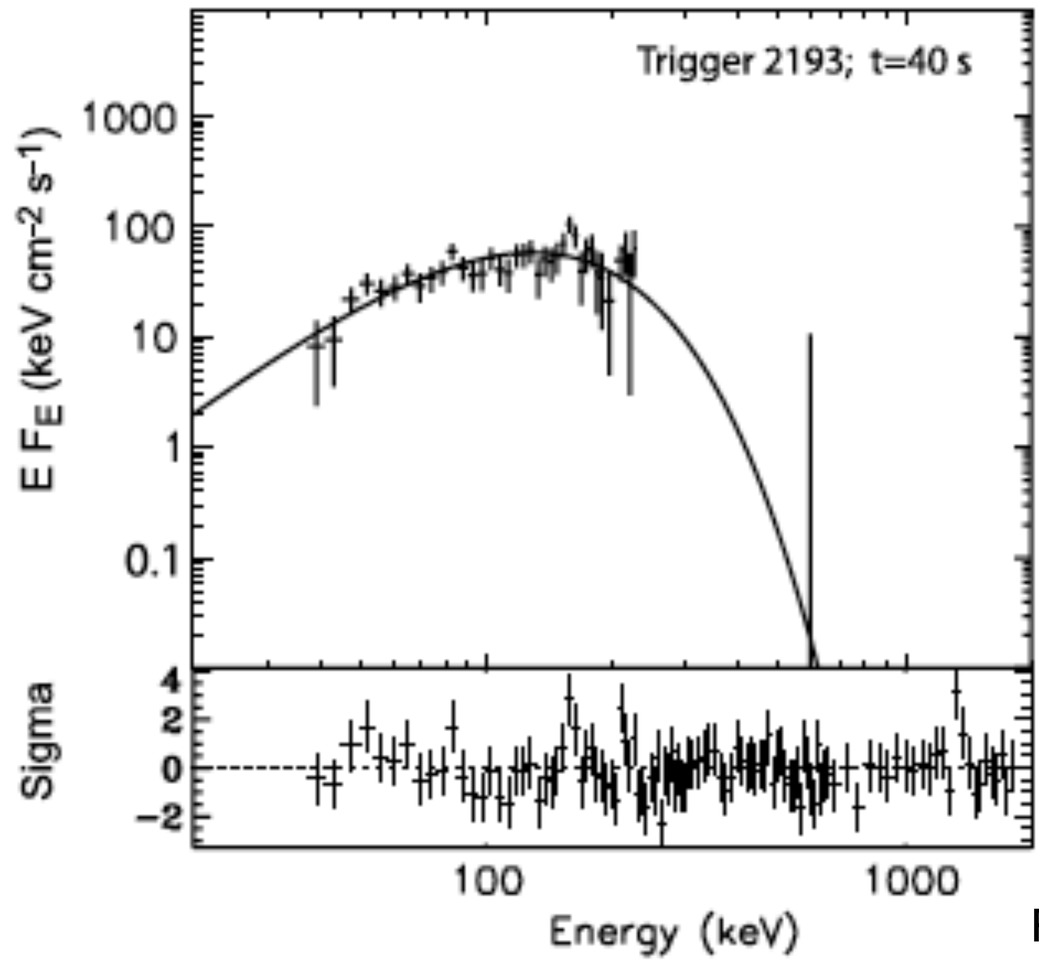

20 keV 1 MeV

Ryde 2004

Spectra from temporally resolved pulses observed by BATSE over the energy range 20-2000 keV.

- **Ryde (2004):** Blackbody through out the pulse
- **Ghirlanda et al. (2003):** Blackbody in initial phase of burst

Single Planck function bursts

Compton Gamma-Ray Observatory

GRB930214

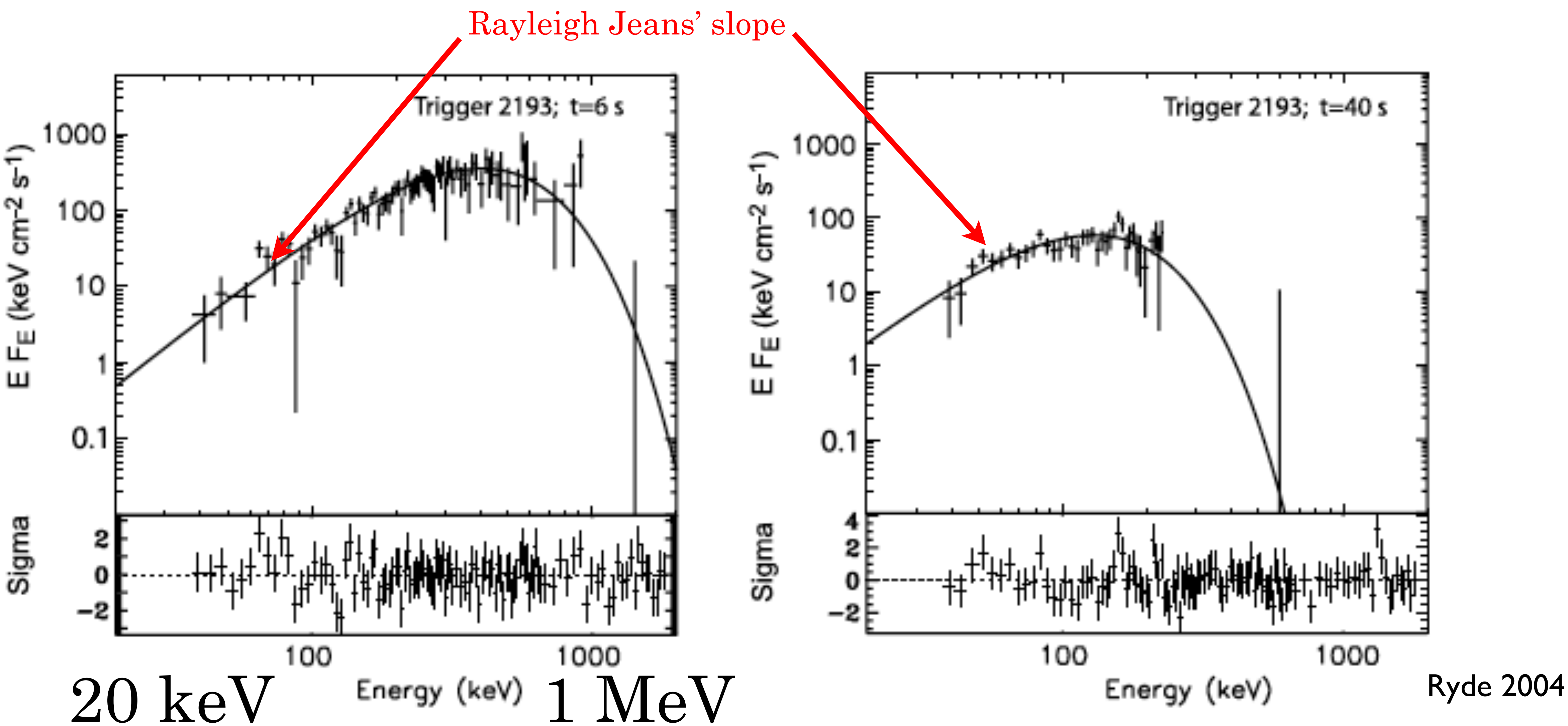

Spectra from temporally resolved pulses observed by BATSE over the energy range 20-2000 keV.

- **Ryde (2004):** Blackbody through out the pulse
- **Ghirlanda et al. (2003):** Blackbody in initial phase of burst

Single Planck function bursts

Compton Gamma-Ray Observatory

GRB930214

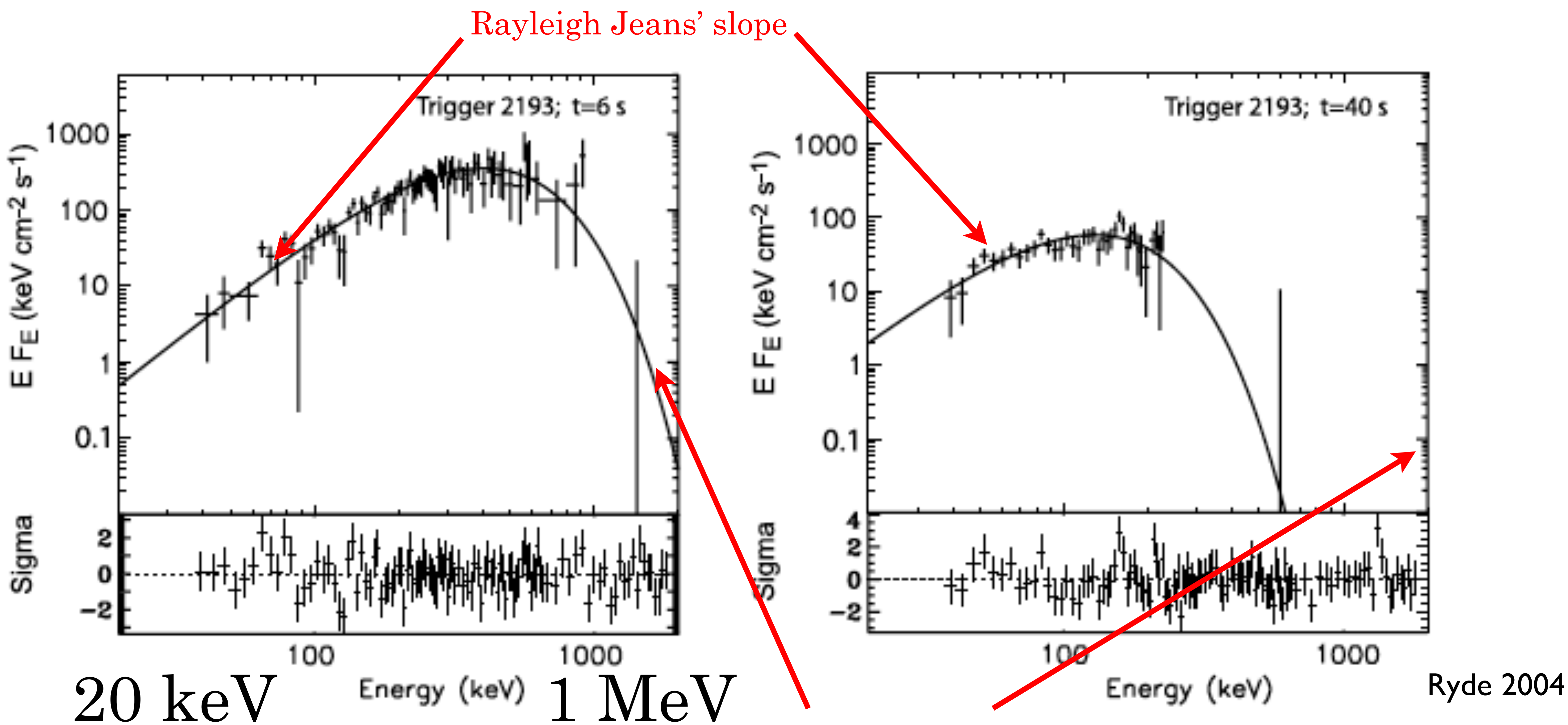

Spectra from temporally resolved pulses observed
by BATSE over the energy range 20-2000 keV.

- **Ryde (2004):** Blackbody through out the pulse
- **Ghirlanda et al. (2003):** Blackbody in initial phase of burst

Single Planck function bursts

Compton Gamma-Ray Observatory

GRB930214

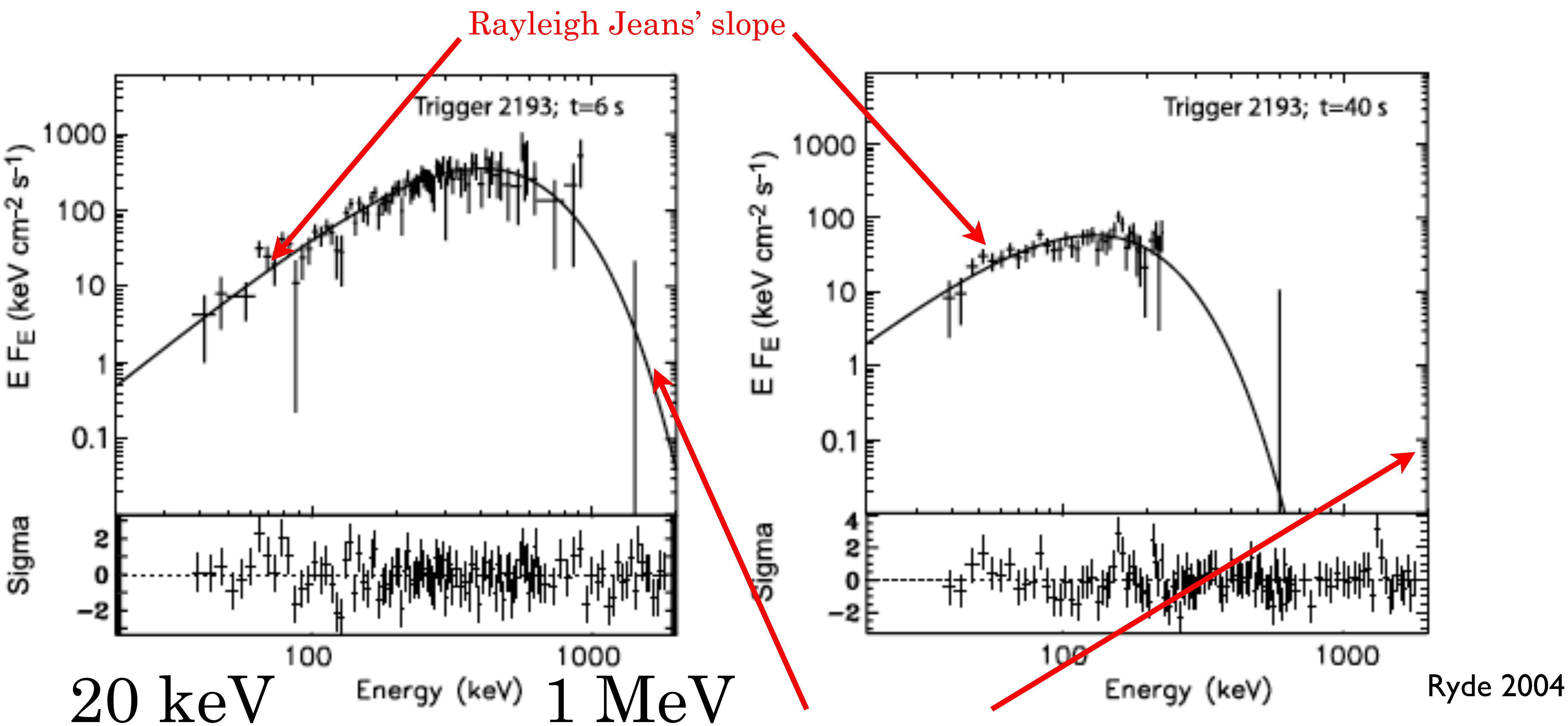

Spectra from temporally resolved pulses observed by BATSE over the energy range 20-2000 keV.

CGRO BATSE: 6 observed bursts out of 2200

- **Ryde (2004):** Blackbody through out the pulse
- **Ghirlanda et al. (2003):** Blackbody in initial phase of burst

Single Planck function bursts

Fermi Gamma Ray Space Telescope

GRB100507

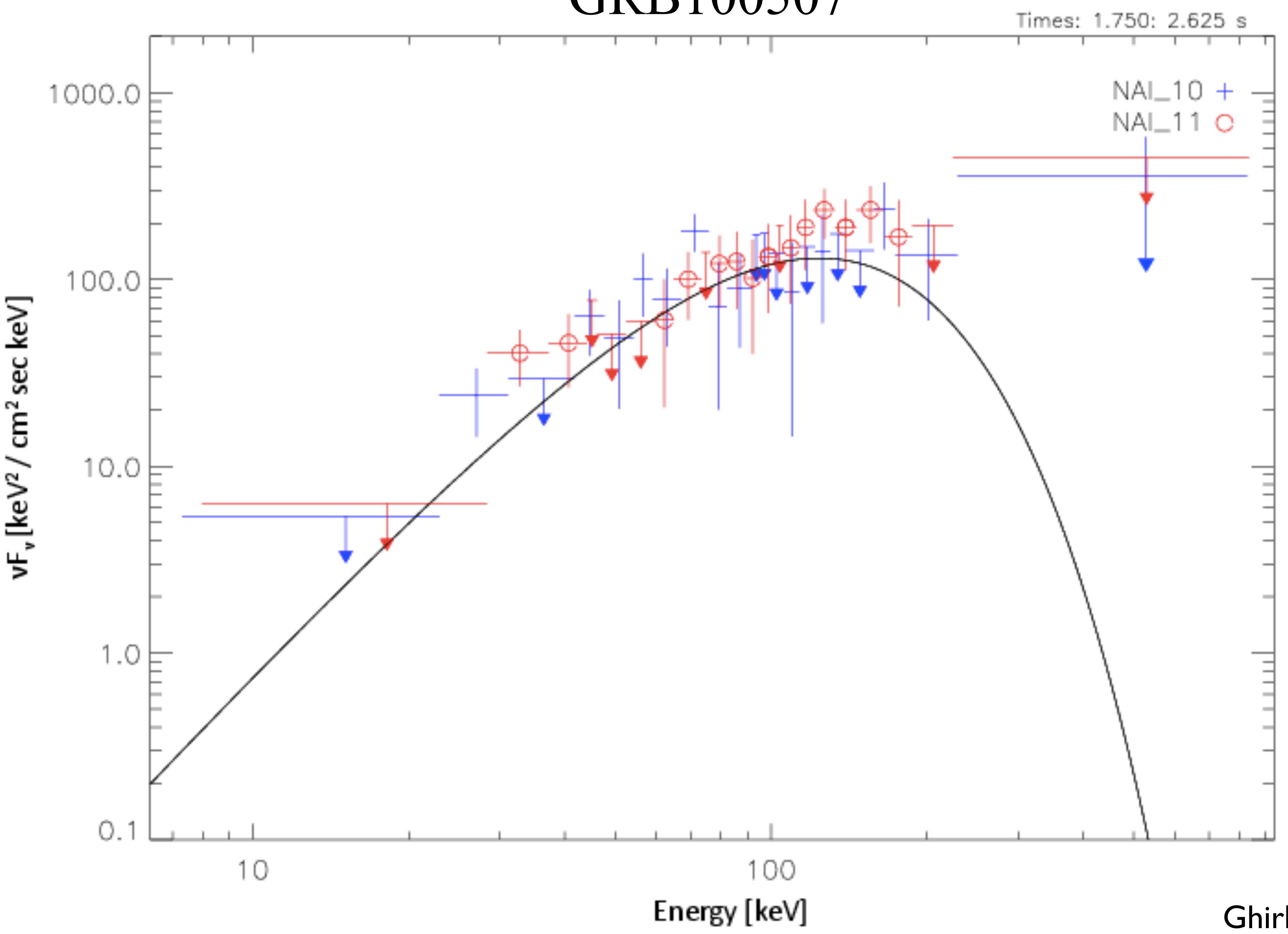

Ghirlanda et al. 2013

Single Planck function bursts

Fermi Gamma Ray Space Telescope

GRB100507

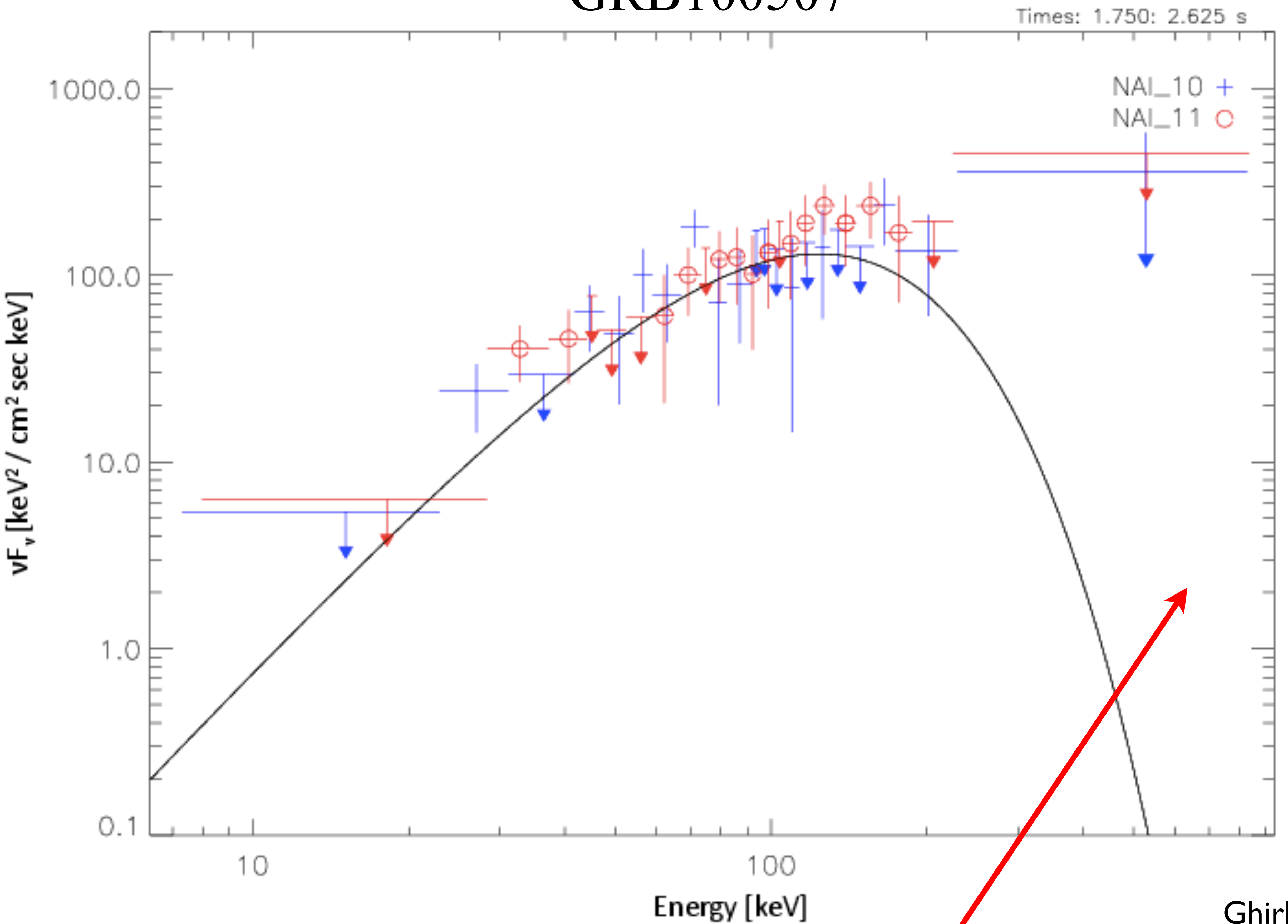

Ghirlanda et al. 2013

Void of photons

Single Planck function bursts

Fermi Gamma Ray Space Telescope

GRB100507

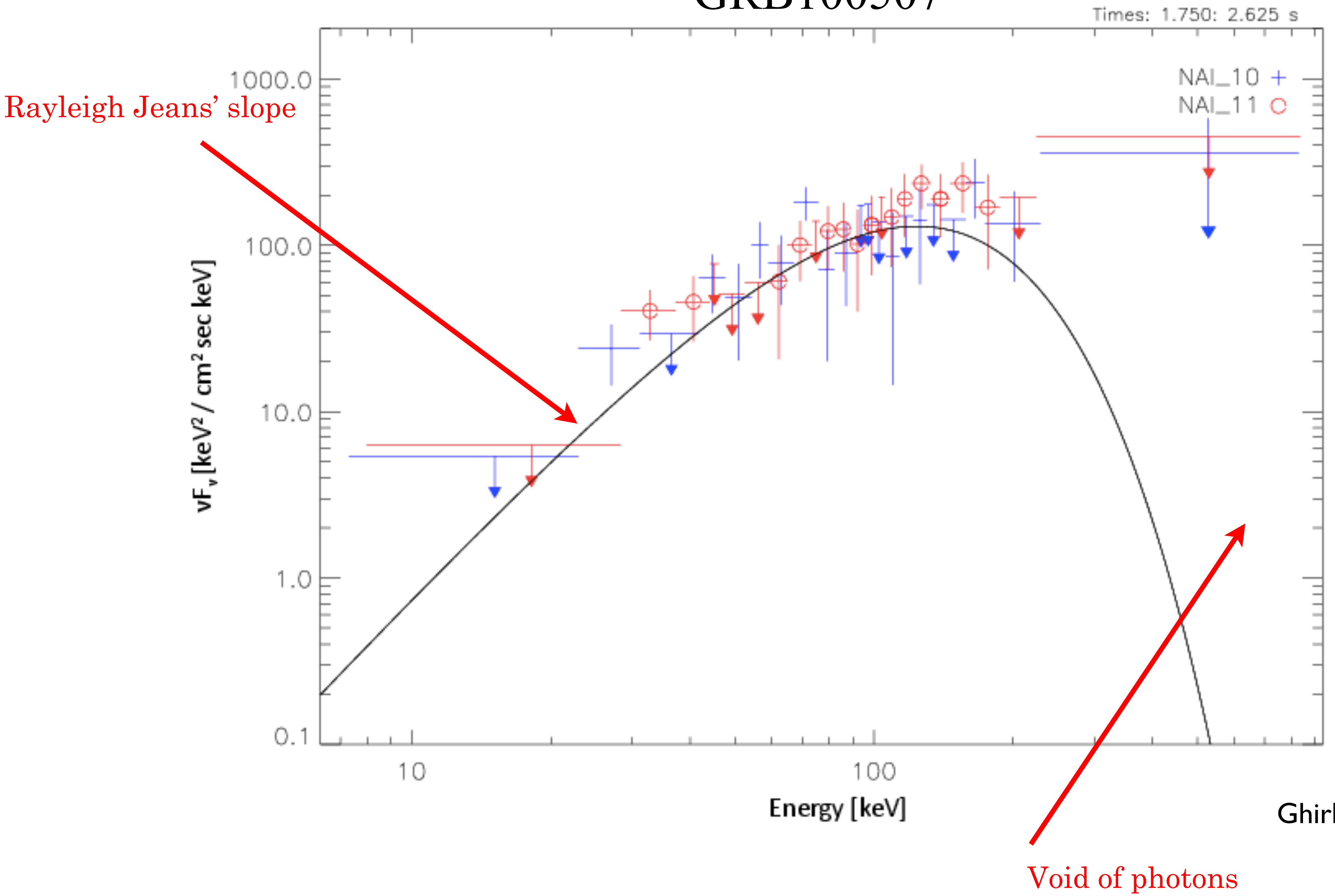

Ghirlanda et al. 2013

Single Planck function bursts

Fermi Gamma Ray Space Telescope

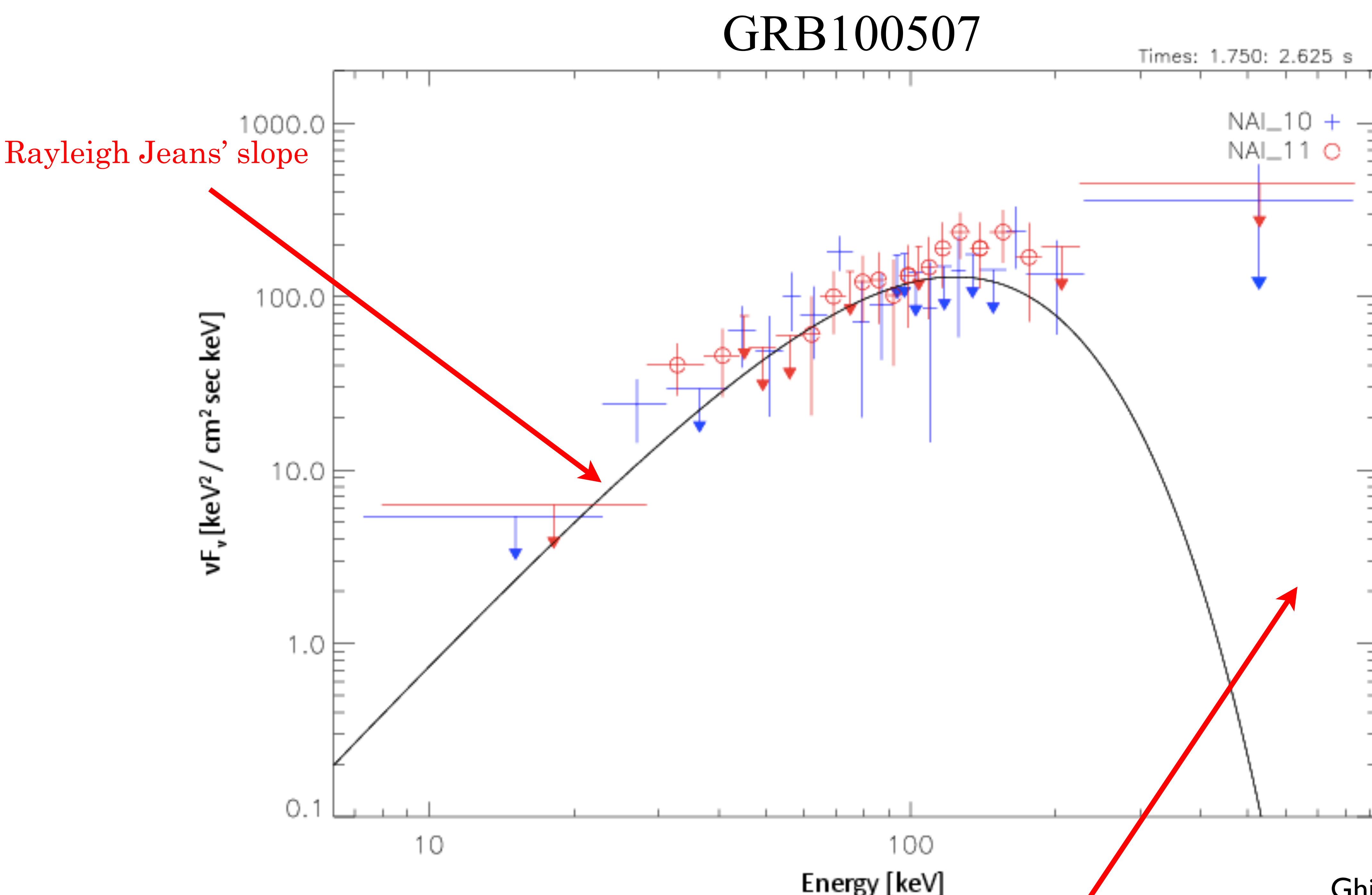

Ghirlanda et al. 2013

Fermi GST: 2 observed bursts out of 1400

Single Planck function bursts

Fermi Gamma Ray Space Telescope

GRB100507

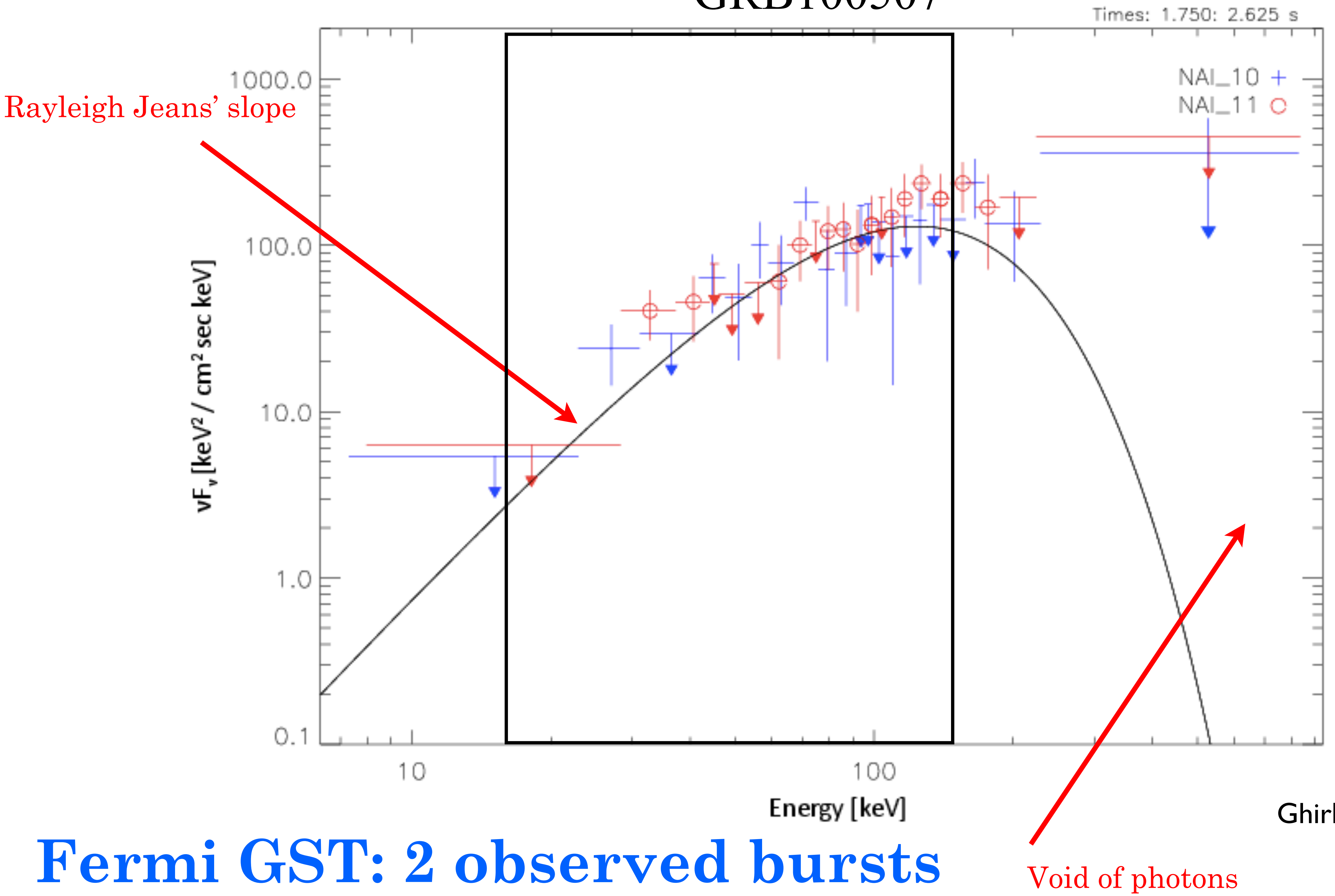

Ghirlanda et al. 2013

Fermi GST: 2 observed bursts out of 1400

GRB090902B

Abdo et al. (2009), Ryde et al. (2010) Zhang et al. (2010)

Time resolved spectrum (11.608-11.880 s)

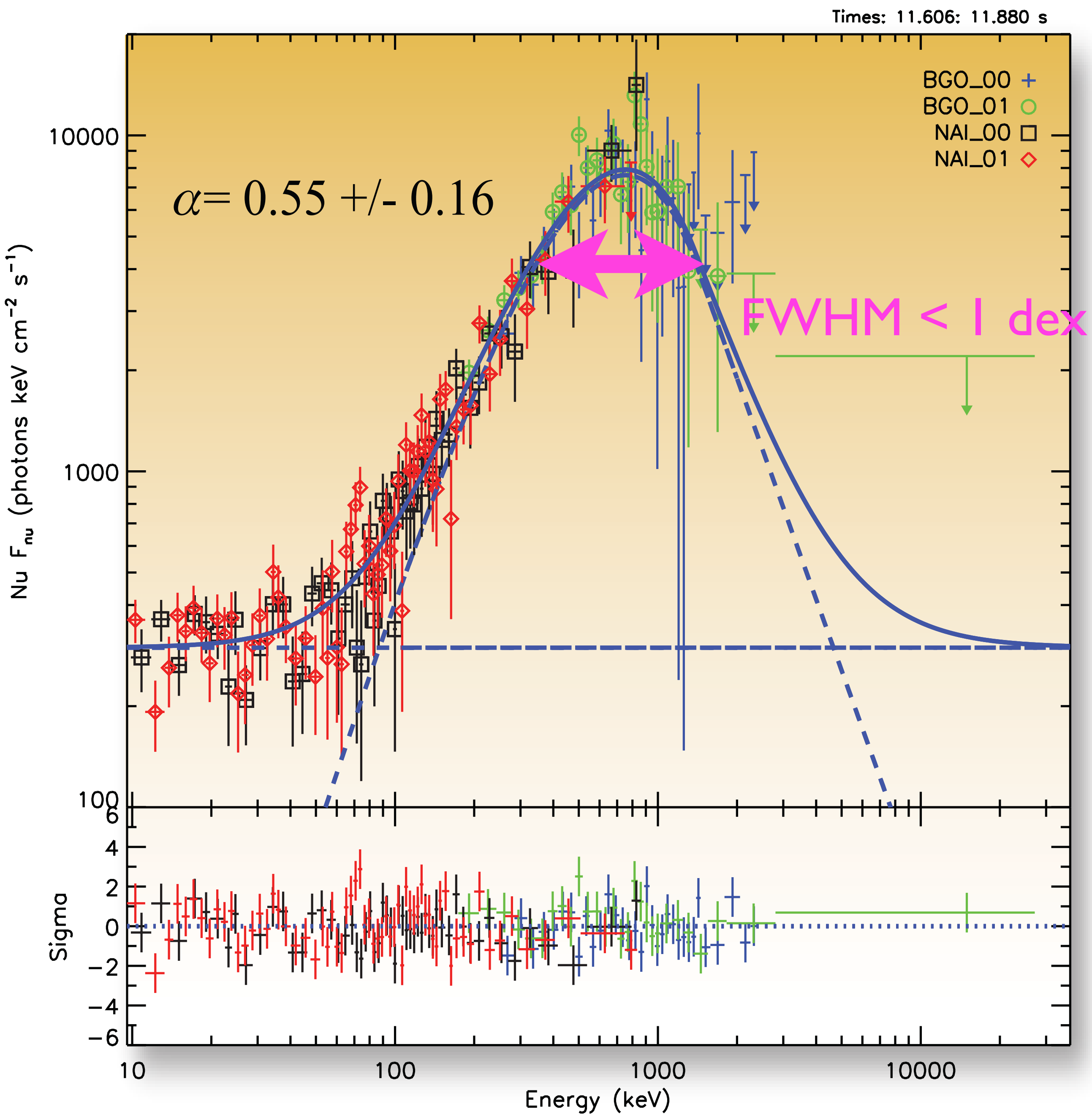

GRB090902B

Abdo et al. (2009), Ryde et al. (2010) Zhang et al. (2010)

Time resolved spectrum (11.608-11.880 s)

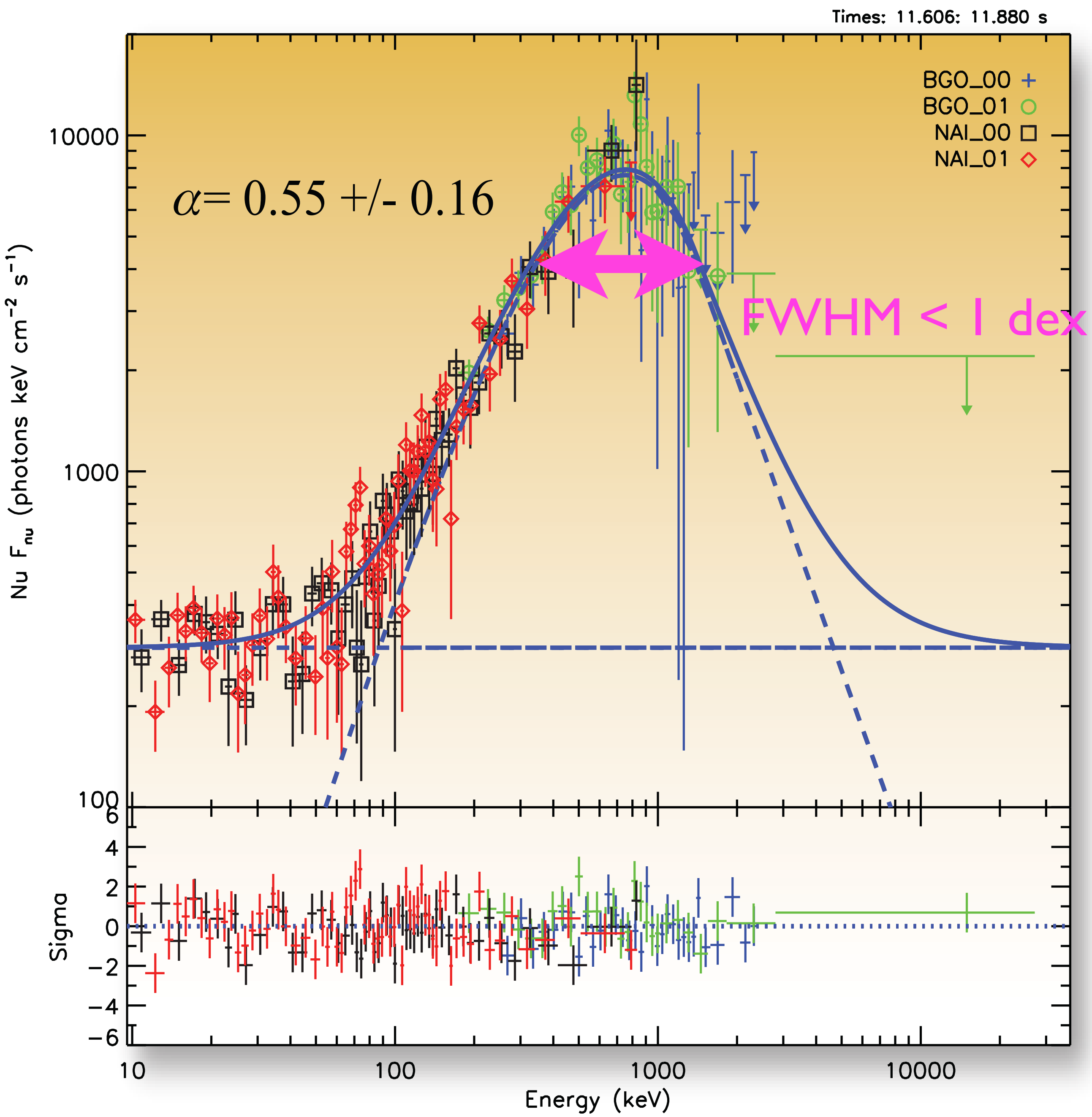

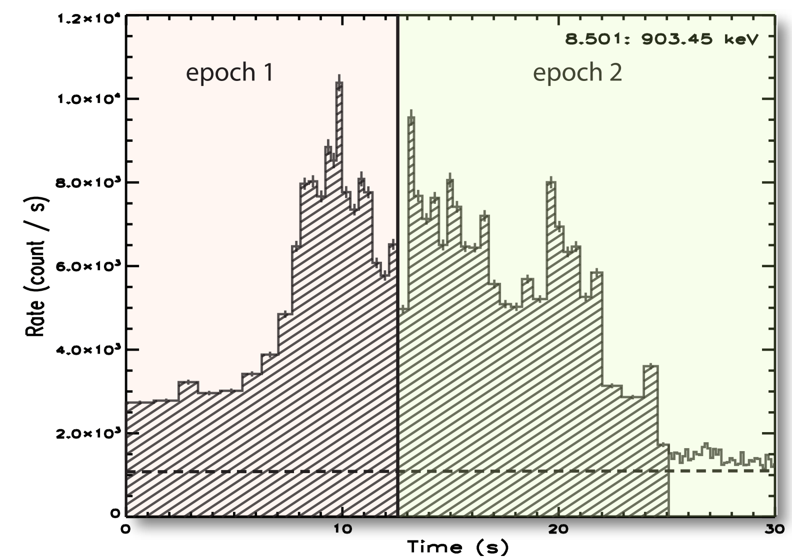

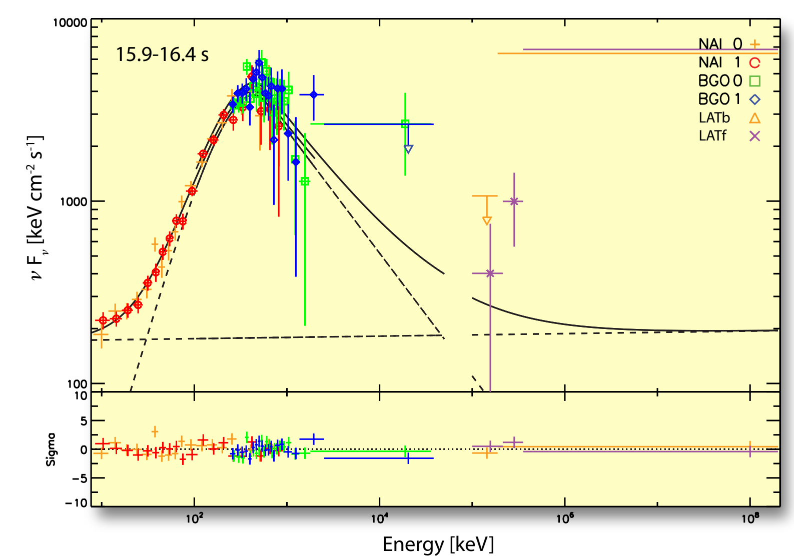

Observed spectral width & Evolution

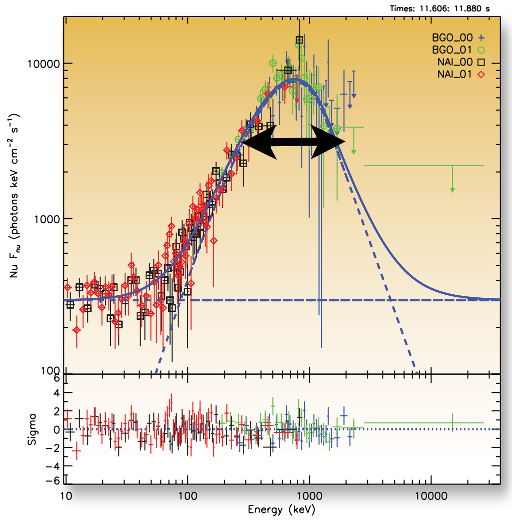

FWHM as ratio E_{high}/E_{low},

Observed spectral width & Evolution

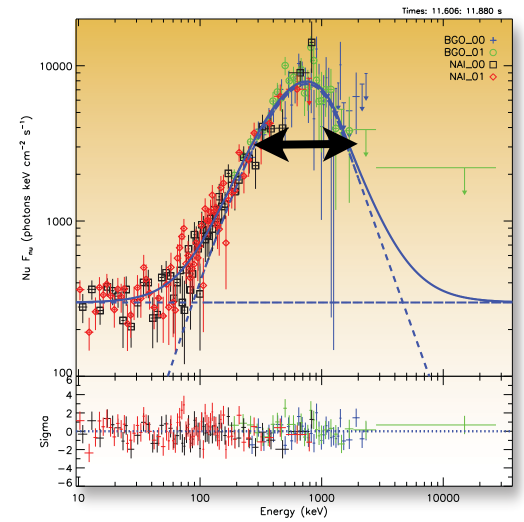

FWHM as ratio E_{high}/E_{low},

~3. ~7 ~70 ~100

Planck High latitude Synchrotron Inverse Compton

Observed spectral width & Evolution

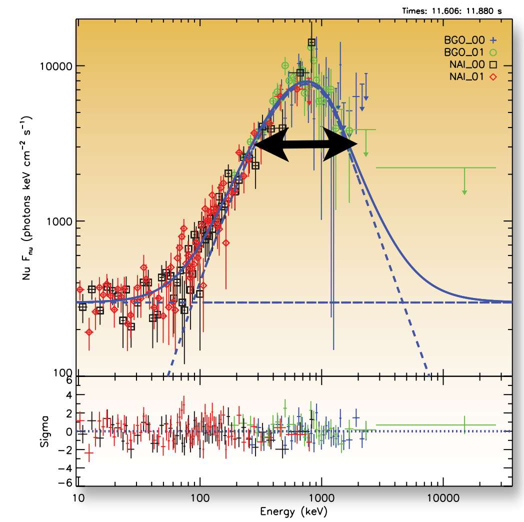

FWHM as ratio Ehigh/Elow,

~3.	~7	~70	~100
Planck	High latitude	Synchrotron	Inverse Compton

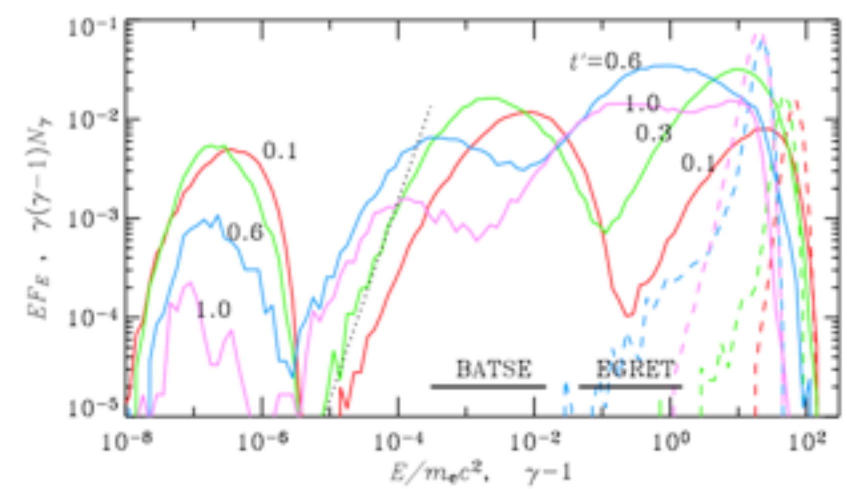

Poutanen & Stern 2004

Observed spectral width & Evolution

FWHM as ratio E_{high}/E_{low},

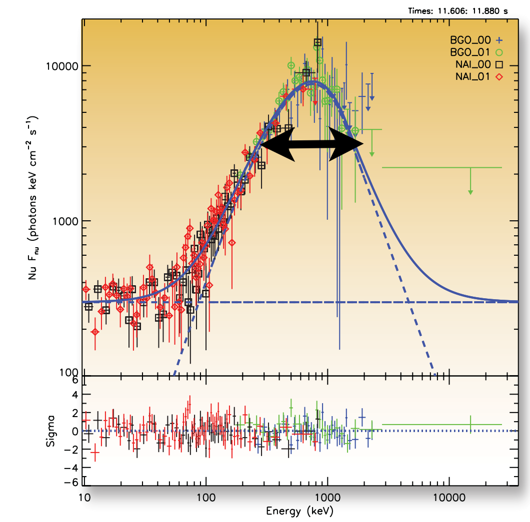

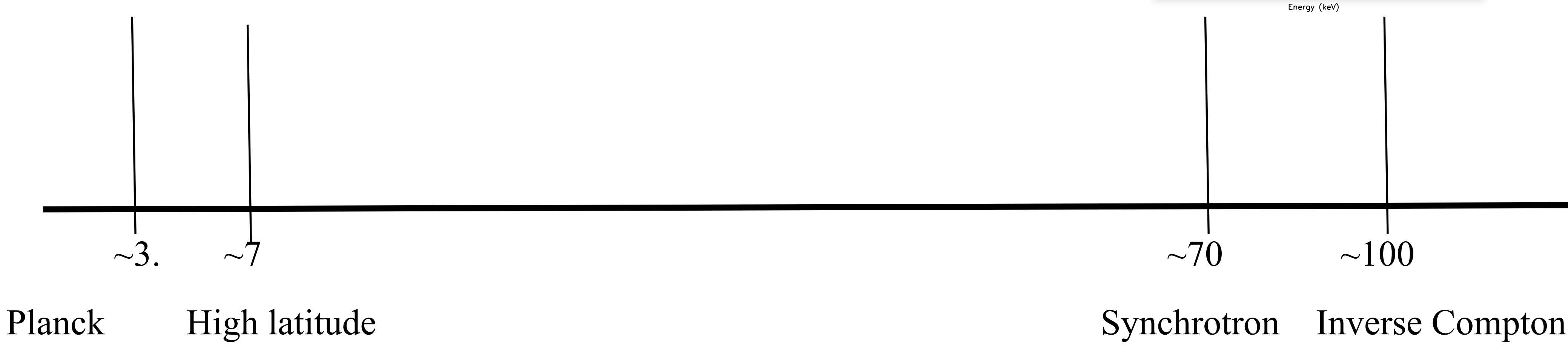

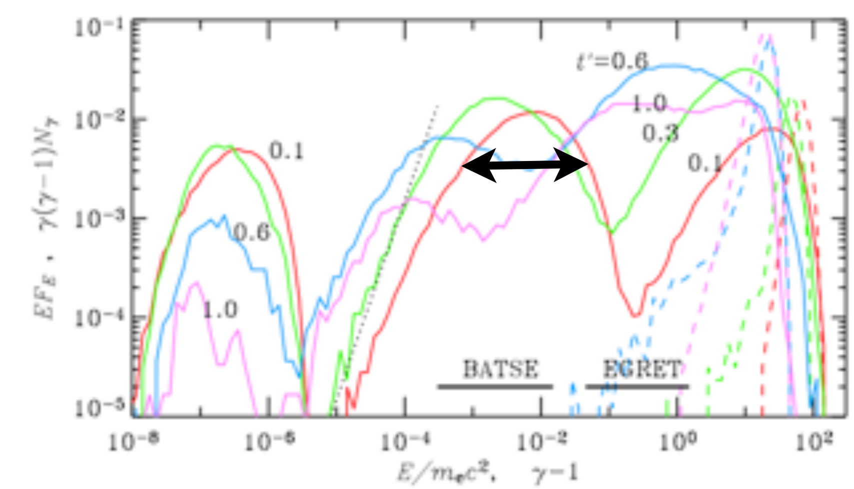

Poutanen & Stern 2004

Observed spectral width & Evolution

FWHM as ratio E_{high}/E_{low},

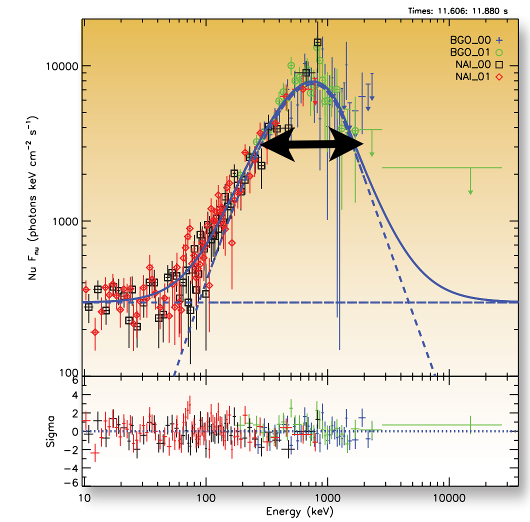

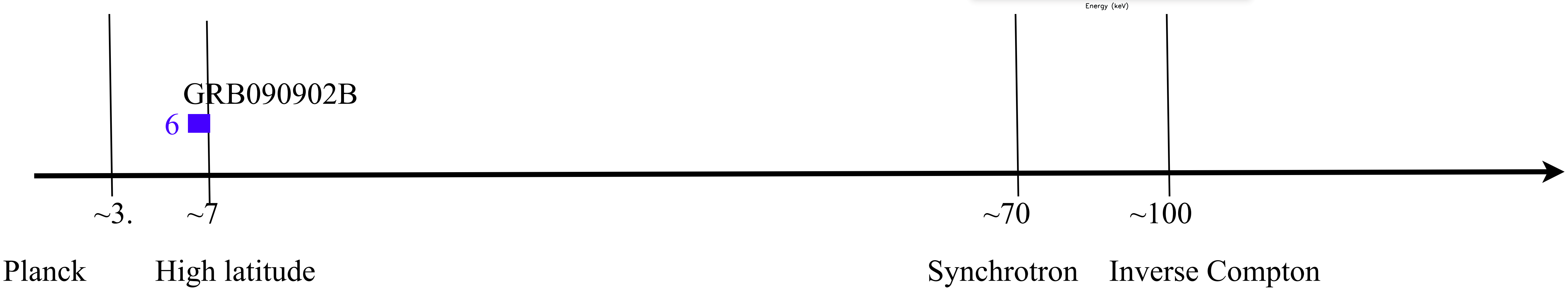

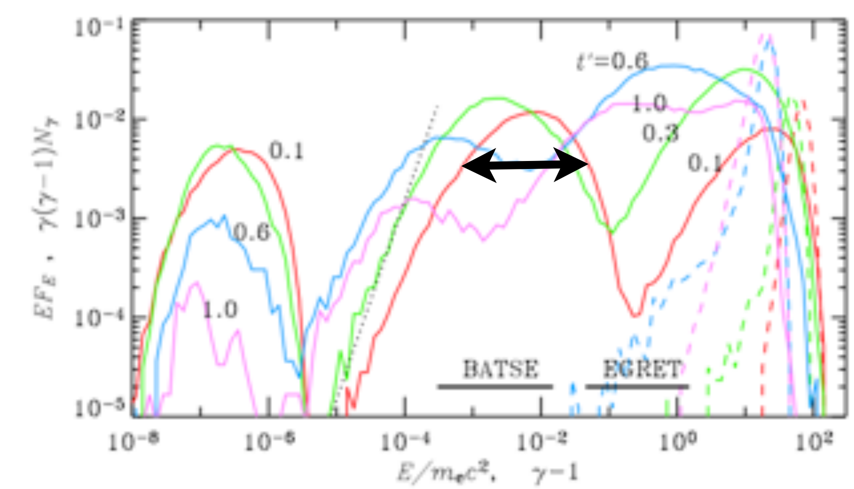

Poutanen & Stern 2004

Observed spectral width & Evolution

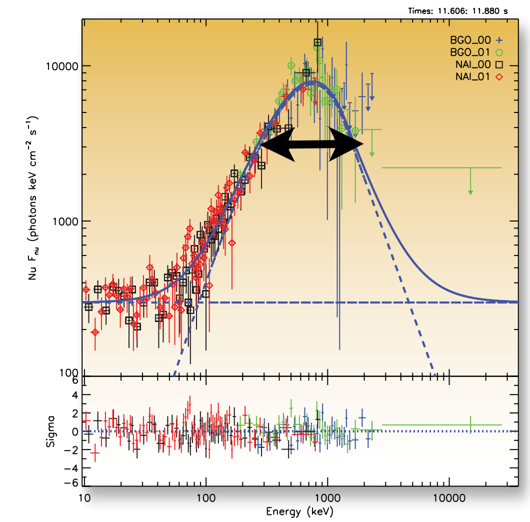

FWHM as ratio E_{high}/E_{low},

GRB090902B

6 → 20

~3. ~7 ~70 ~100

Planck High latitude Synchrotron Inverse Compton

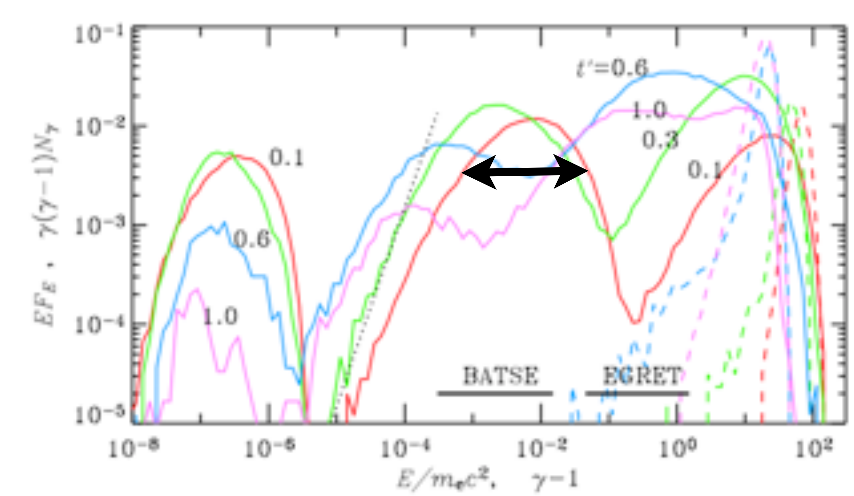

Poutanen & Stern 2004

Observed spectral width & Evolution

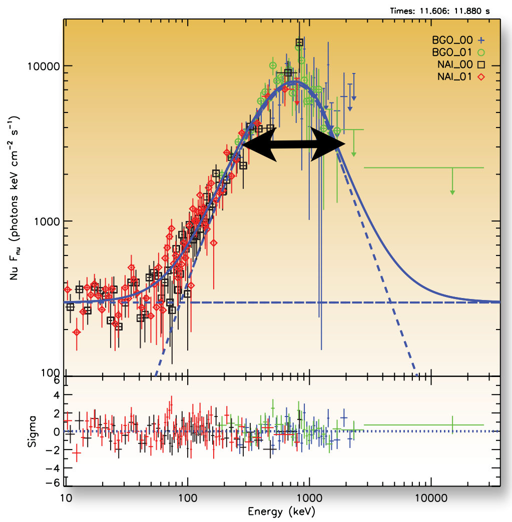

FWHM as ratio Ehigh/Elow,

GRB110920

12

GRB090902B

6

20

~3.

~7

~70

~100

Planck

High latitude

Synchrotron

Inverse Compton

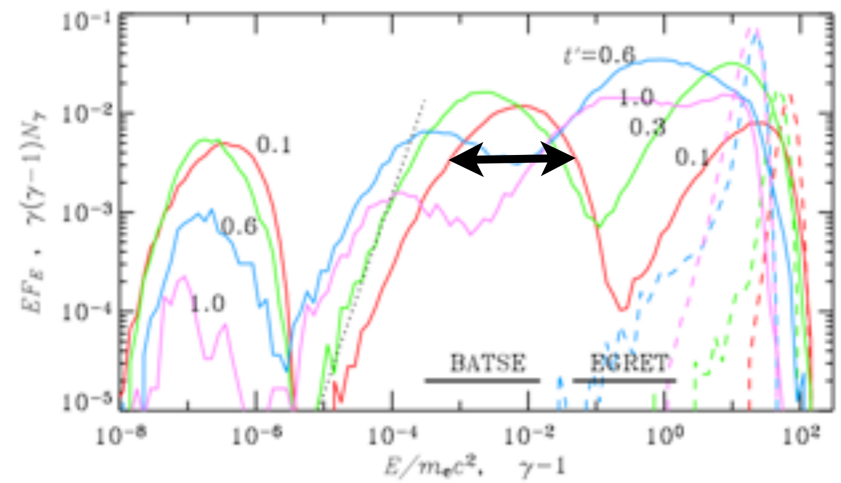

Poutanen & Stern 2004

Observed spectral width & Evolution

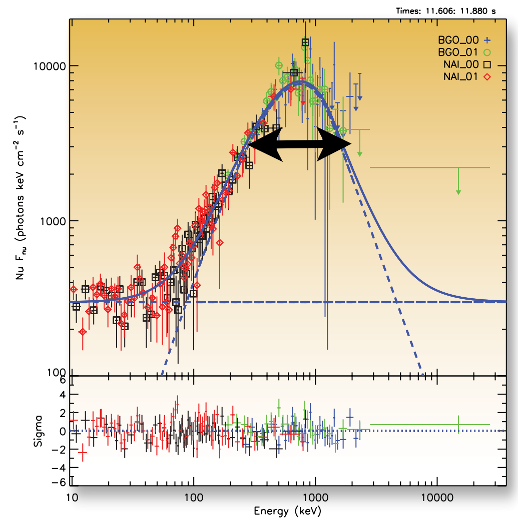

FWHM as ratio Ehigh/Elow,

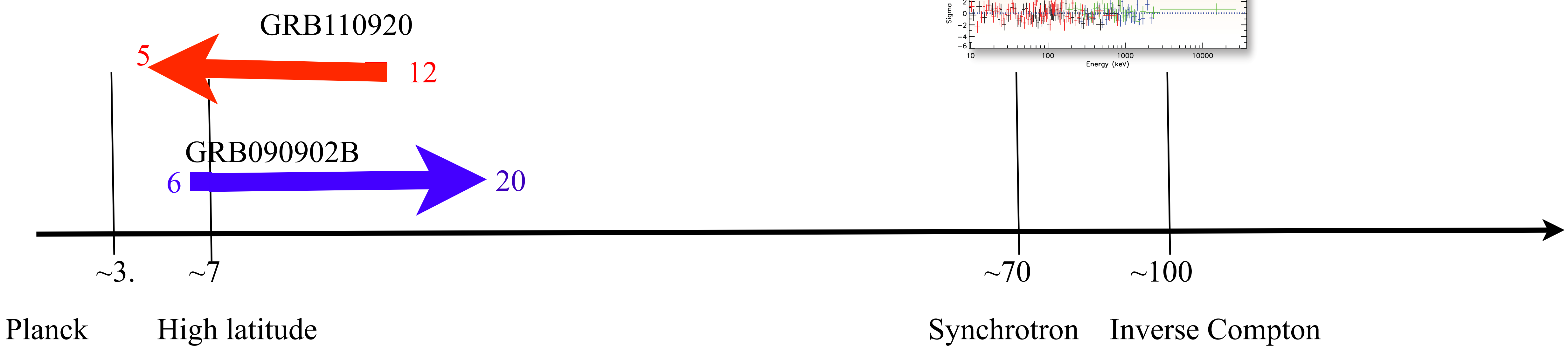

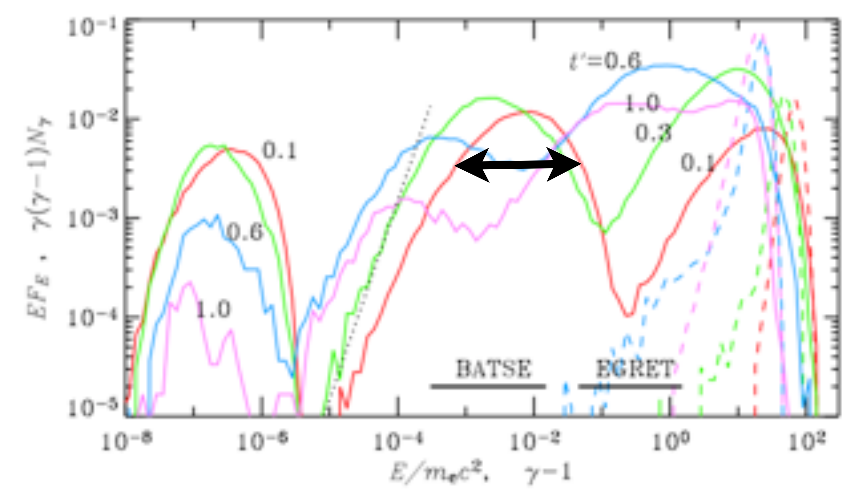

Poutanen & Stern 2004

Observed spectral width & Evolution

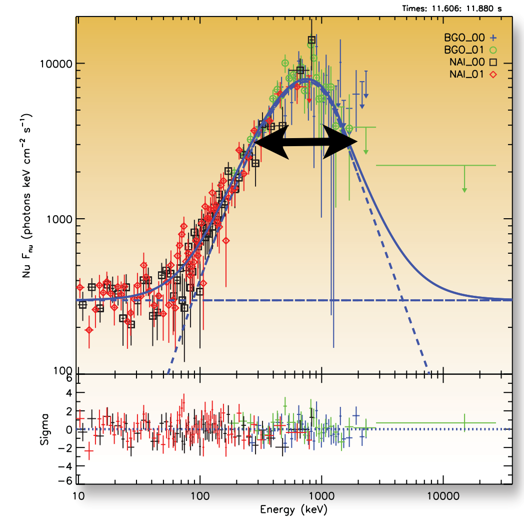

FWHM as ratio Ehigh/Elow,

GRB110920

5 ← 12

GRB090902B

6 → 20

~3. ~7 ~70 ~100

Planck High latitude Synchrotron Inverse Compton

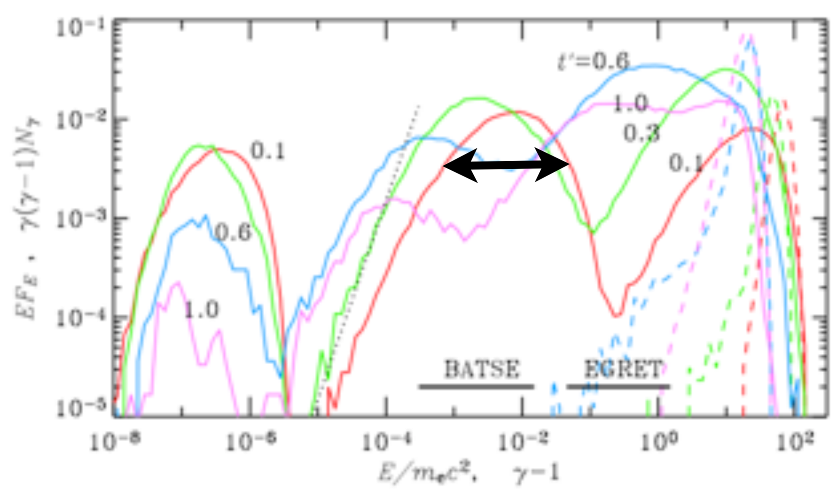

Poutanen & Stern 2004

The narrowness of GRB spectra are equally as important as the hard α values

What do these bursts tell us?

1. Jet photosphere is detected! Photosphere has an effect on the formation of the GRB spectra.

2. Some spectra are pure blackbodies -> strong theoretical implications!

3. Some spectra are slightly broader than a BB, but still optically thick -> broadening mechanisms

4. Typical spectra are not this kind: Theoretical explanation.

5. Motivation to search for blackbodies in the data

Multi component bursts

Band only

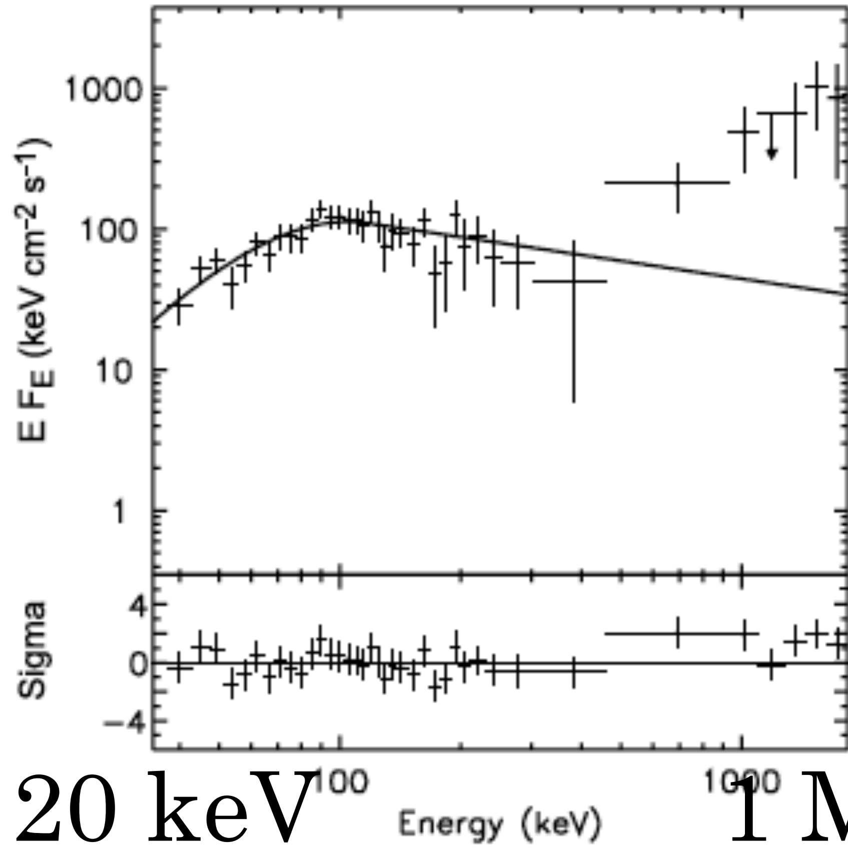

20 keV 1 MeV

Multi component bursts

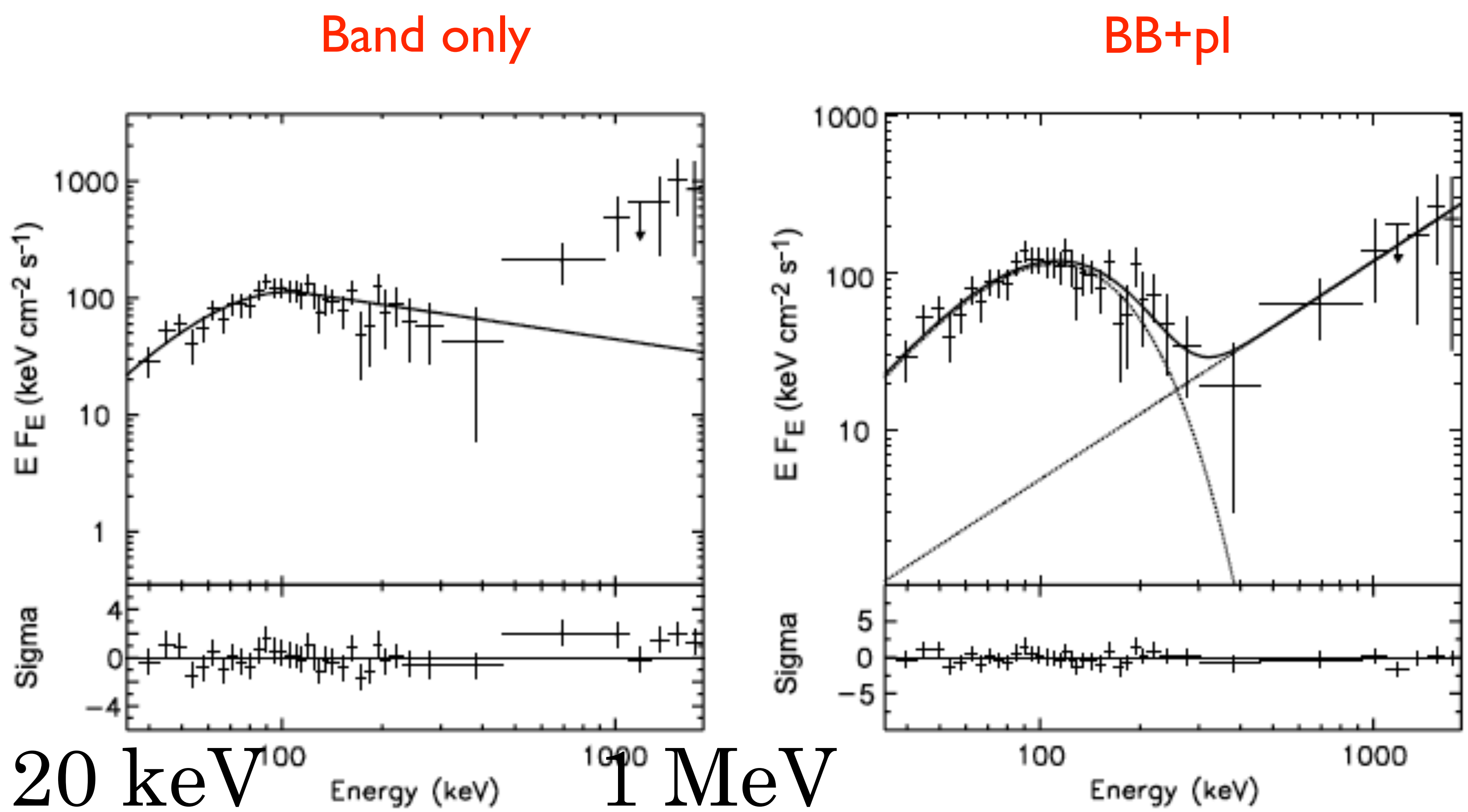

Ryde 2005

Multi component bursts

Band only   BB+pl

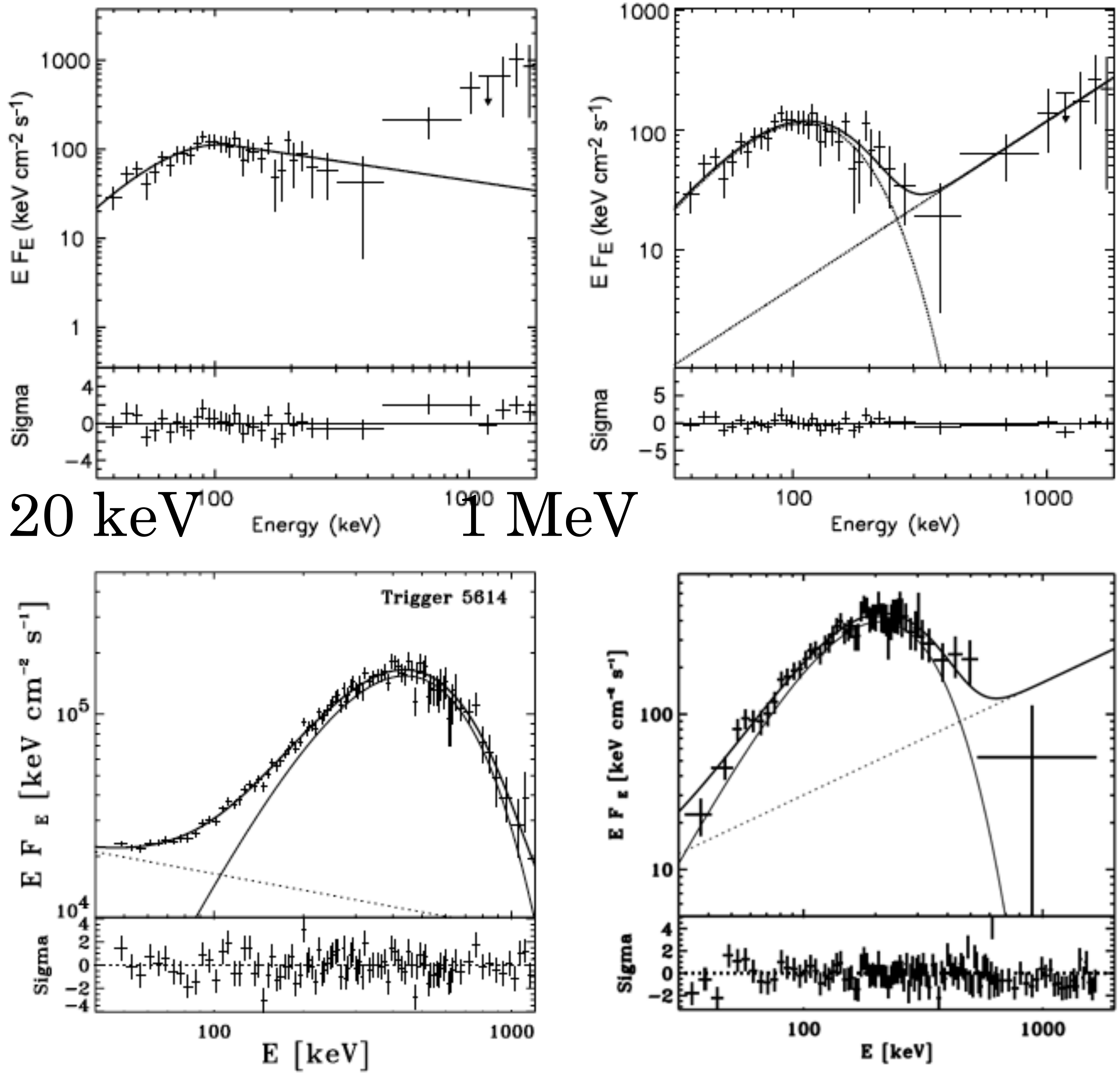

Ryde 2005

Examples of multi-peaked spectra observed by *Fermi*:

The photospheric component is modelled by a Planck function.
Is expected to be broadened to some extent.

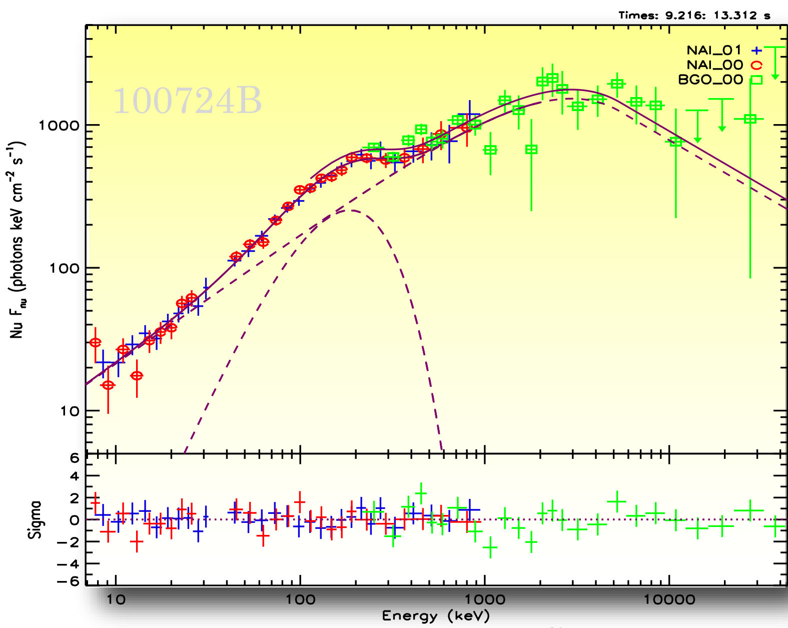

Guiriec et al. 2011

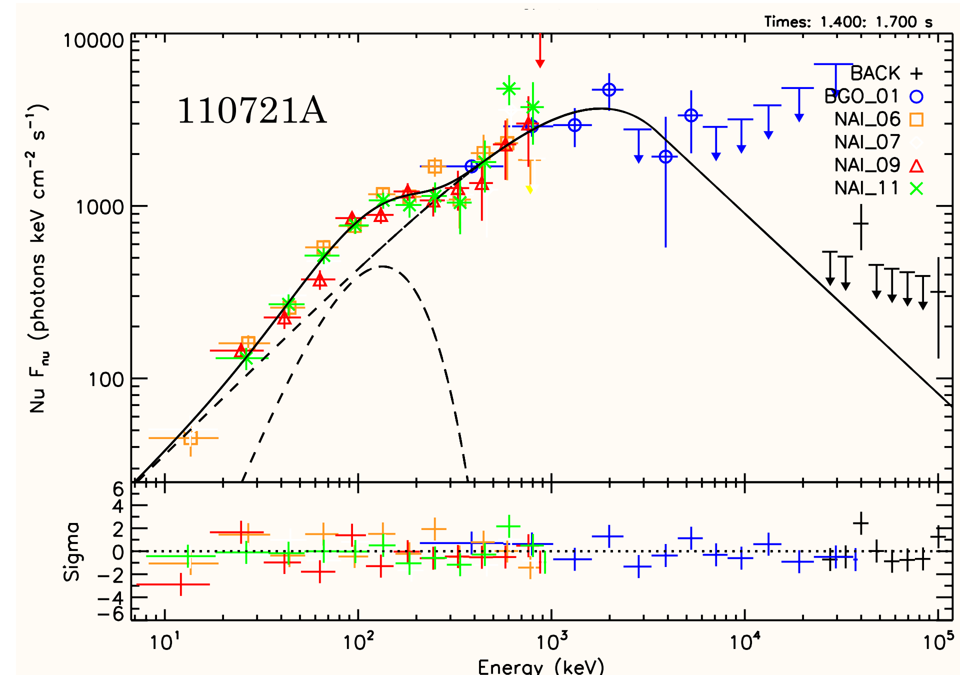

Axelsson et al. 2012

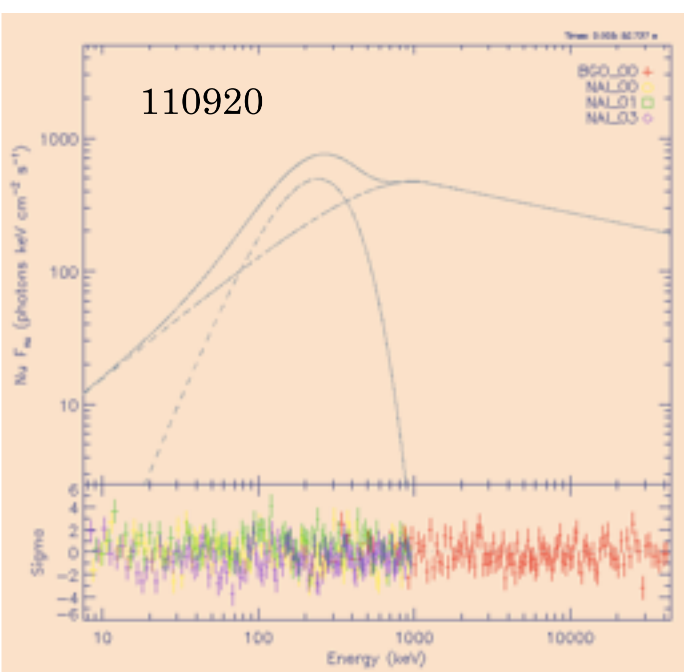

McGlynn et al. 2012

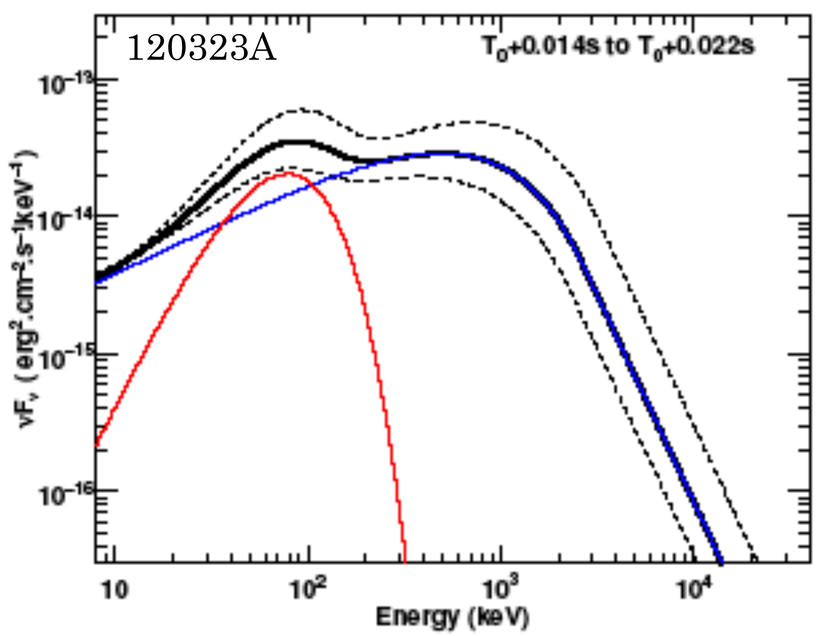

Guiriec et al. 2013

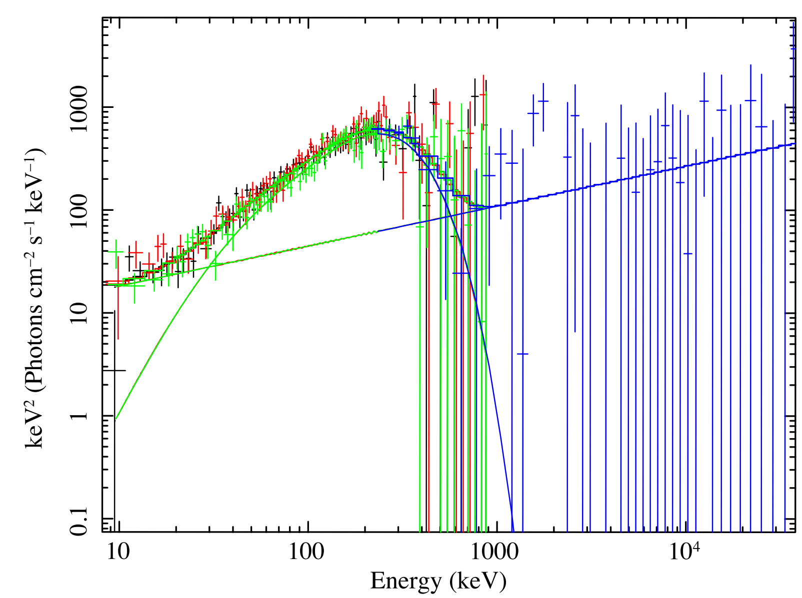

Iyyani et al. 2014

<u>Two component spectra:</u> Blackbody component typically 5-10% of total flux.
But many cases with 40-60 %.

Examples of multi-peaked spectra observed previous to *Fermi*:

PHEBUS/Fregate 1990'ies

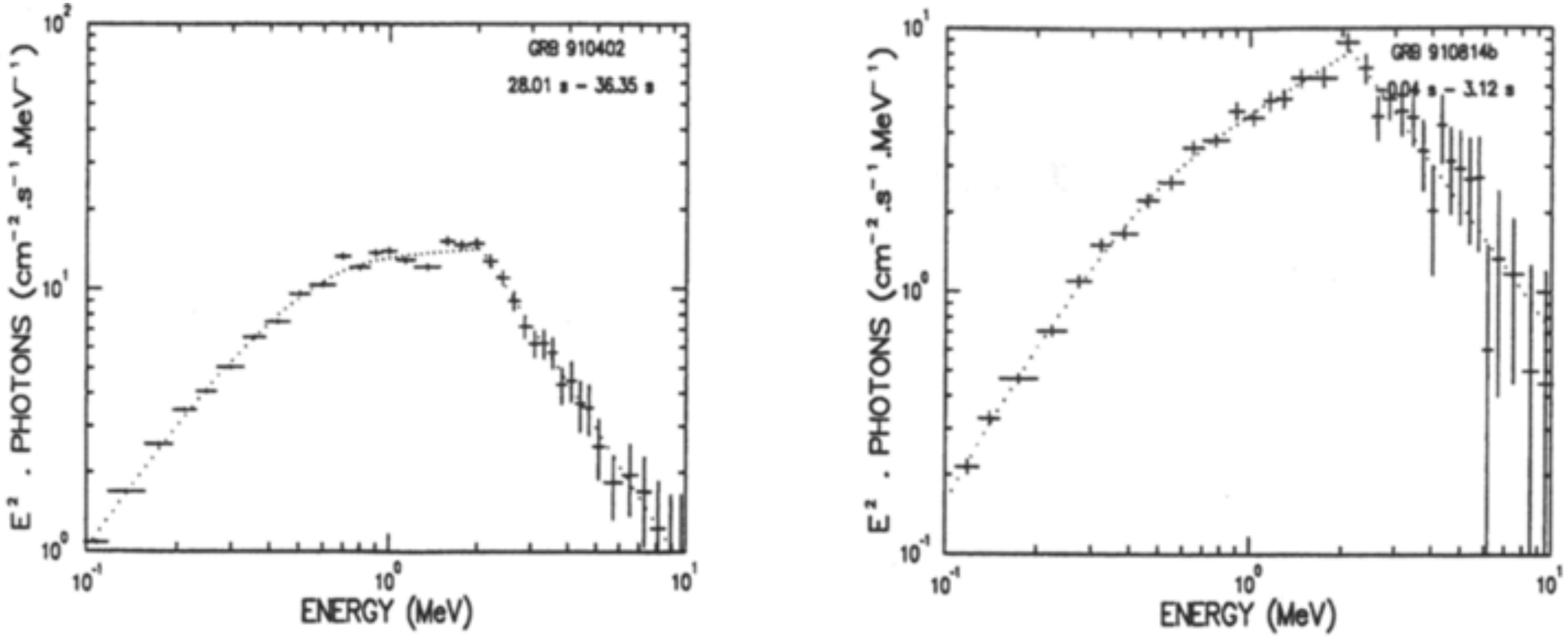

Barat et al. 2000

Multiple components in the *short* burst GRB120323A

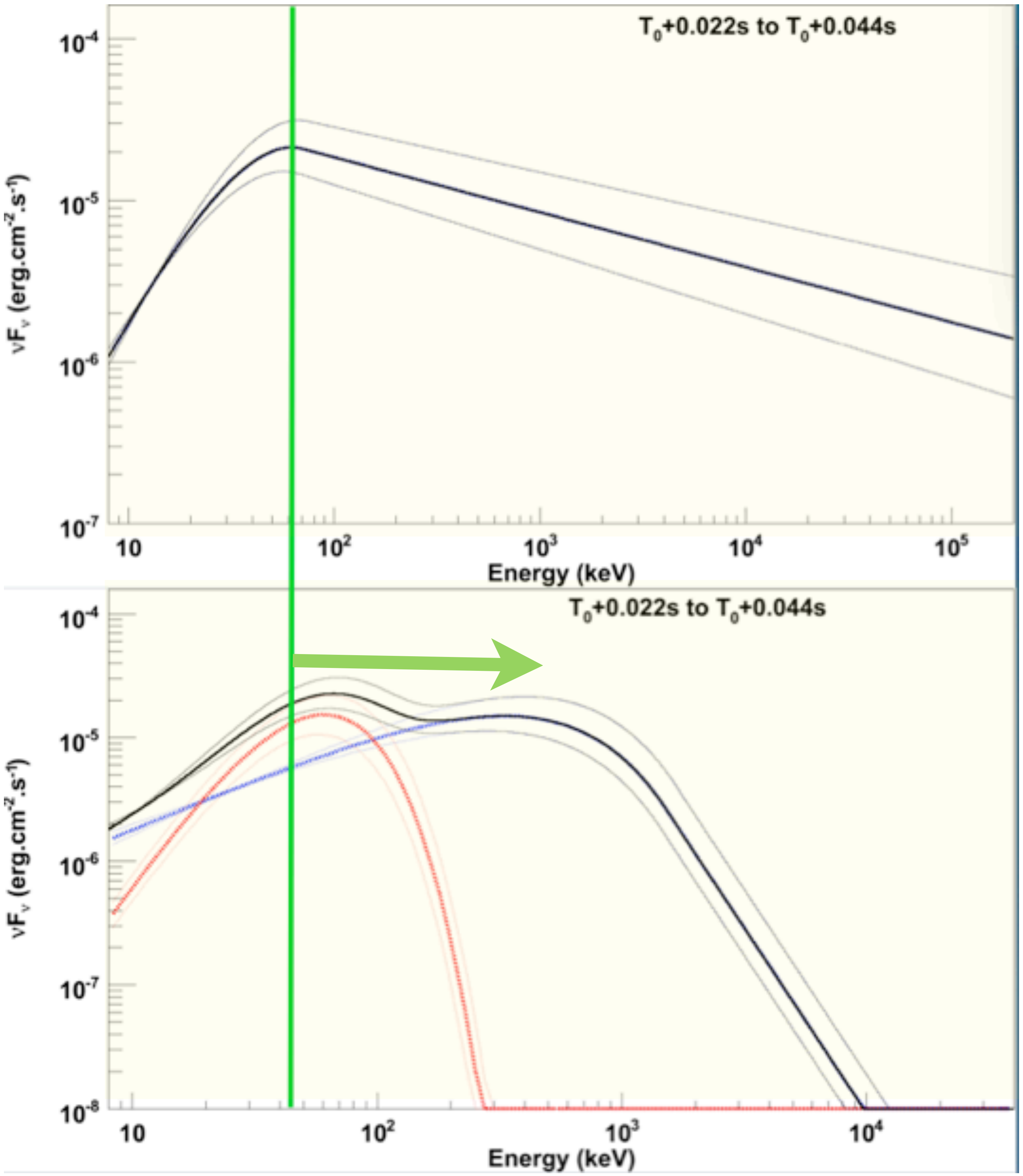

Changes the interpretations!

1. Change in Epeak
2. Change in alpha (synchrotron?)
3. Change in emission zones

Guiriec et al. 2013

Paradigm shift

nature
International weekly journal of science

NATURE | NEWS

Cosmic blasts powered by a hot glow

Spectral sensitivity of Fermi satellite reveals physics of gamma-ray generation

Eric Hand

08 May 2012

Since its launch in 2008, the Fermi space telescope has recorded hundreds of gamma-ray bursts (GRBs), flashes of light that, for just a few seconds or minutes, are the brightest objects in the Universe. And now the telescope is yielding data that is starting to explain the mechanisms that unleash these beam-like jets of light, which are thought to emanate from the poles of a spinning star as it collapses to form a black hole and explode in a supernova.

New light

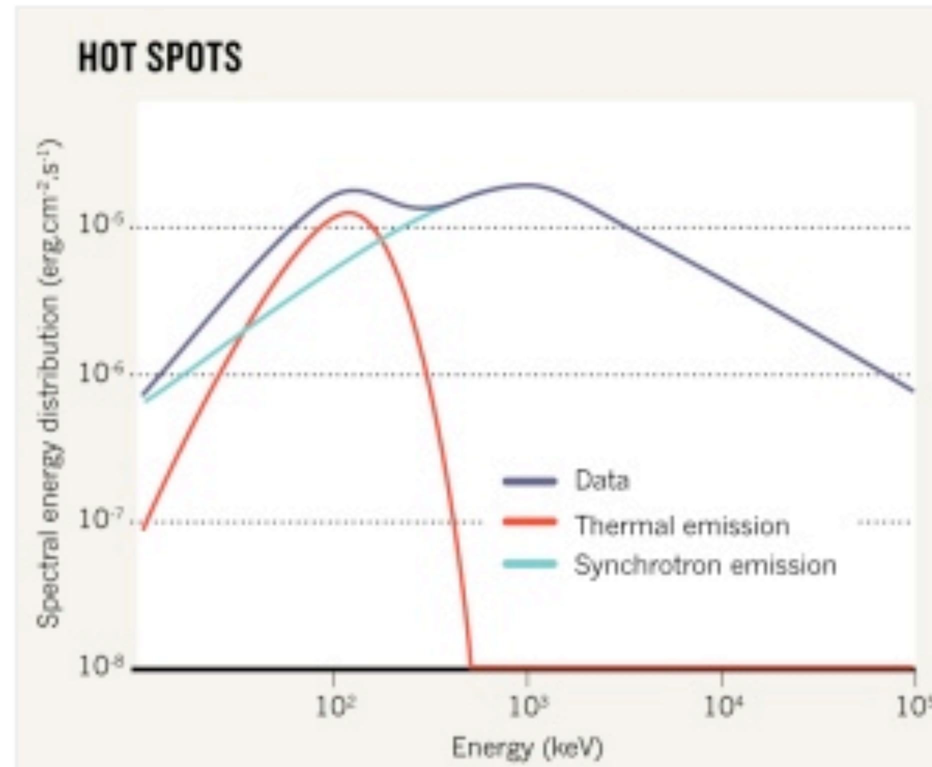

A preliminary model for the energy spectrum of gamma-ray burst 120323A, discovered in March by the Fermi telescope, shows a bump that is likely to come from thermal emissions — casting doubt on a long-held view that synchrotron emissions alone could explain the

But at t
team m
in Gree
cache c
that we
high-re
of these
hump c
tell-tale

The fiel
importa
years, t
emitting
were di
would h

Interpretation

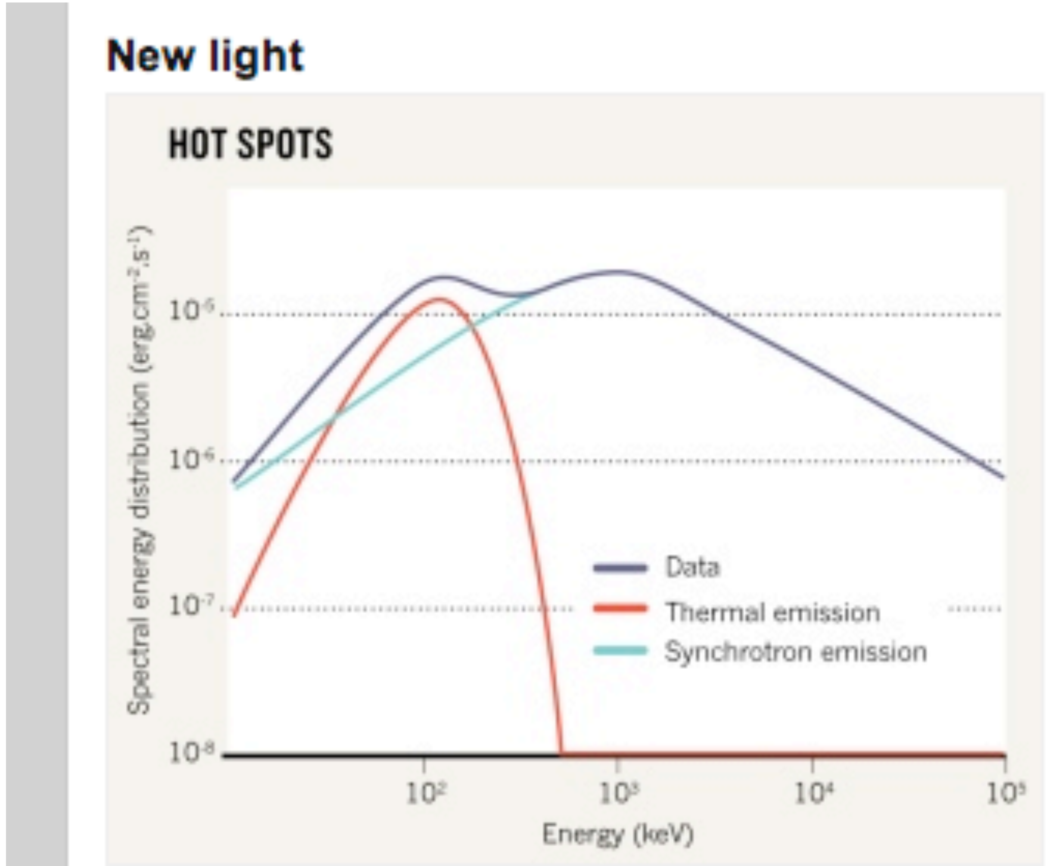

Interpretation

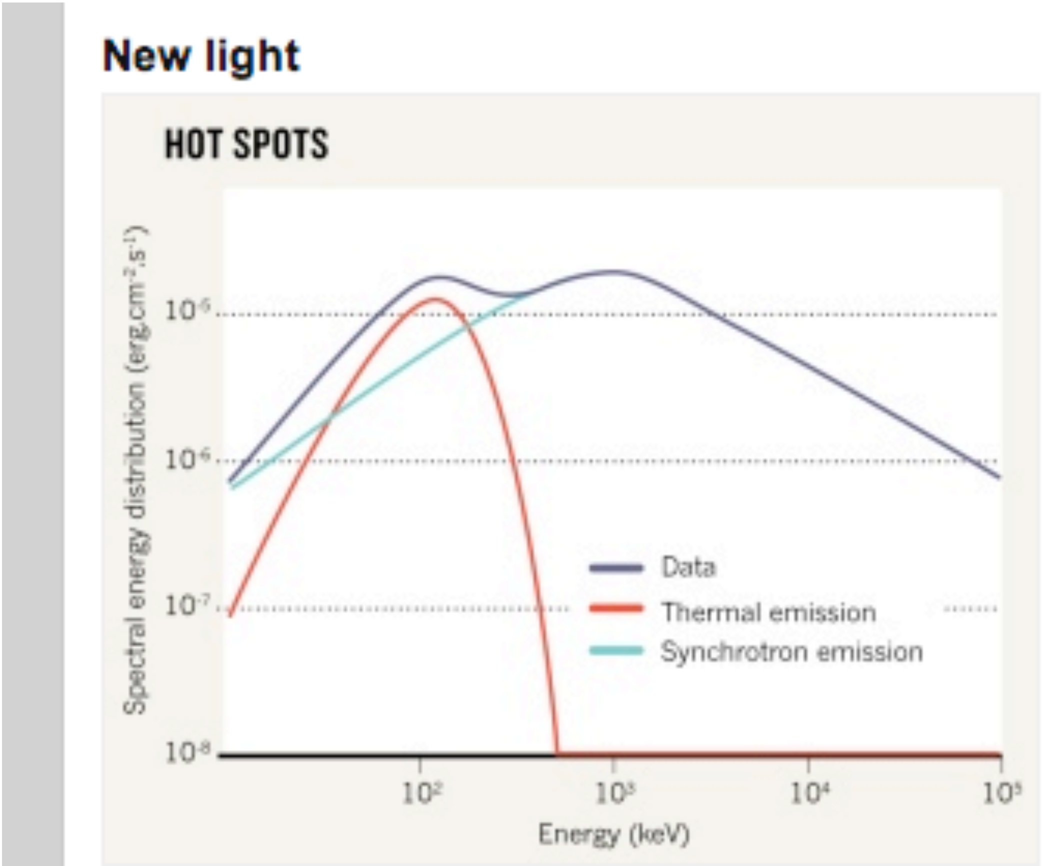

1. *Multi-zone emission:* initially passive jets, Shocks, ICMART, synchrotron emission

2. *Photospheric emission:* including heated jets and geometrical effects

Interpretation 1: Multiple Emission Zones

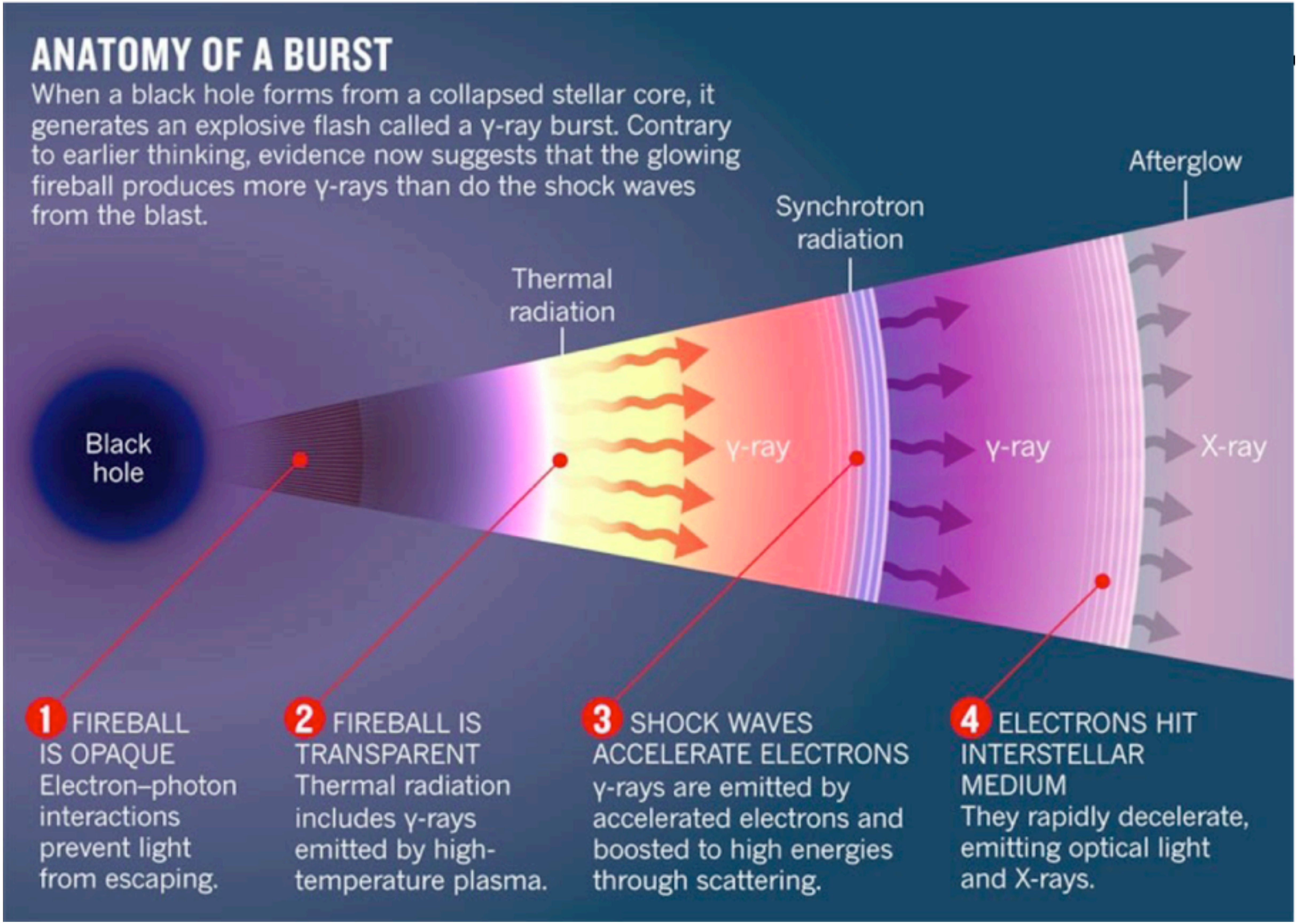

Basic framework: the fireball model

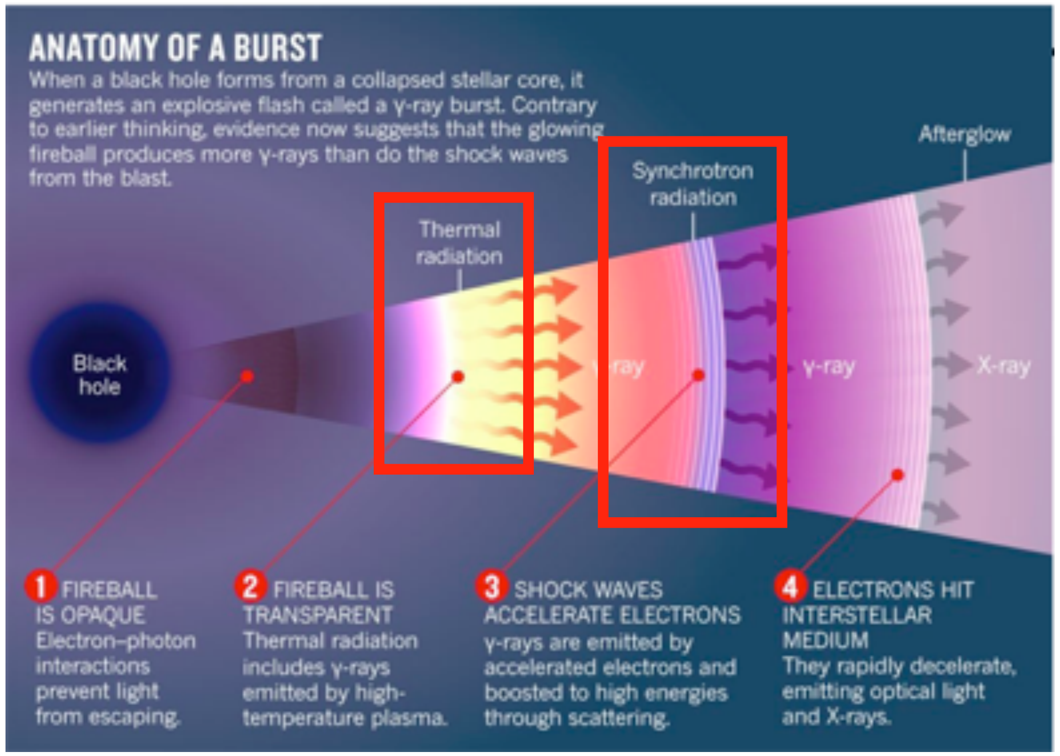

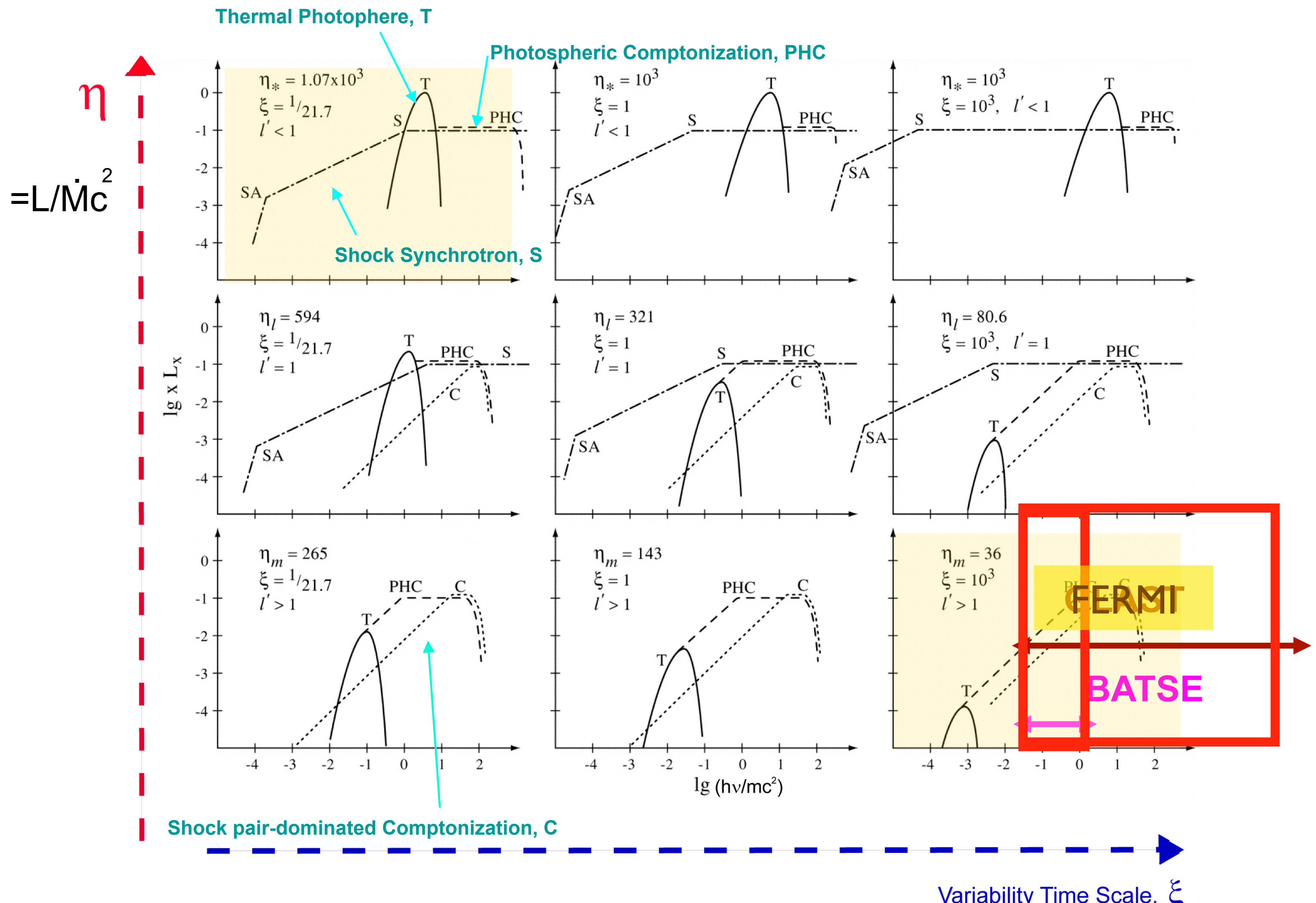

Mészáros et al. (2000)

Guiriec+, Daigne+, Ryde+, Zhang+, Axelsson+, Burgess+, McGlynn+, etc.

Need high time resolution, strong bursts, broad energy range

Two Emission zone - model

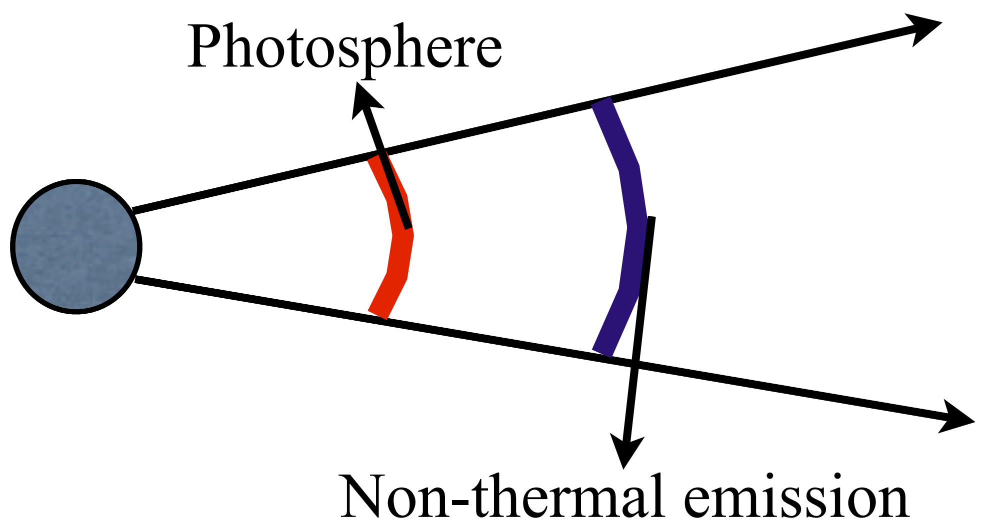

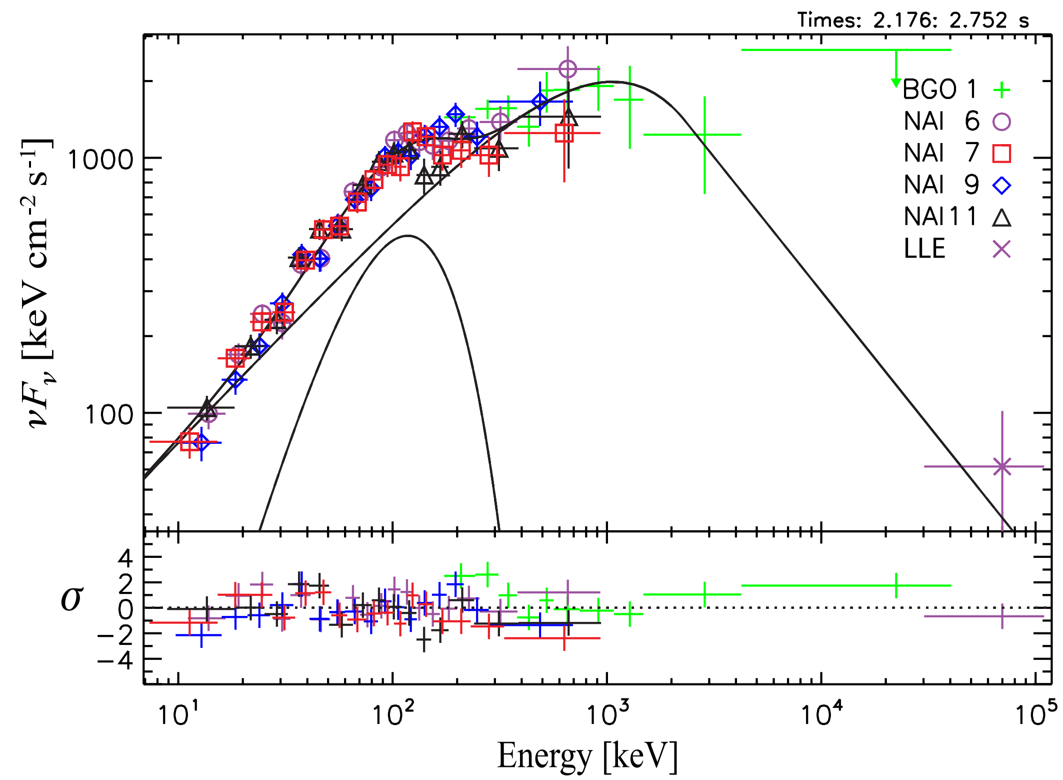

Axelsson+12

Photosphere
(Passive jet)

Thermal component - (quasi) Planck function (BB)

Above photosphere
(Optically thin)

Non-thermal component - Band function
synchrotron, ICMART...

2 zone emission, various realisations

If below the saturation radius - strong black body
If above saturation radius - adiabatic cooling

$$\left(\frac{r_{\rm ph}}{r_{\rm s}}\right)^{-2/3} = \frac{F_{\rm BB}}{F_{\rm NT}},$$

Magnetisation of the jet allows the ratio to vary (Daigne+ 2013, Zhang+ 2013)

Interpretation 2: Photospheric emission

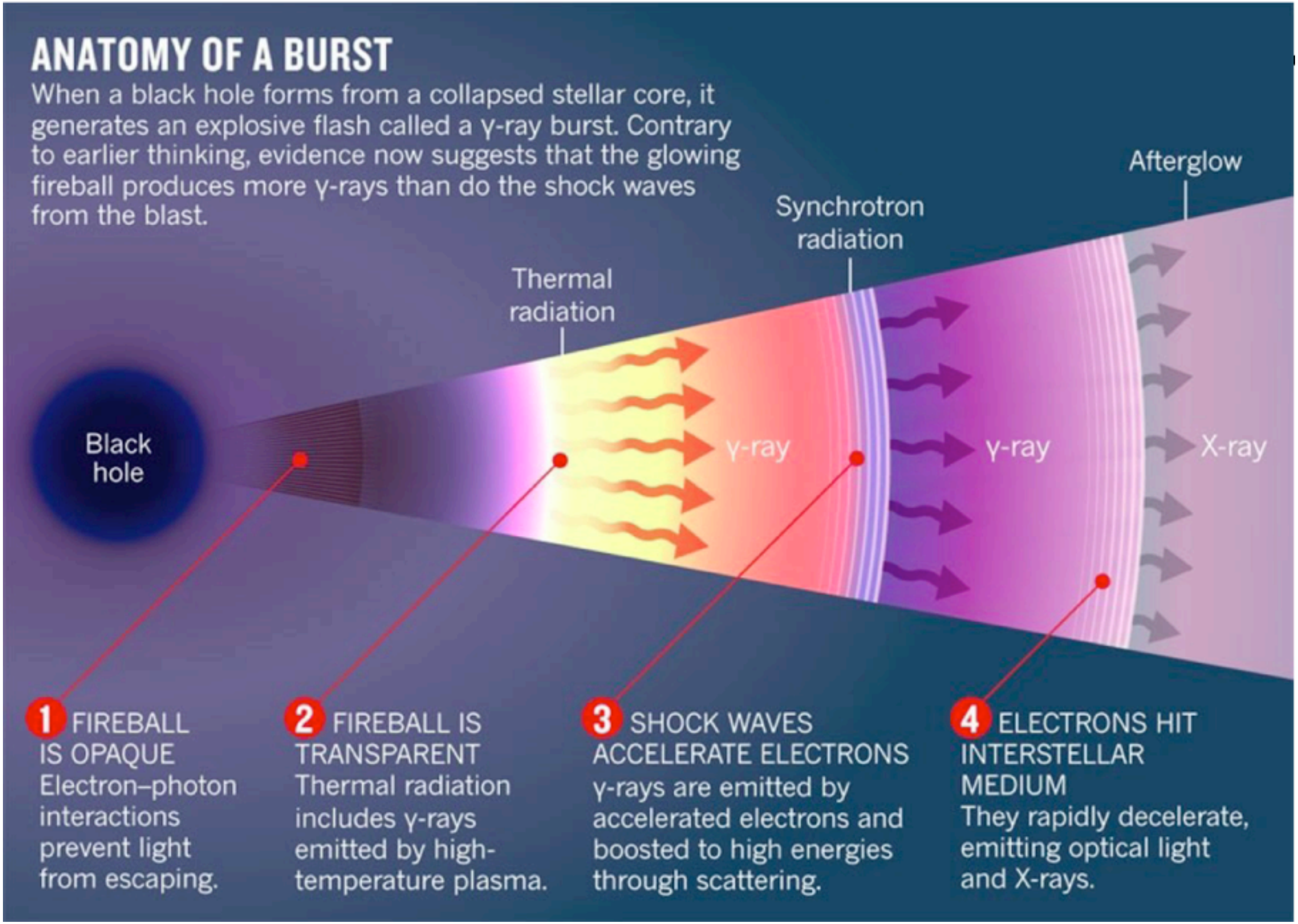

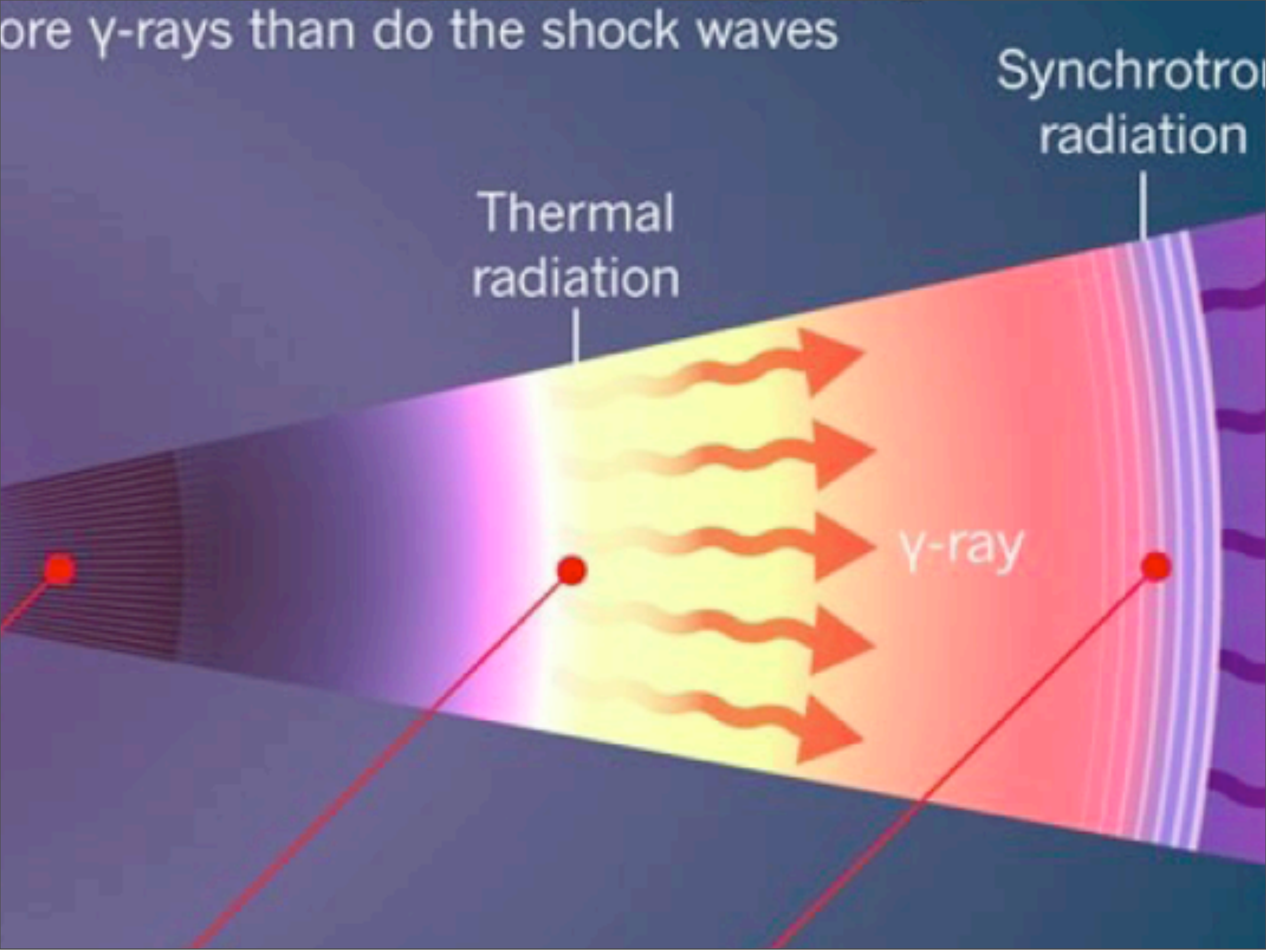
ore γ-rays than do the shock waves
Synchrotron
radiation
Thermal
radiation
γ-ray

Modification of Planck spectrum

Heating mechanism below the photosphere modifies the Planck spectrum

- Internal shocks
  (Peer, Meszaros, Rees 06, Ryde+10, Toma+10, Ioka10)
- Magnetic reconnection
  (Giannions 06, 08)
- Weak / oblique shocks
  (Lazzati, Morsonoi & Begelman 11, Ryde & Peer 11)
- Collisional dissipation
  (Beloborodov 10, Vurm, Beloborodov & Poutanen 11)

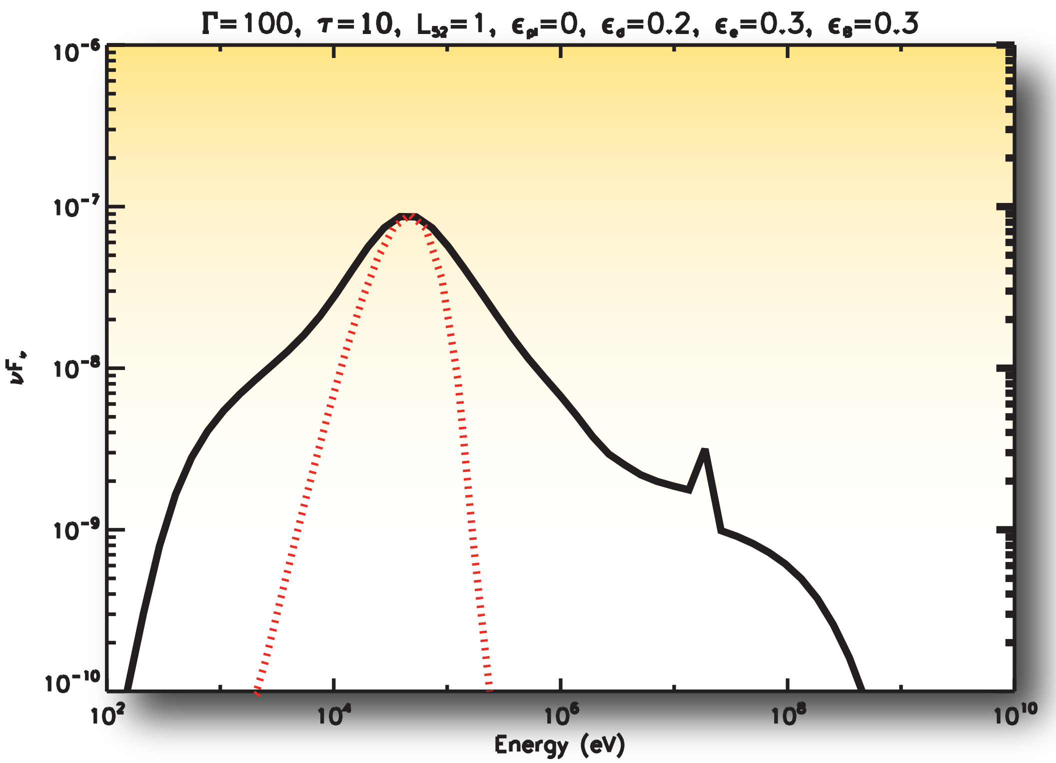

Emission from the photosphere is NOT seen as Planck !

Modification of Planck spectrum

Geometrical broadening: 'photosphere' is NOT a single radius, but is 3-dimensional

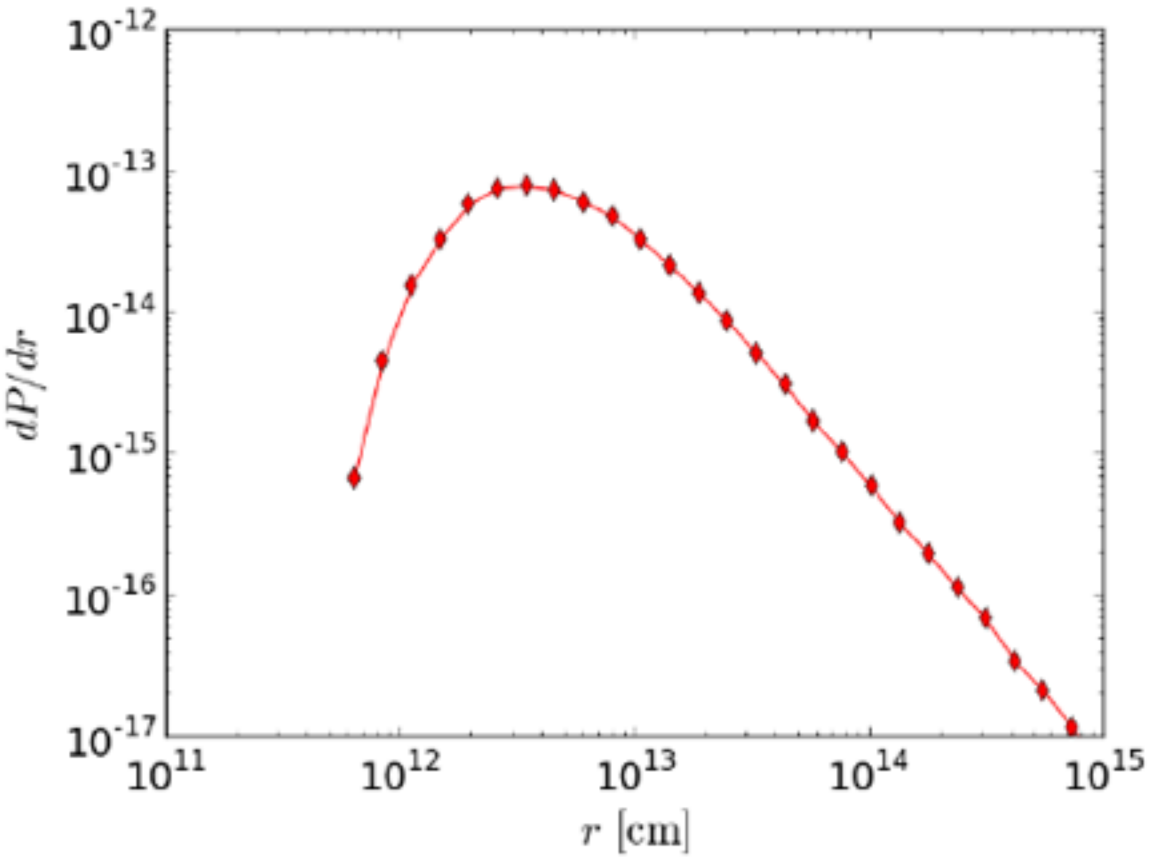

Lundman, Peer, Ryde 2012

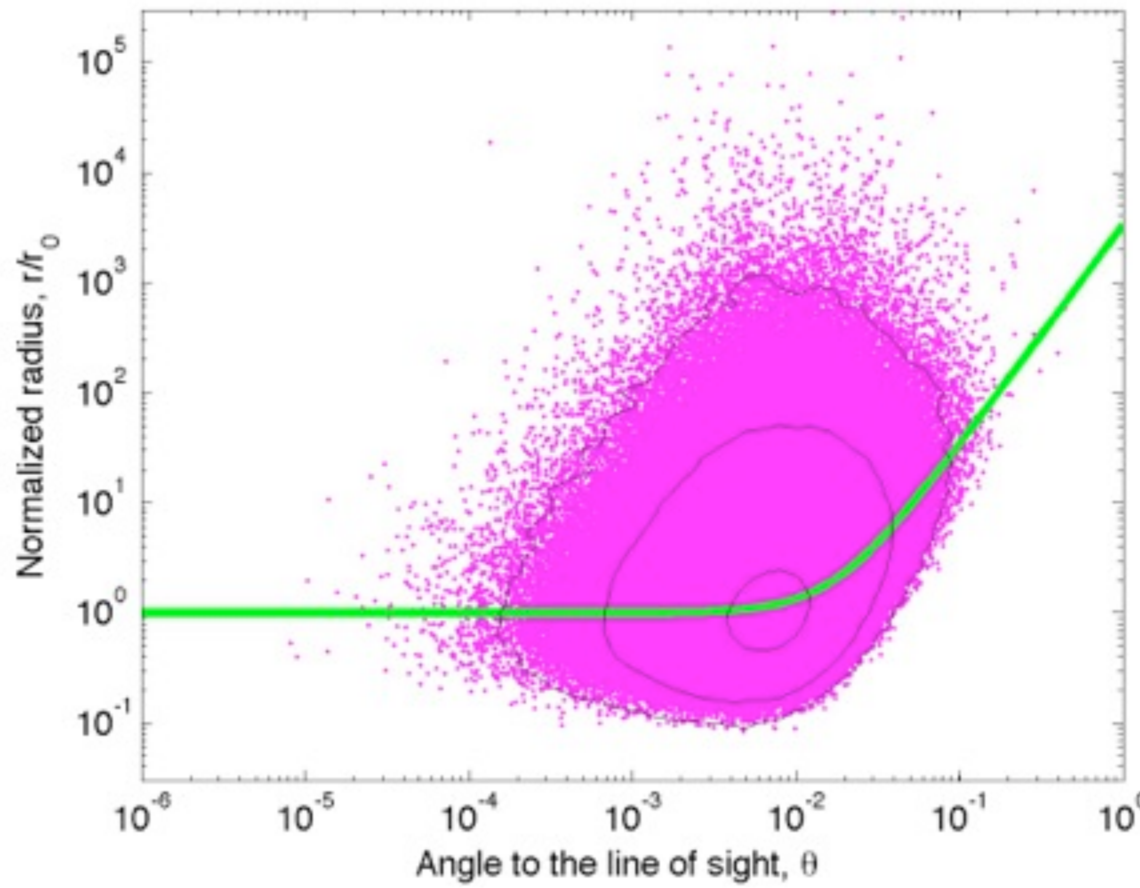

Pe'er 2008; Pe'er & Ryde 2011

'Limb darkening' in relativistically expanding plasma;
Emission from the photosphere is NOT seen as Planck !

Observed spectral width & Evolution

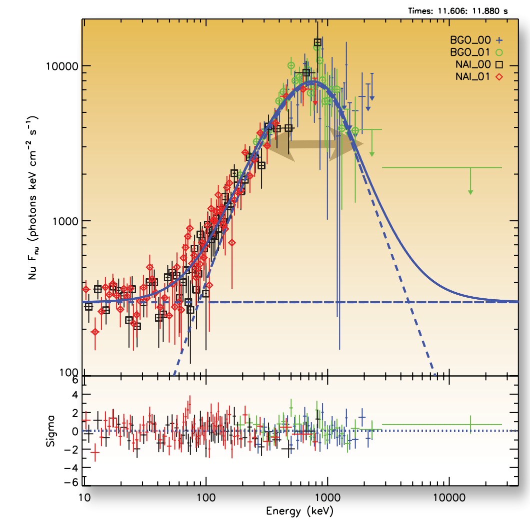

FWHM as ratio Ehigh/Elow,

GRB110920

5 ← 12

GRB090902B

6 → 20

~3. ~7 ~70 ~100

Planck High latitude Synchrotron Inverse Compton

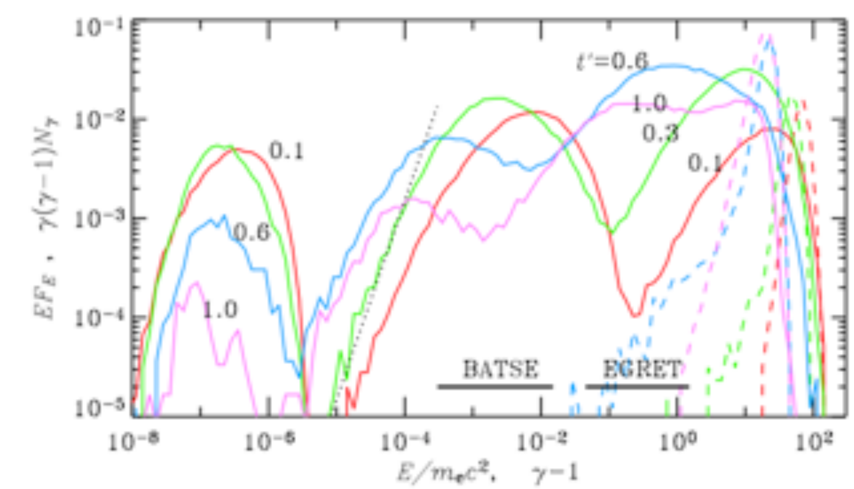

Observed spectral width & Evolution

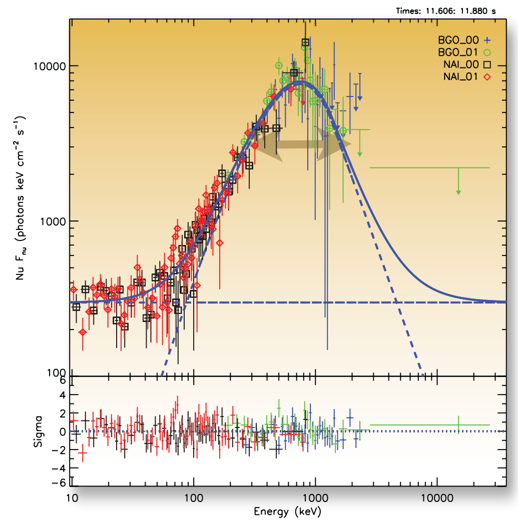

FWHM as ratio E_{high}/E_{low},

GRB110920

5 12

GRB090902B

6 20

~3. ~7 ~70 ~100

Planck High latitude Synchrotron Inverse Compton

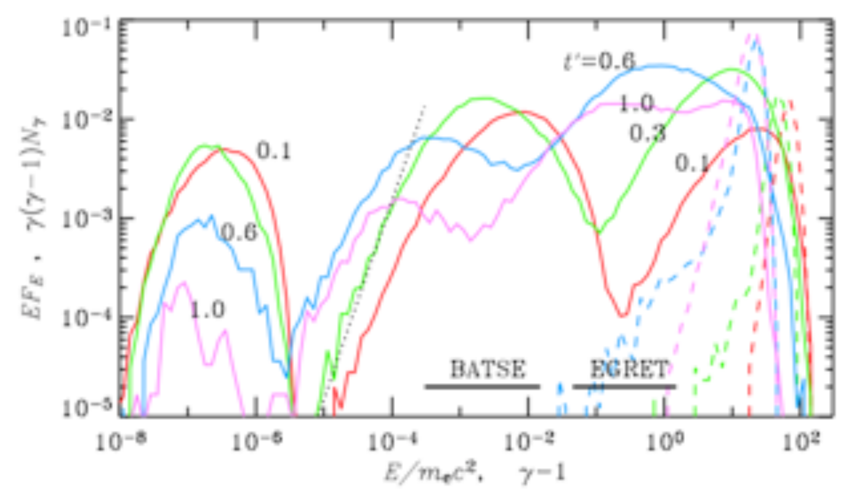

Poutanen & Stern 2004

Observed spectral width & Evolution

FWHM as ratio Ehigh/Elow,

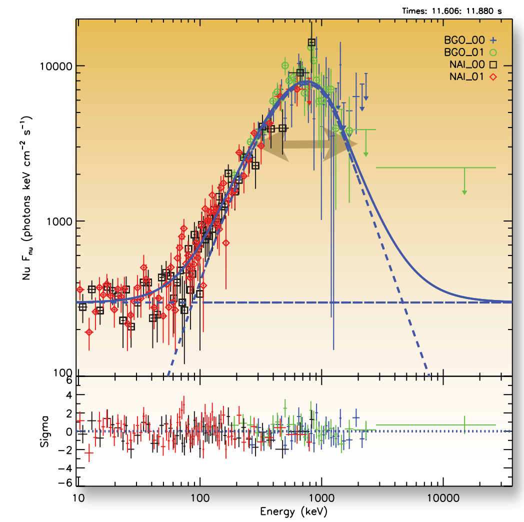

GRB110920

5 ← 12

GRB090902B

6 → 20

~3. ~7 ~70 ~100

Planck

High latitude

Synchrotron

Inverse Compton

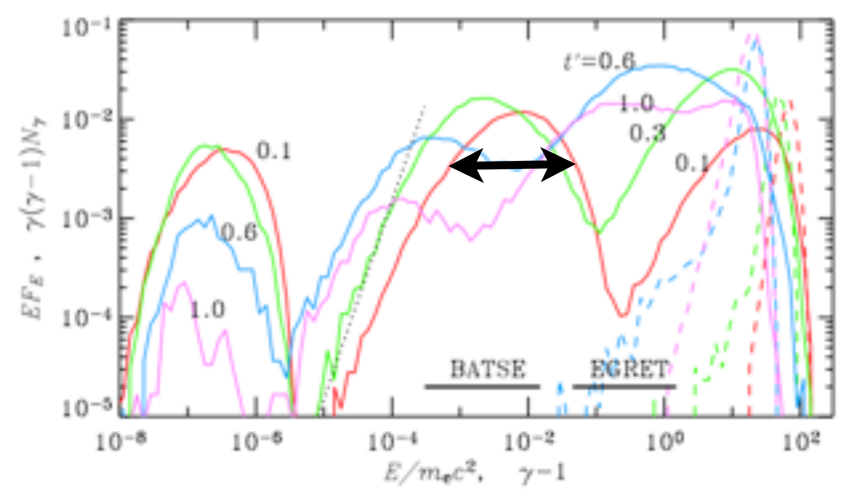

Poutanen & Stern 2004

Observed spectral width & Evolution

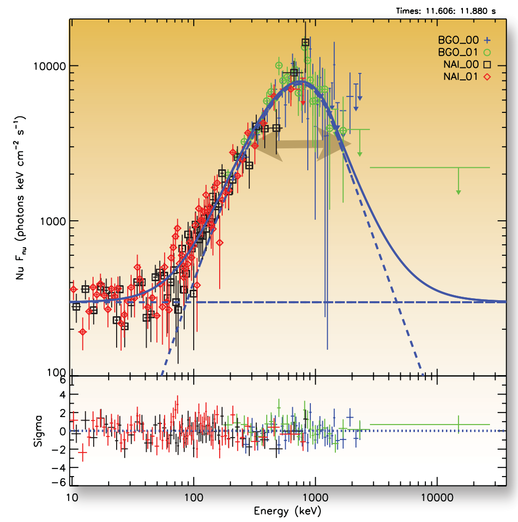

FWHM as ratio Ehigh/Elow,

GRB110920

5 ← 12

GRB090902B

6 → 20

~3. ~7 ~70 ~100

Planck

High latitude

Synchrotron

Inverse Compton

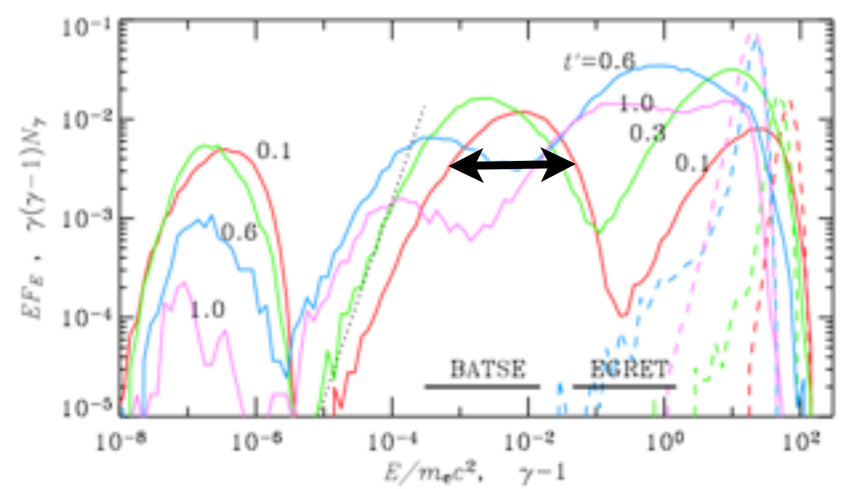

Poutanen & Stern 2004

Subphotospheric dissipation
Rees+, Peer+, Beloborodov+
Geometrical broadening
Peer+, Lundman+, Ito+

Observed spectral width & Evolution

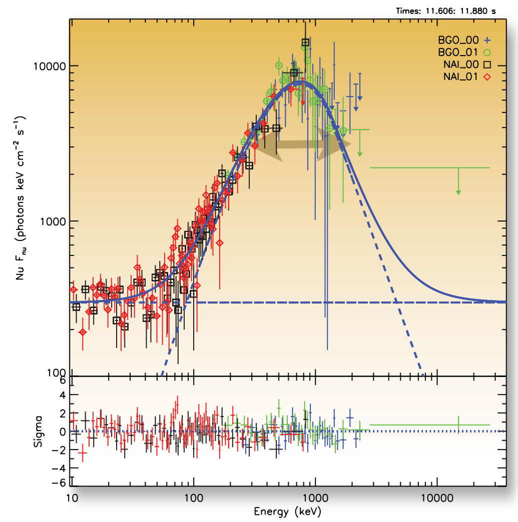

FWHM as ratio E_{high}/E_{low},

GRB110920

5 ← 12

GRB090902B

6 → 20

~3. ~7 ~70 ~100

Planck | High latitude | Synchrotron | Inverse Compton

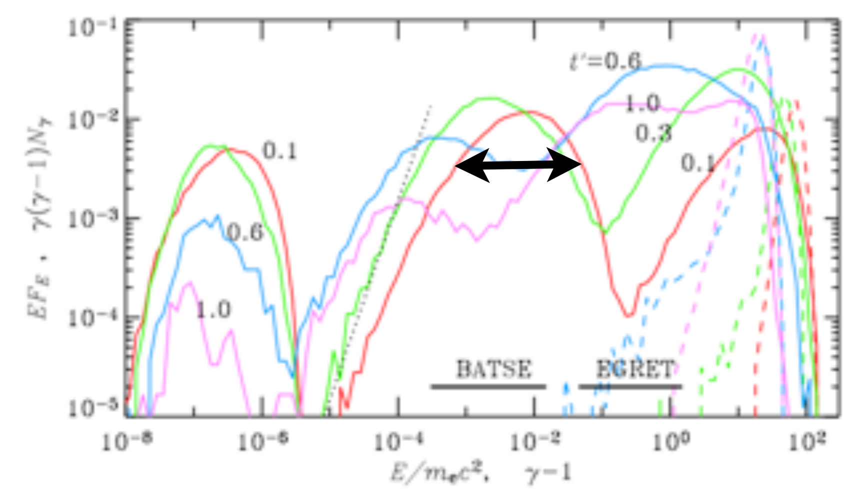

Poutanen & Stern 2004

Subphotospheric dissipation
Rees+, Peer+, Beloborodov+
Geometrical broadening
Peer+, Lundman+, Ito+

IC in the Klein Nishina regime
Decaying B field
Thermalisation

Observed spectral width & Evolution

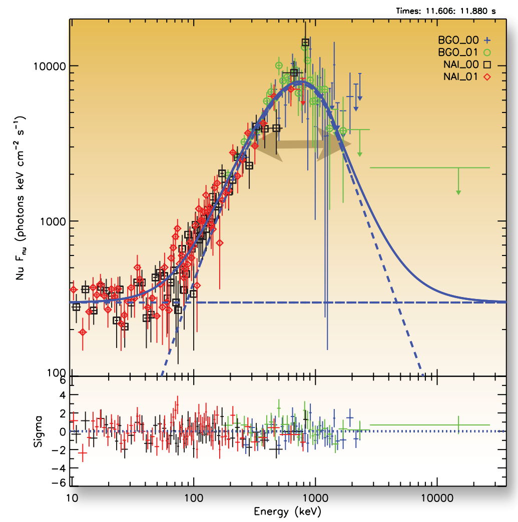

FWHM as ratio E_{high}/E_{low},

GRB110920

5 ← 12

GRB090902B

6 → 20

~3. ~7 ~70 ~100

Planck

High latitude

Synchrotron

Inverse Compton

Subphotospheric dissipation
Rees+, Peer+, Beloborodov+
Geometrical broadening
Peer+, Lundman+, Ito+

IC in the Klein Nishina regime
Decaying B field
Thermalisation

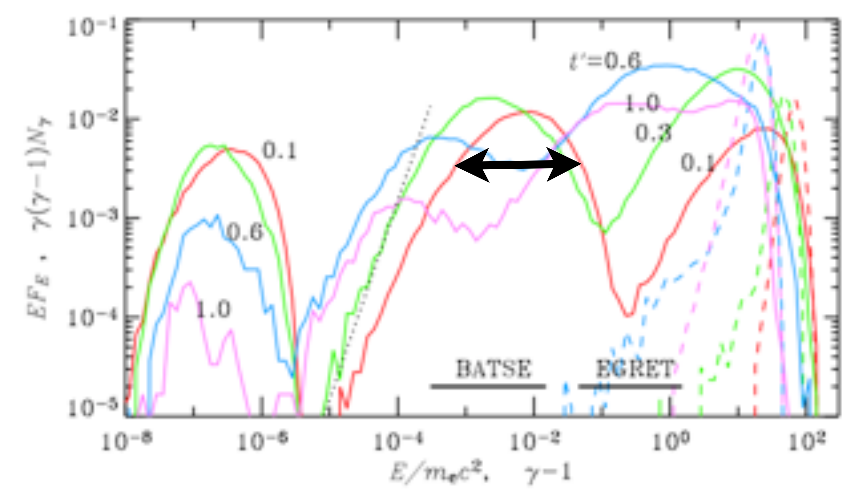

Poutanen & Stern 2004

Observed spectral width & Evolution

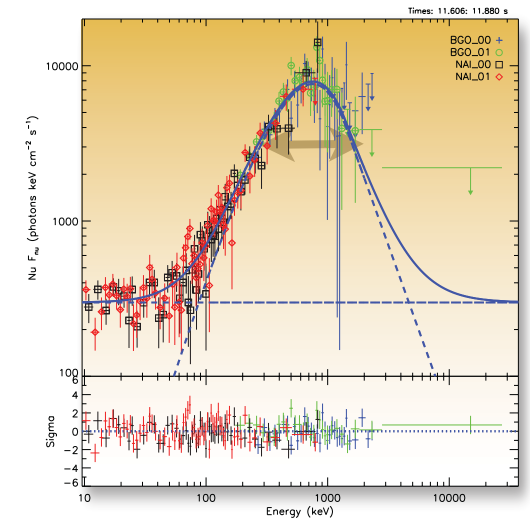

FWHM as ratio Ehigh/Elow,

GRB110920

5 ← 12

GRB090902B

6 → 20

~3. ~7 ~70 ~100

Planck High latitude Synchrotron Inverse Compton

Subphotospheric dissipation
Rees+, Peer+, Beloborodov+
Geometrical broadening
Peer+, Lundman+, Ito+

Incomplete thermalisation
Geometrical broadening

IC in the Klein Nishina regime
Decaying B field
Thermalisation

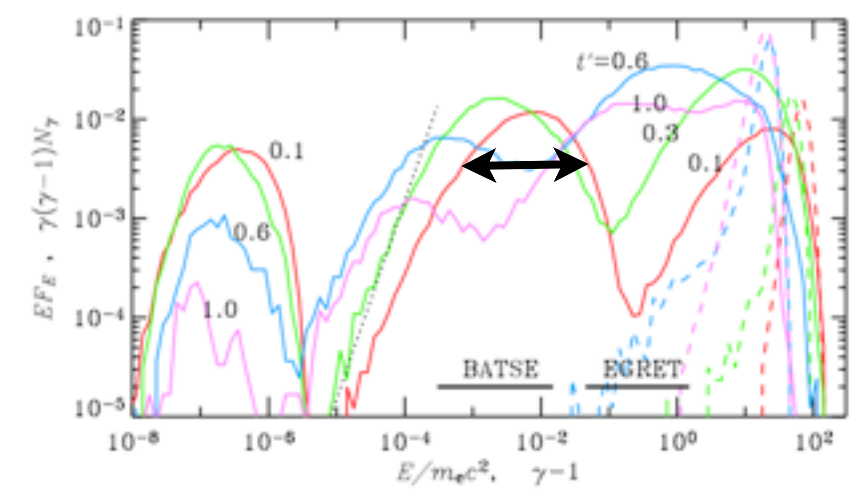

Poutanen & Stern 2004

Observed spectral width & Evolution

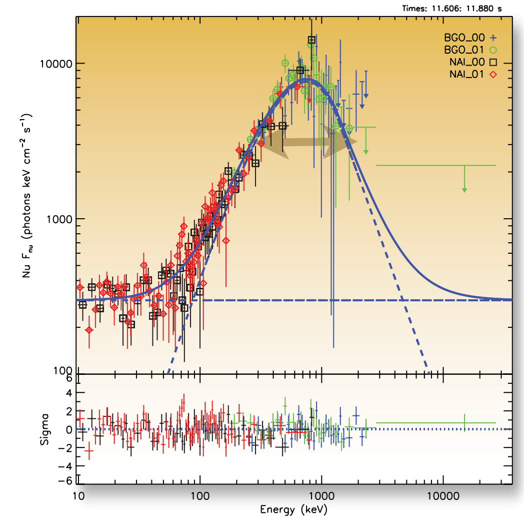

FWHM as ratio Ehigh/Elow,

GRB110920

5 ← 12

GRB090902B

6 → 20

~3. ~7 ~70 ~100

Planck High latitude Synchrotron Inverse Compton

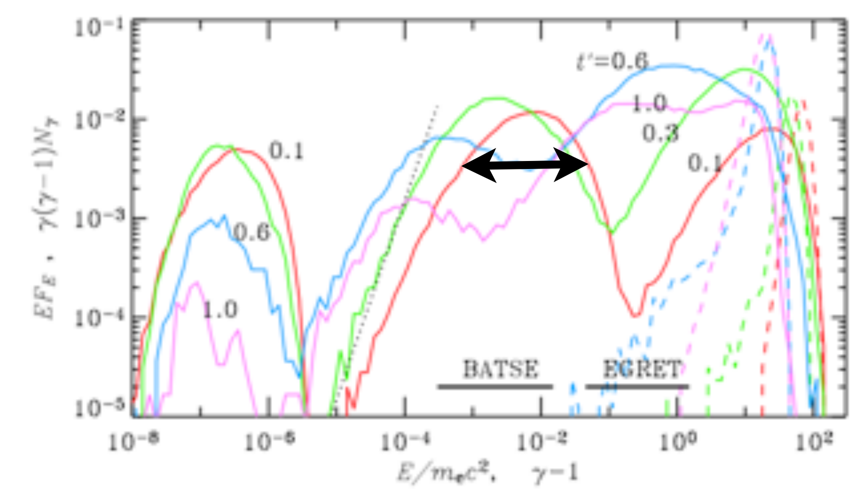

IC in the Klein Nishina regime
Decaying B field
Thermalisation

Poutanen & Stern 2004

Subphotospheric dissipation
Rees+, Peer+, Beloborodov+
Geometrical broadening
Peer+, Lundman+, Ito+

Incomplete thermalisation
Geometrical broadening

The narrowness of GRB spectra are equally as important as the hard α values

Modelling of GRB090902B with subphpotospheric dissipation

Ryde+10

- Our code (by Pe'er & Waxman 2004) solves the kinetic equations for internal shocks
- Includes cyclo/synchrotron emission, SSA, Compton scattering (direct/inverse), pair production, pair annihilation

Dissipation at optical depth τ = 10

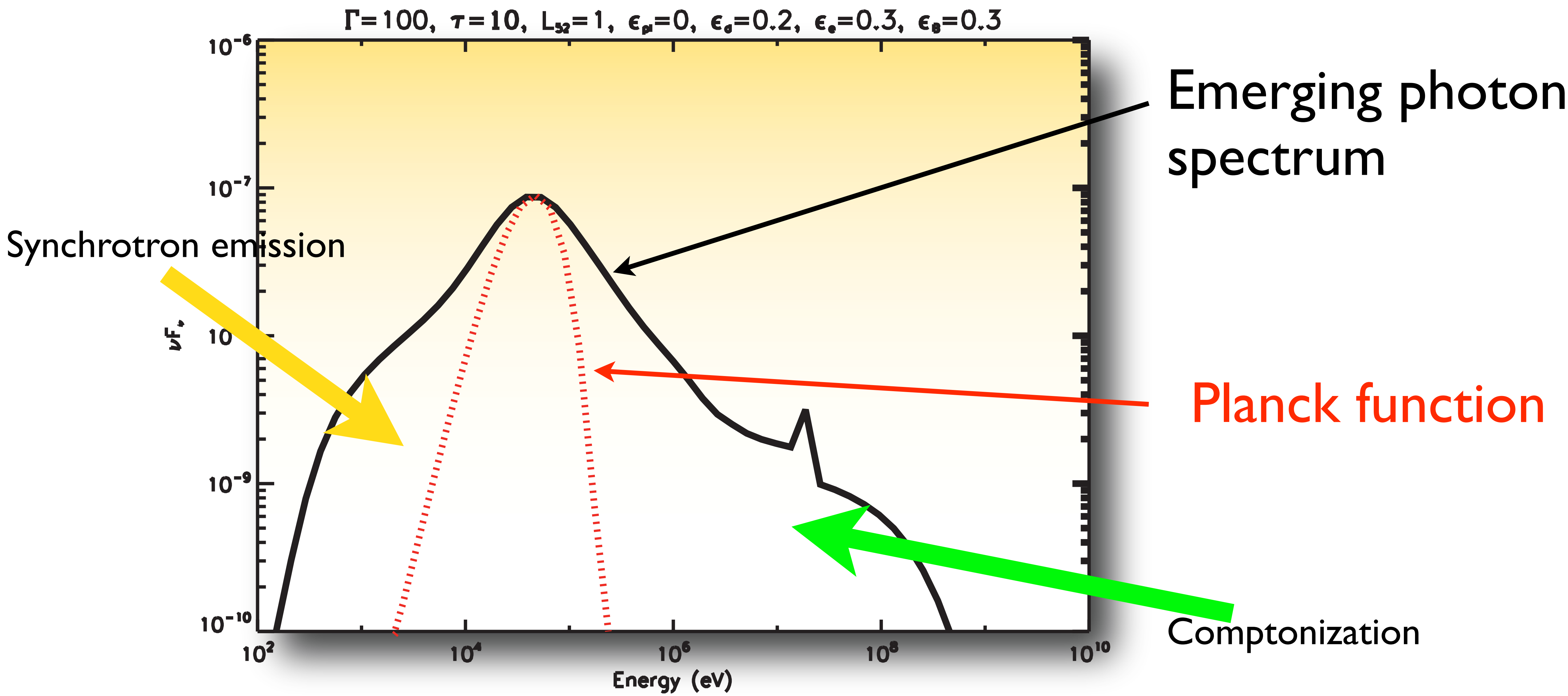

Another interesting example: GRB110920A

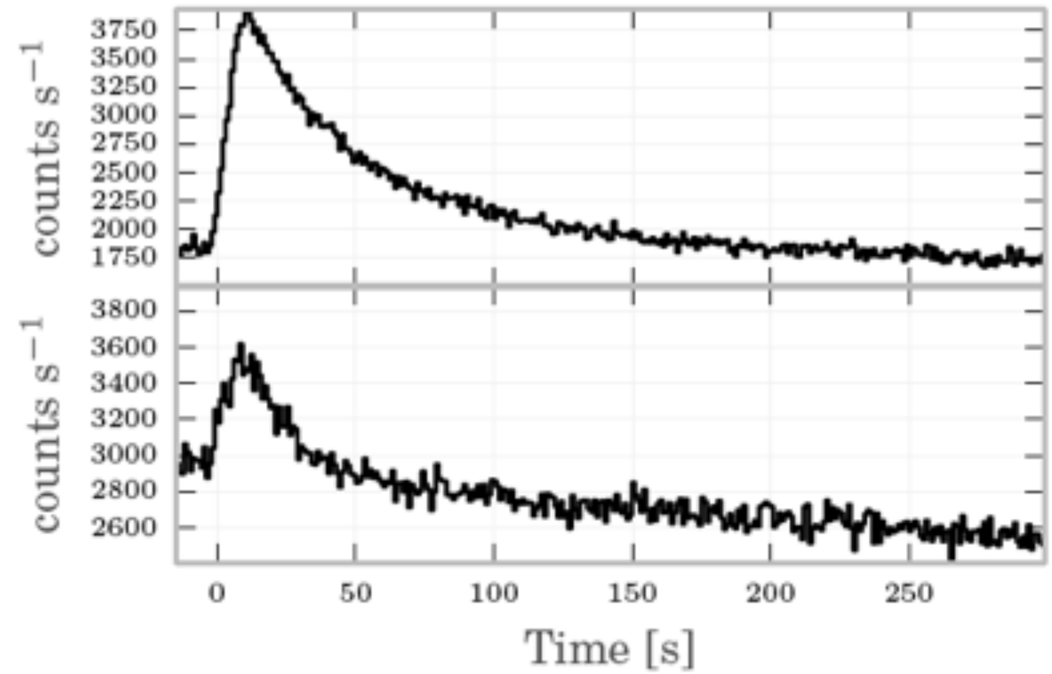

Iyyani & Ryde (in prep.)

Band function fits

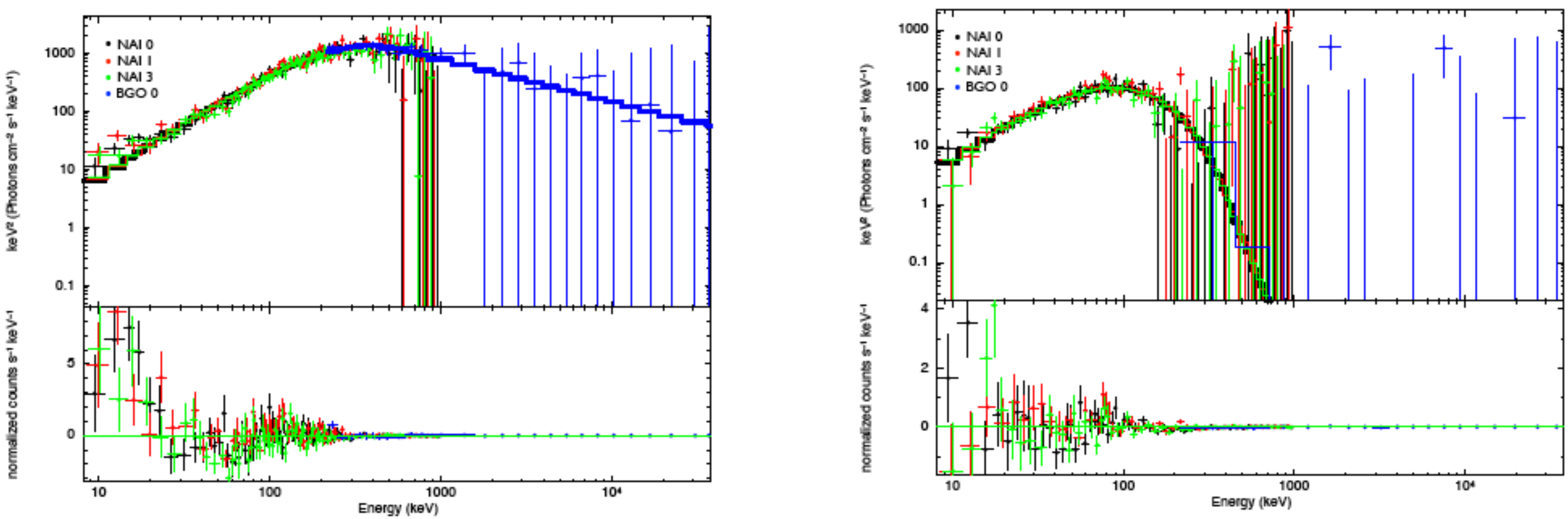

(a) (b)

Band function fits

Spectral Width

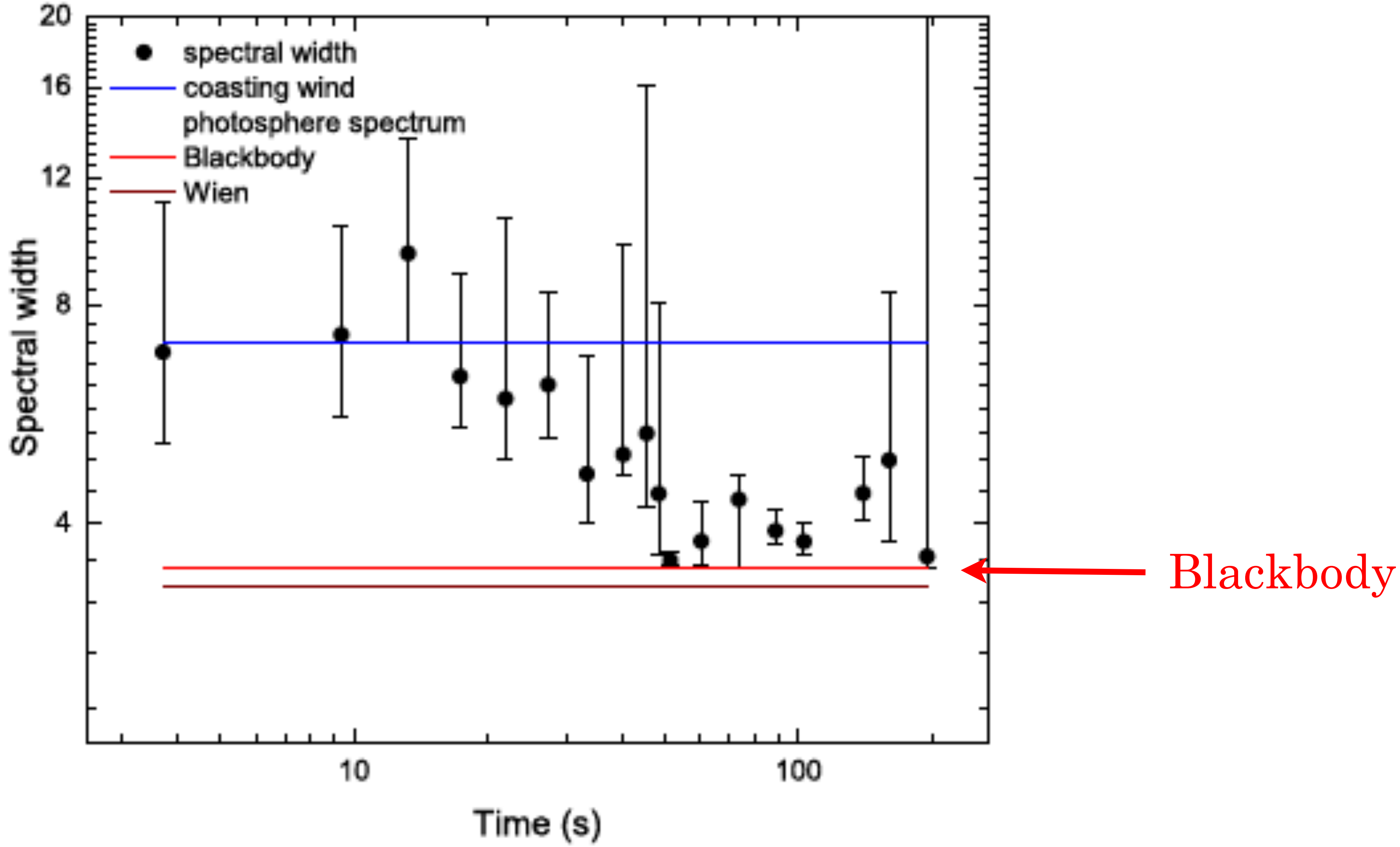

Another interesting example: GRB110920A

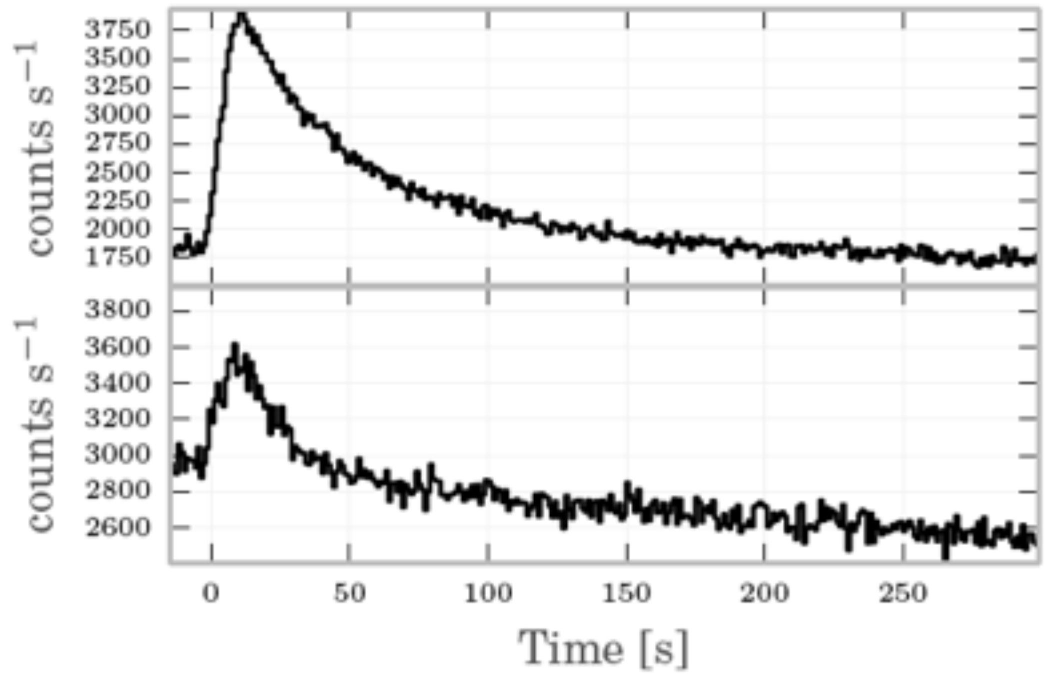

Iyyani & Ryde (in prep.)

Band function fits

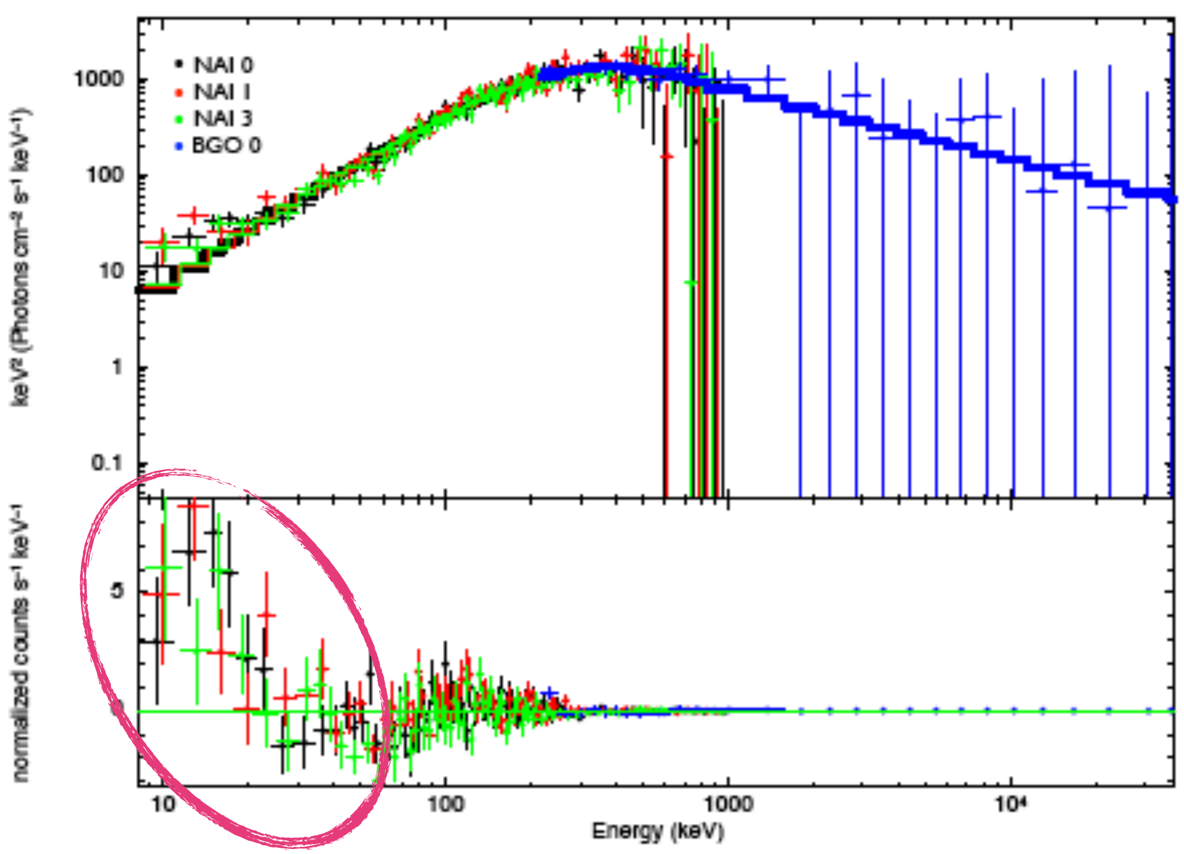

(a)

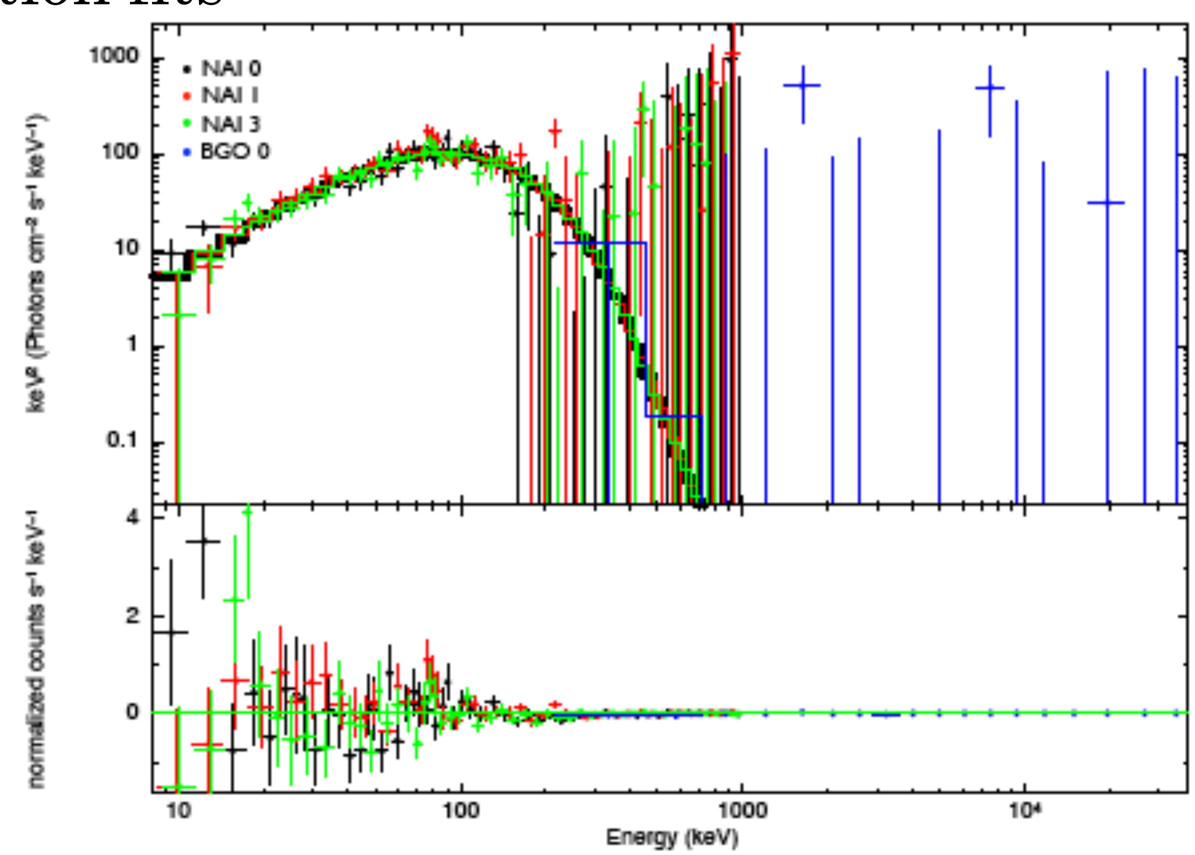

(b)

GRB110920

Two component fit

Band + BB

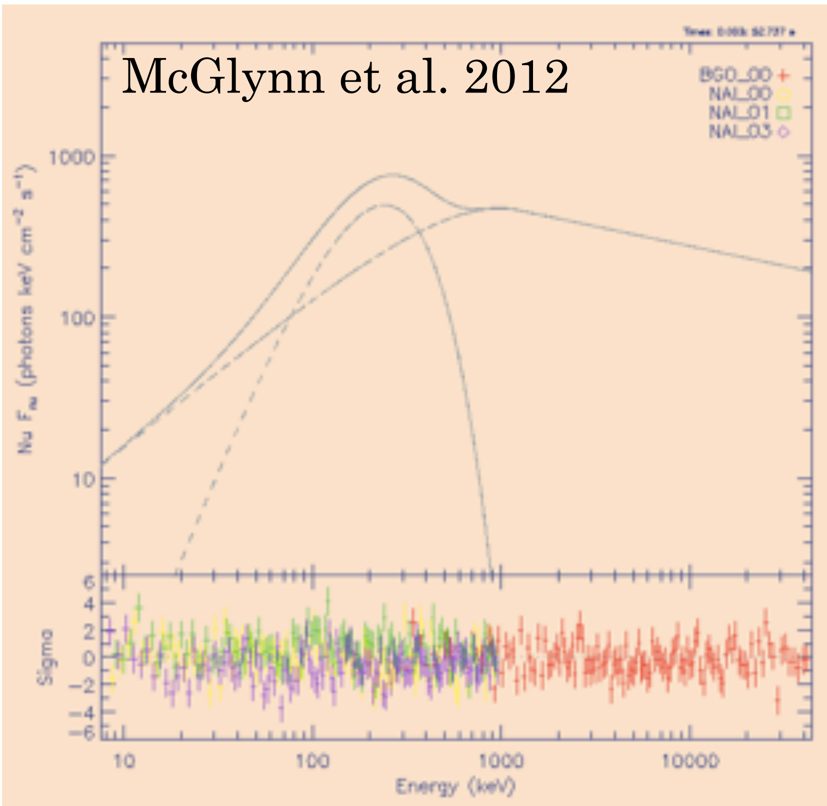

Synchrotron + BB

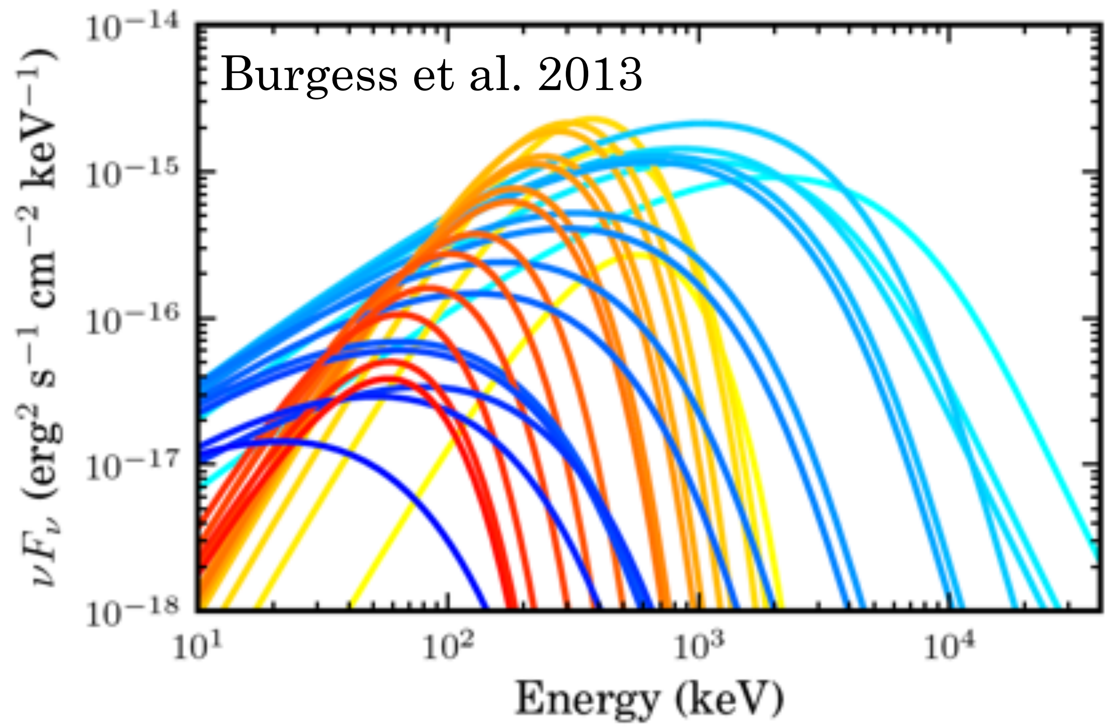

GRB110920

Two component fit

Band + BB

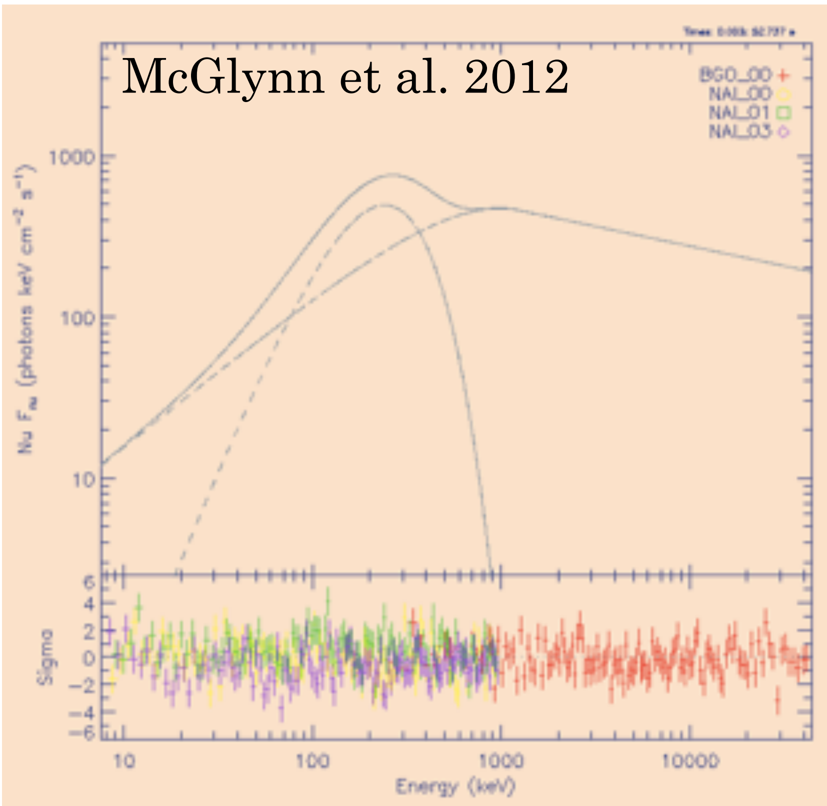

Synchrotron + BB

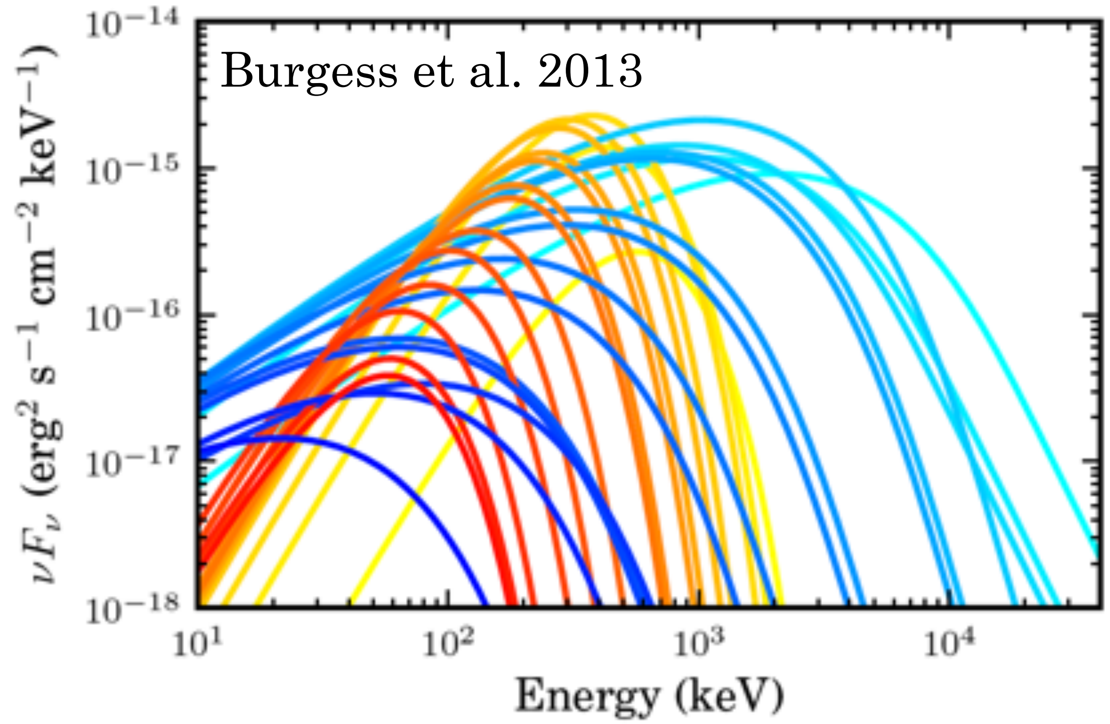

Single component fit

<u>Best fit:</u> Thermal Comptonization from a localised dissipation at τ~10 occurring close to the saturation radius

Iyyani & Ryde (in prep.)

GRB110920

Two component fit

Band + BB

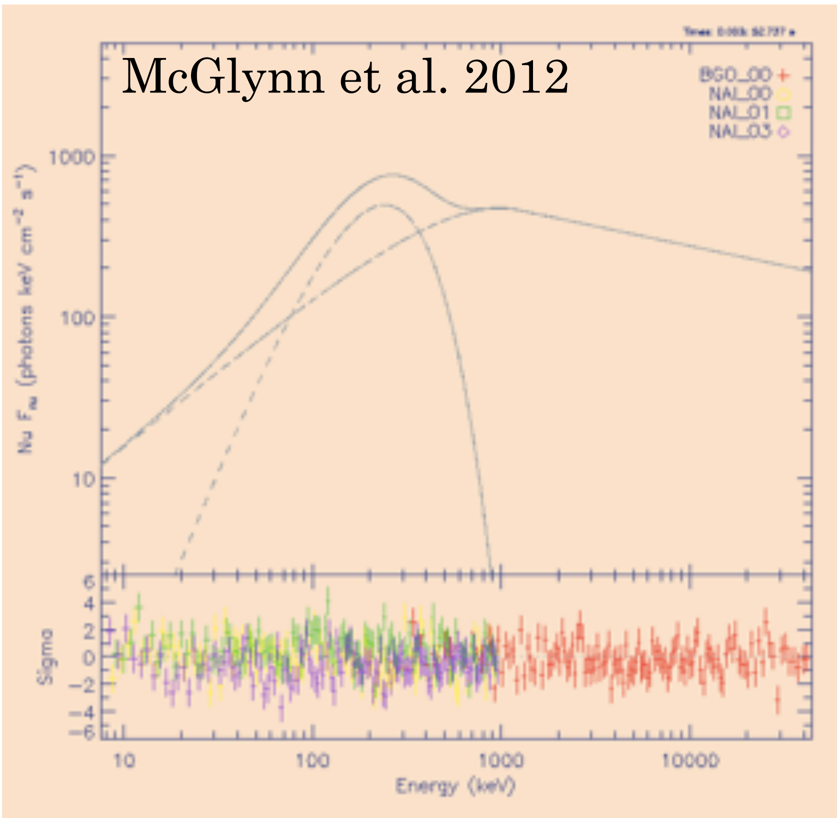

Synchrotron + BB

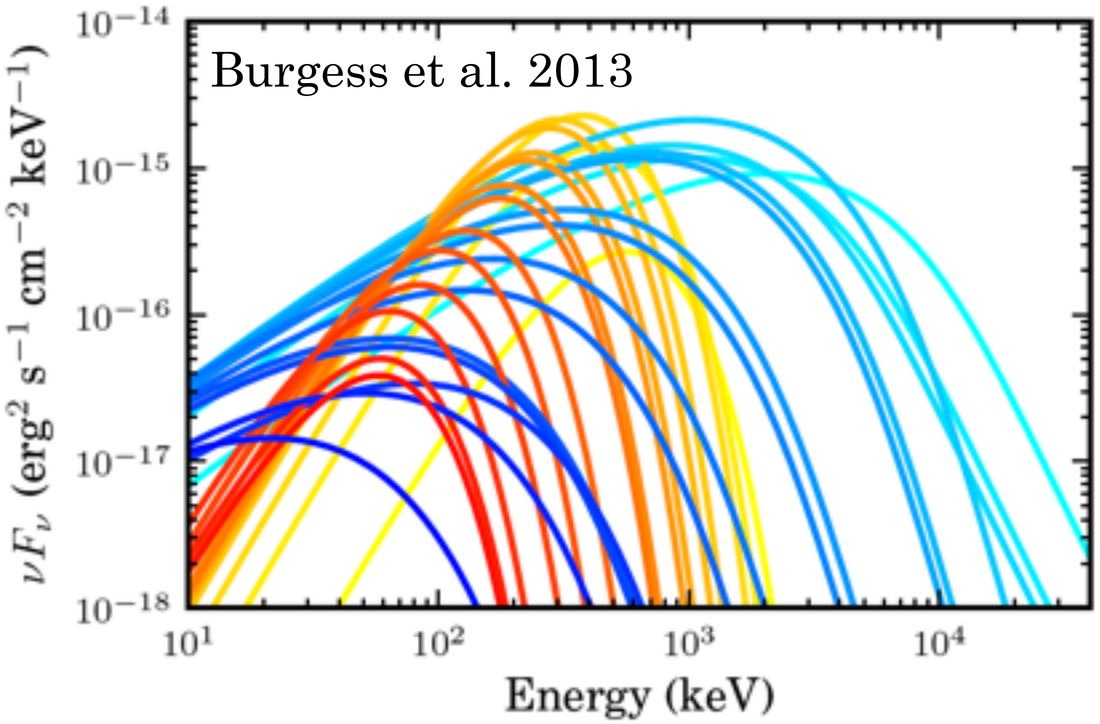

Single component fit

<u>Best fit:</u> Thermal Comptonization from a localised dissipation at τ~10 occurring close to the saturation radius

Iyyani & Ryde (in prep.)

Favours pure photospheric emission - including dissipation

GRB110920

2 zone emission

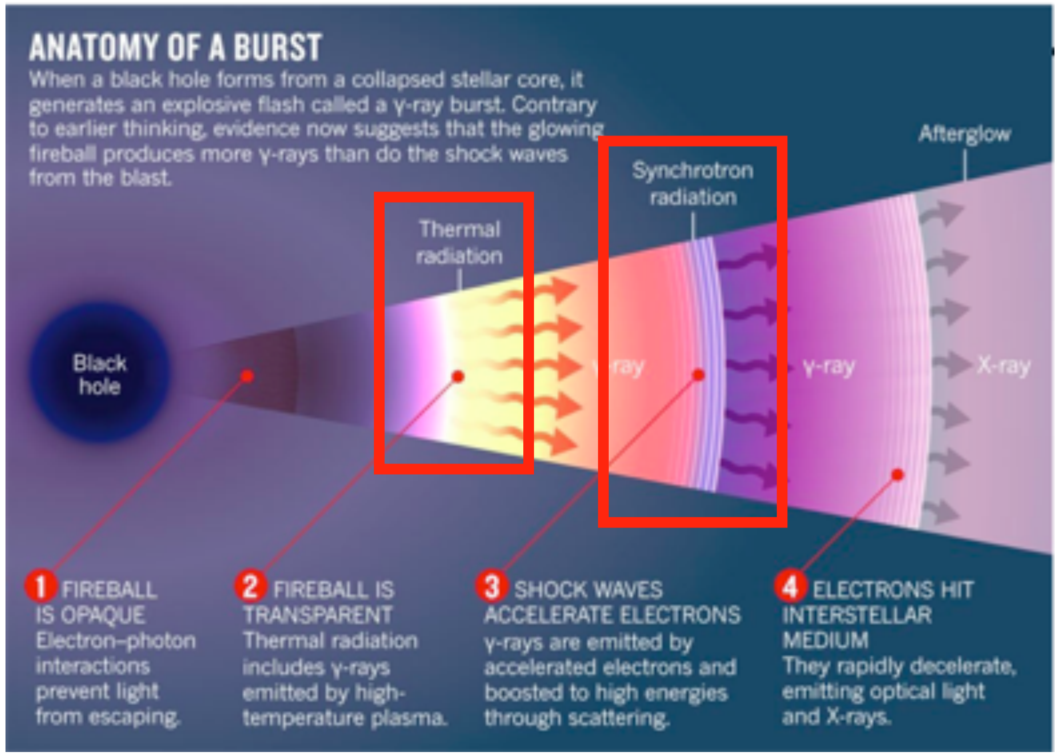

Photosphere

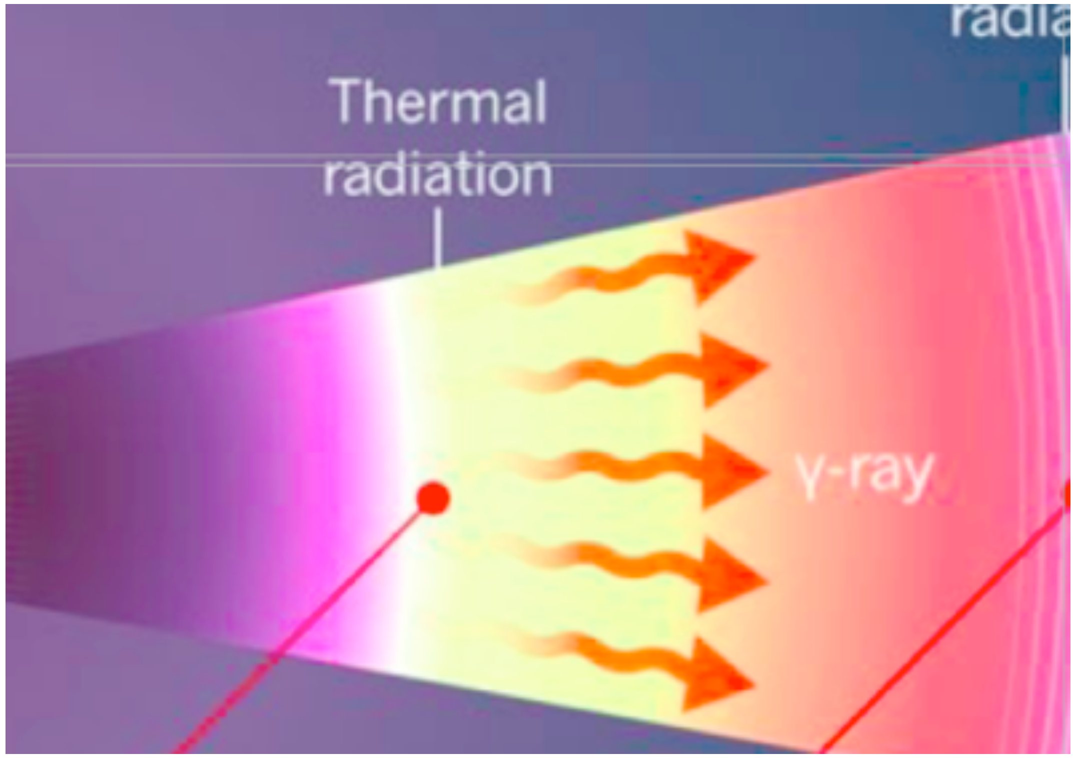

GRB110920

2 zone emission

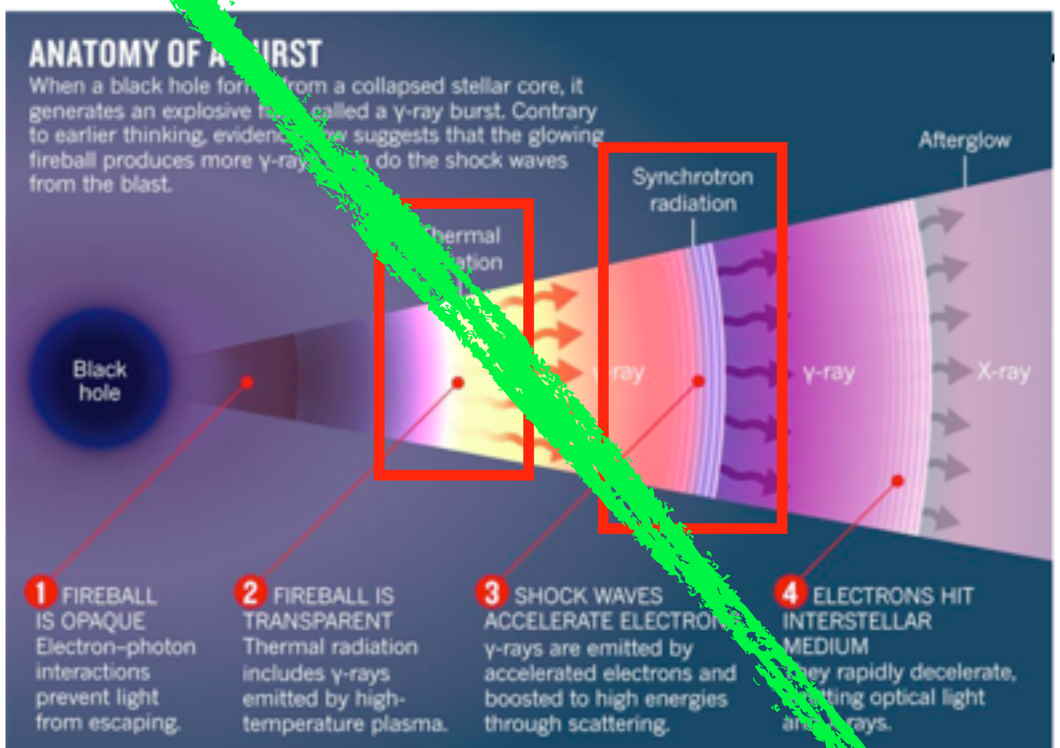

Photosphere

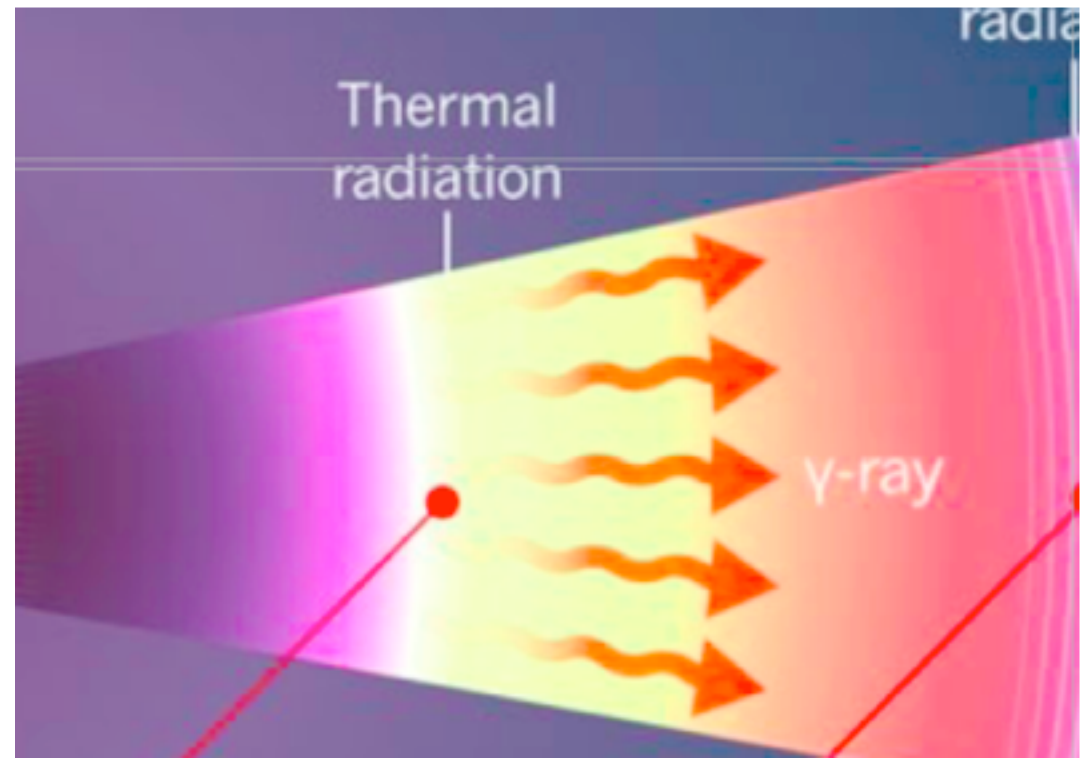

GRB110920

2 zone emission

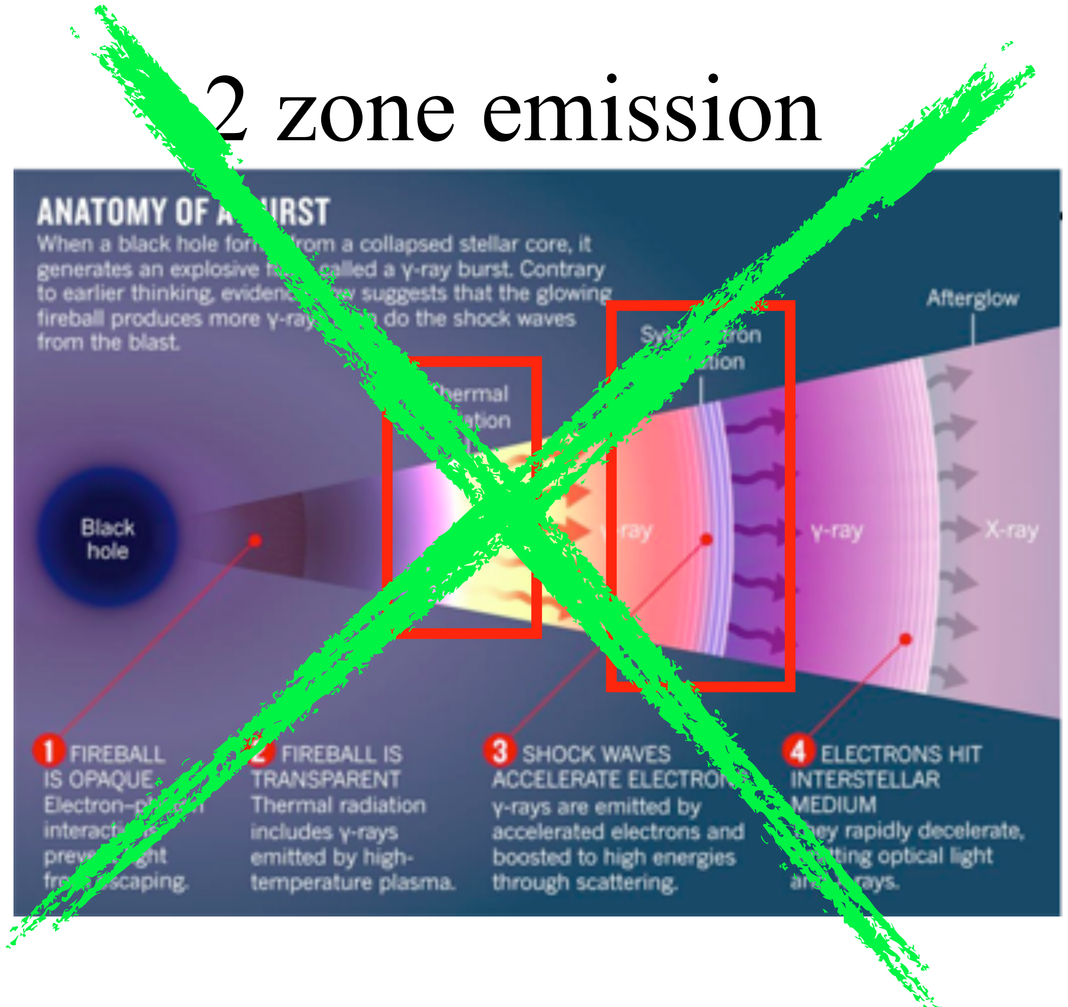

Photosphere

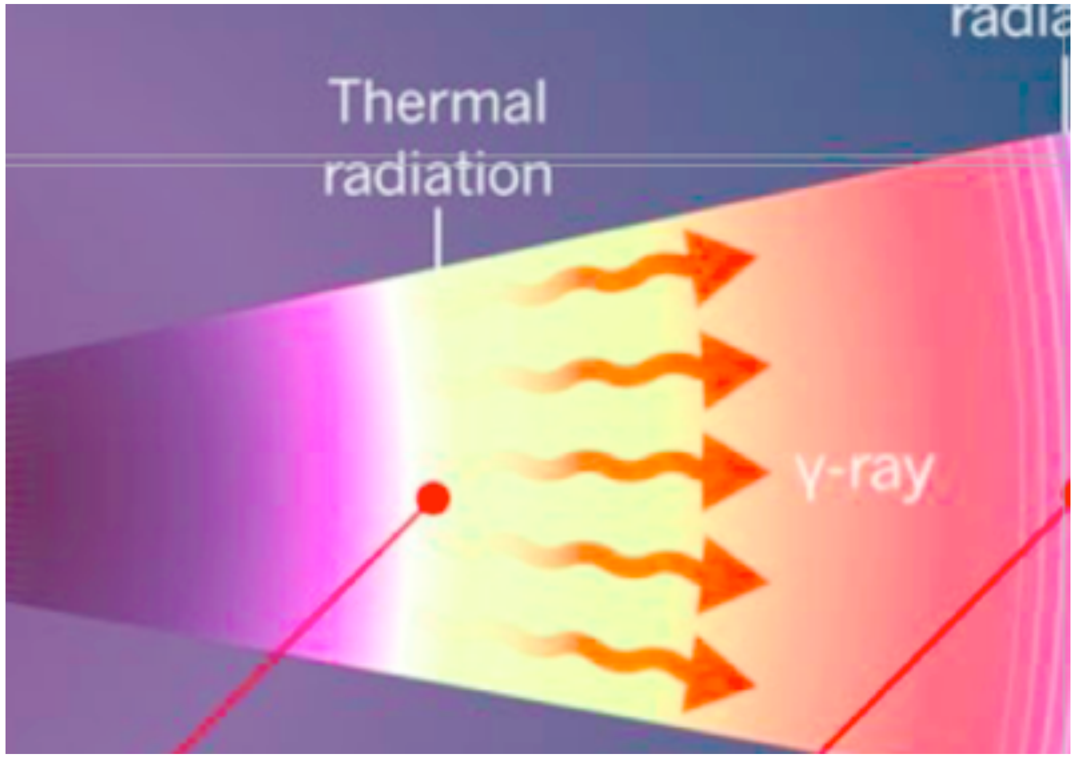

GRB110920

2 zone emission

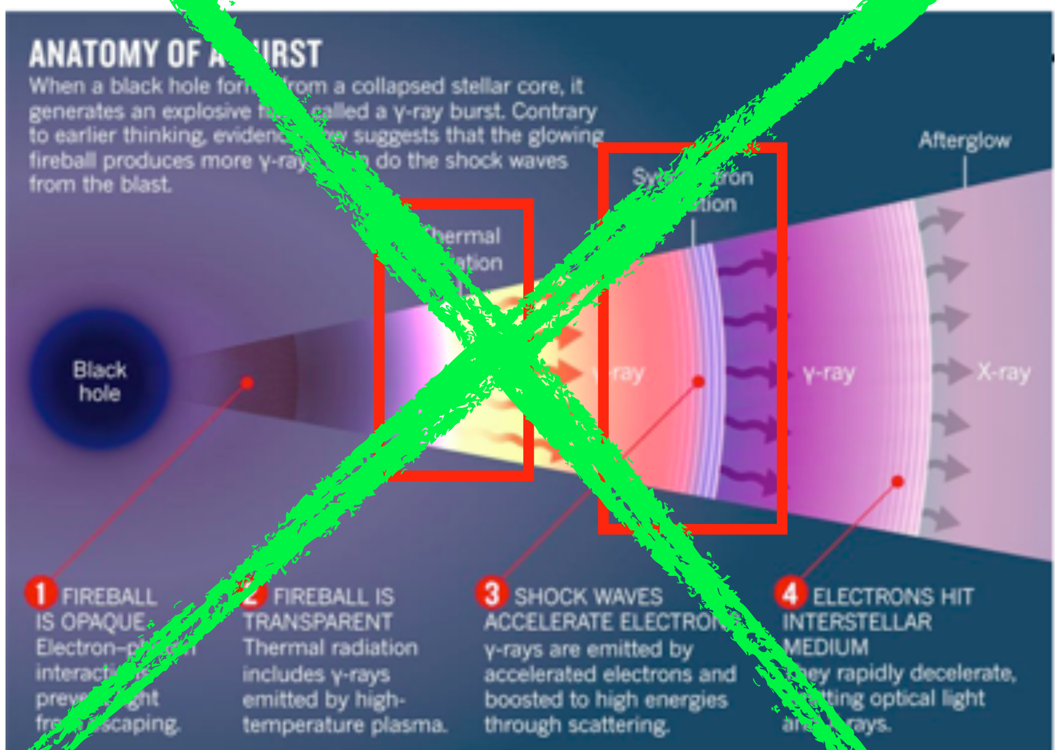

Photosphere

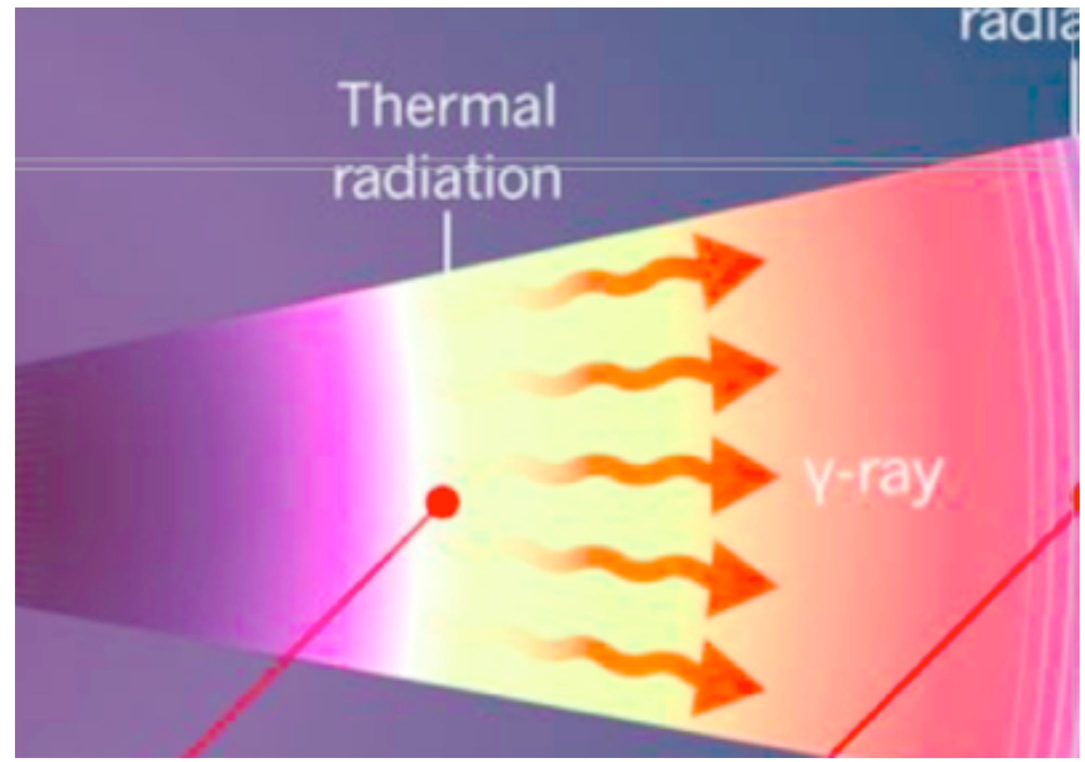

Depending on the dissipation many spectral shapes can be produced including double breaks and pure Band functions

Observable to discriminate between interpretations: *Polarisation*

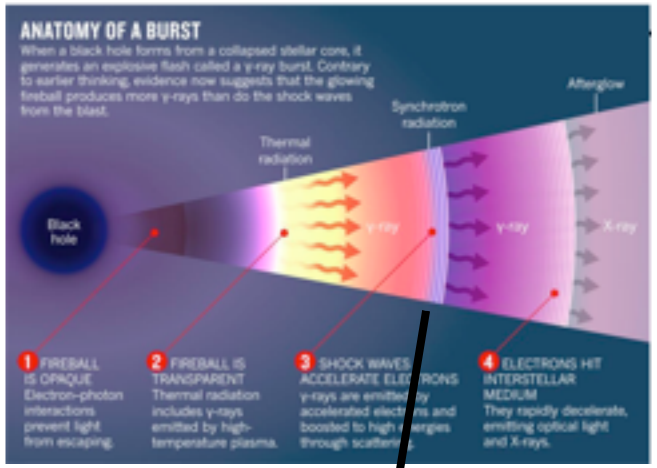

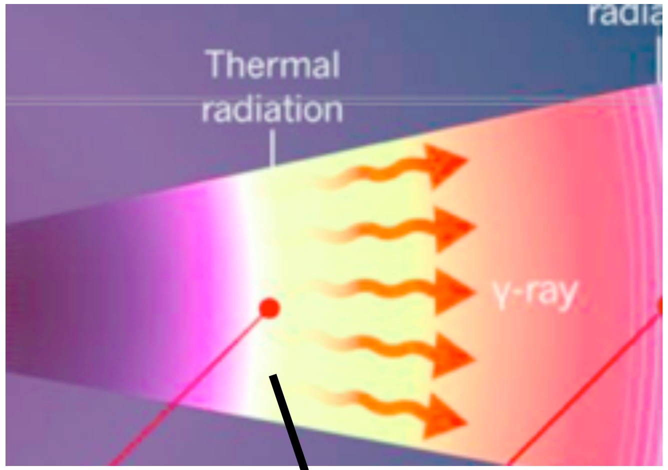

Synchrotron emission
easily polarised

Observable to discriminate between interpretations: *Polarisation*

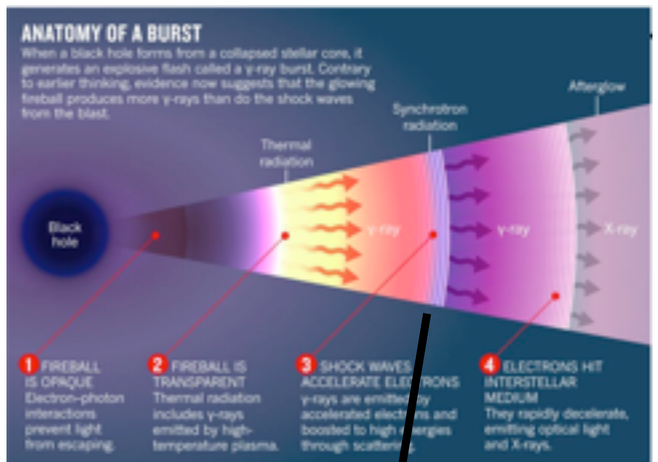

Synchrotron emission easily polarised

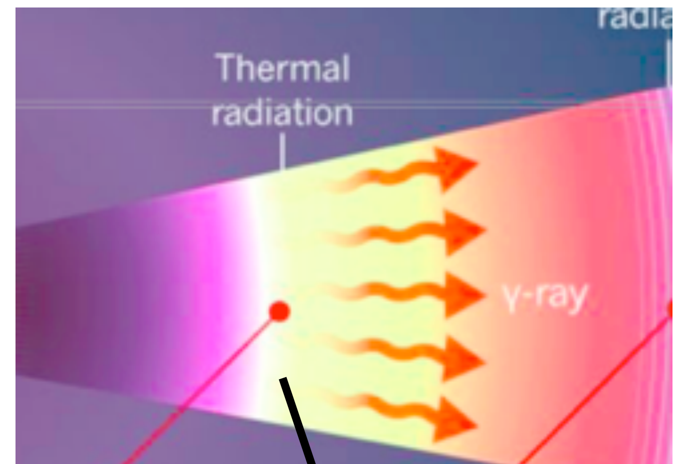

Is the photosphere polarised?

Observable to discriminate between interpretations: *Polarisation*

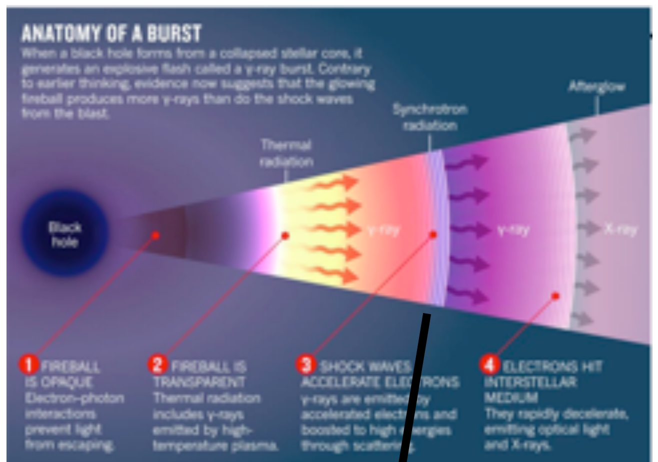

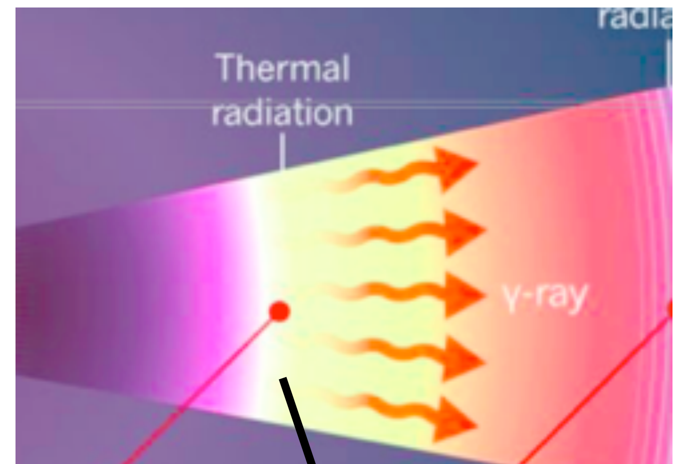

Synchrotron emission
easily polarised

Is the photosphere polarised?

Observable to discriminate between interpretations: *Polarisation*

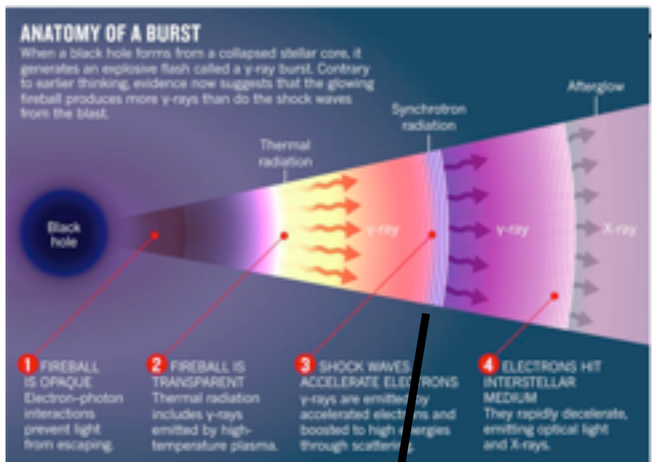

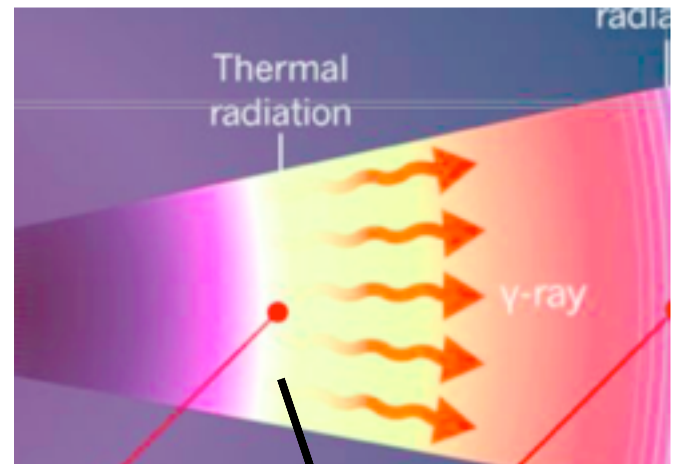

Synchrotron emission easily polarised

Is the photosphere polarised?

- Opacity dominated by scattering
- Photon field in the local comoving frame is anisotriopic
- Symmetry must be broken

Observable to discriminate between interpretations: *Polarisation*

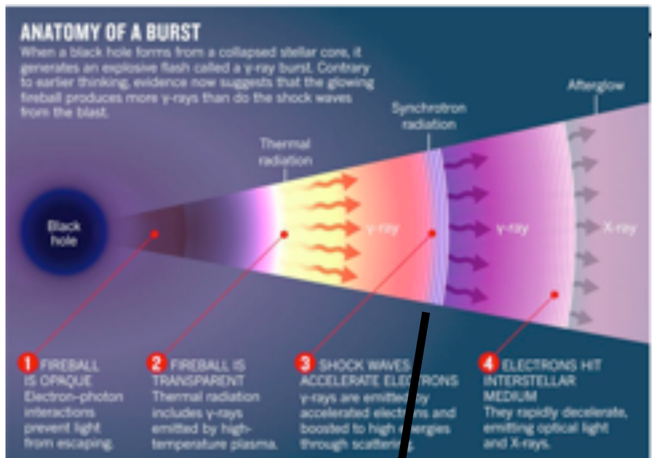

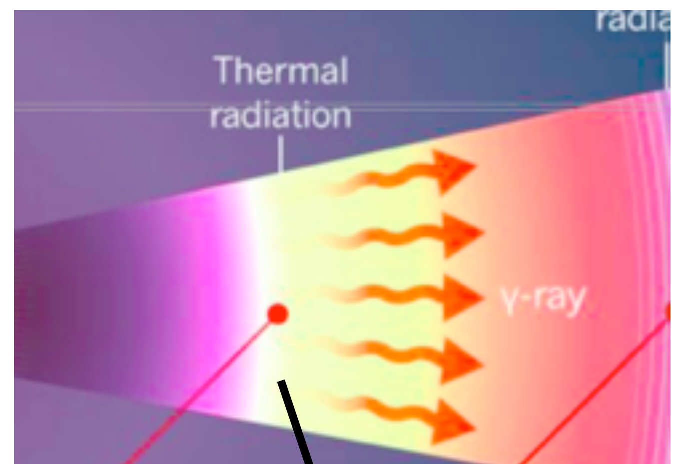

Synchrotron emission easily polarised

Is the photosphere polarised?

- Opacity dominated by scattering
- Photon field in the local comoving frame is anisotriopic
- Symmetry must be broken

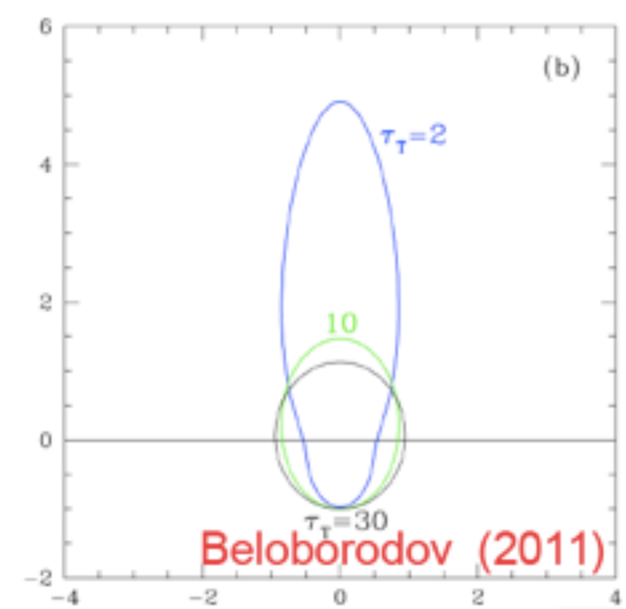

Natural way to break symmetry: Jet structure

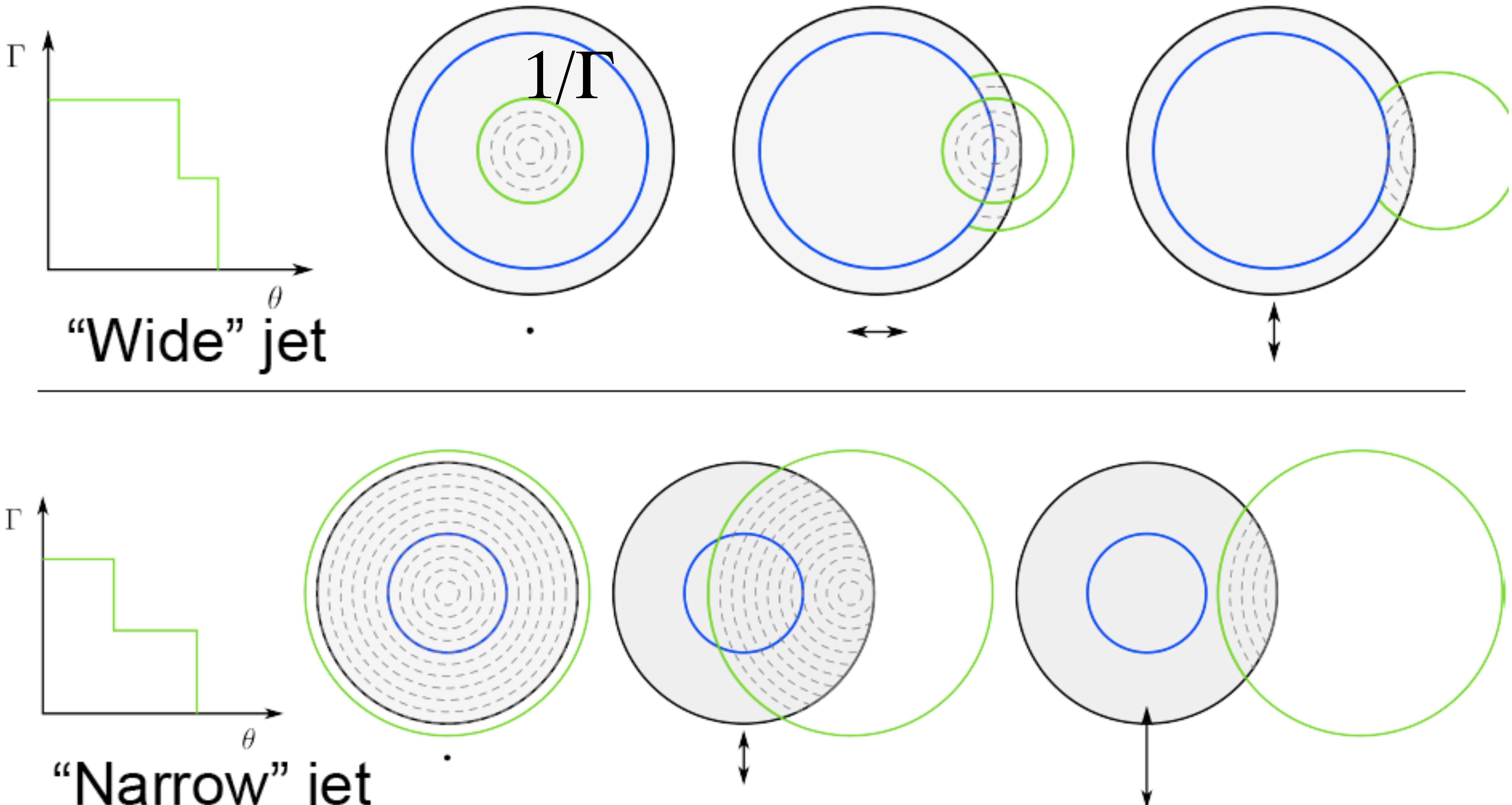

Lundman, Pe'er, & Ryde 2014

Natural way to break symmetry: Jet structure

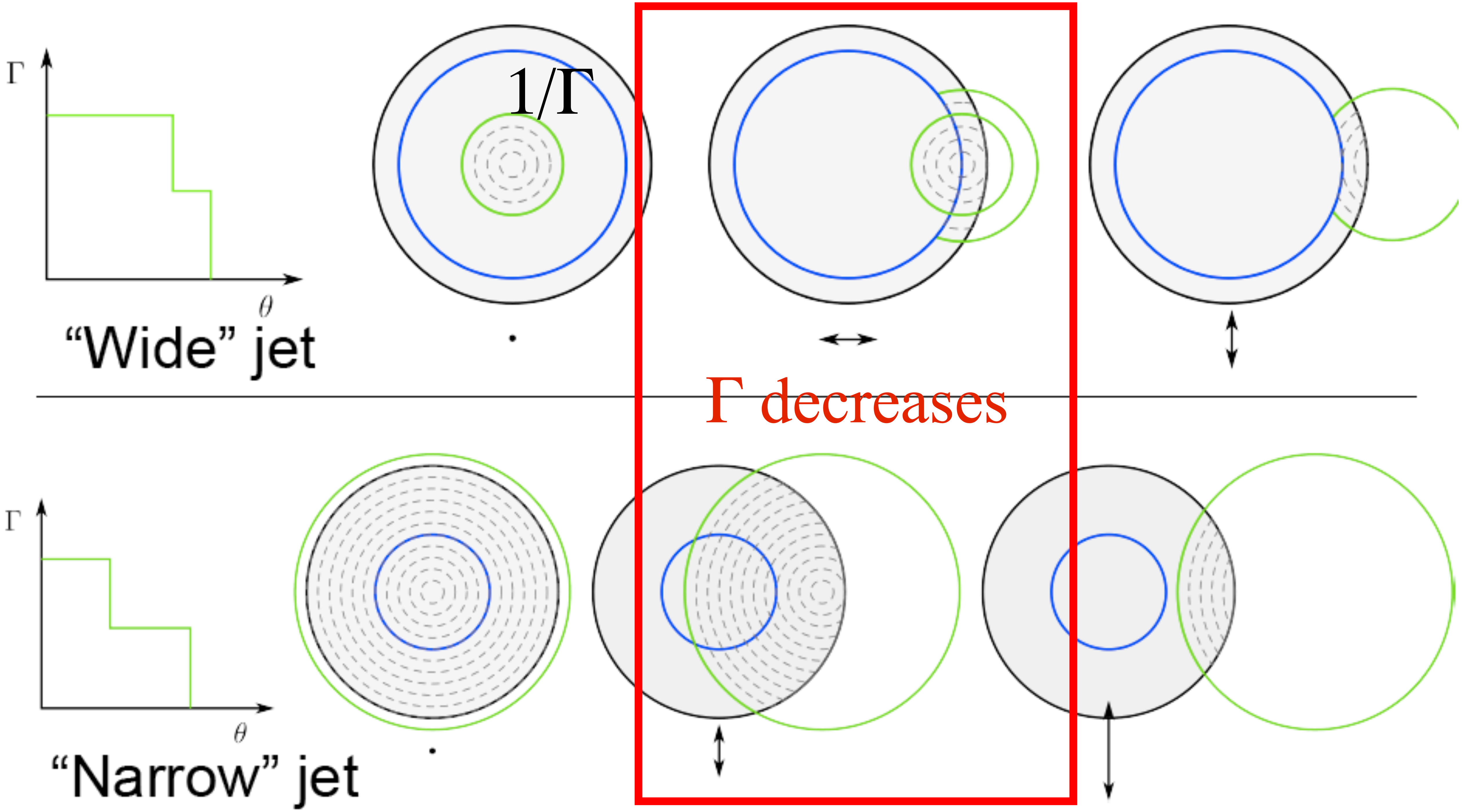

Lundman, Pe'er, & Ryde 2014

Solving the polarised radiative transfer
Lundman, Pe'er & Ryde 2014

Narrow jet results: Breaking the symmetry of the emitting region

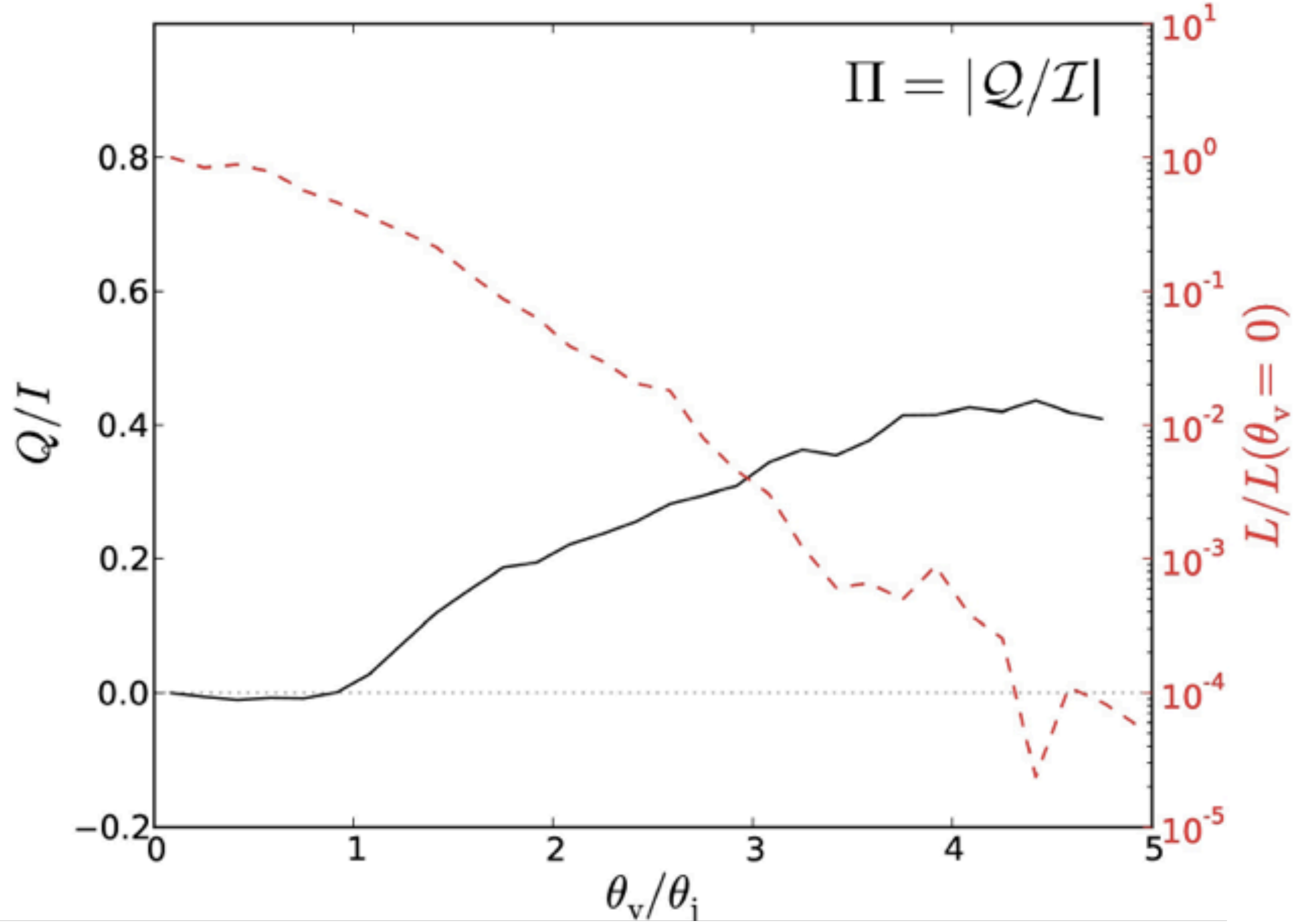

Wide jet results: Breaking the symmetry of the emitting region

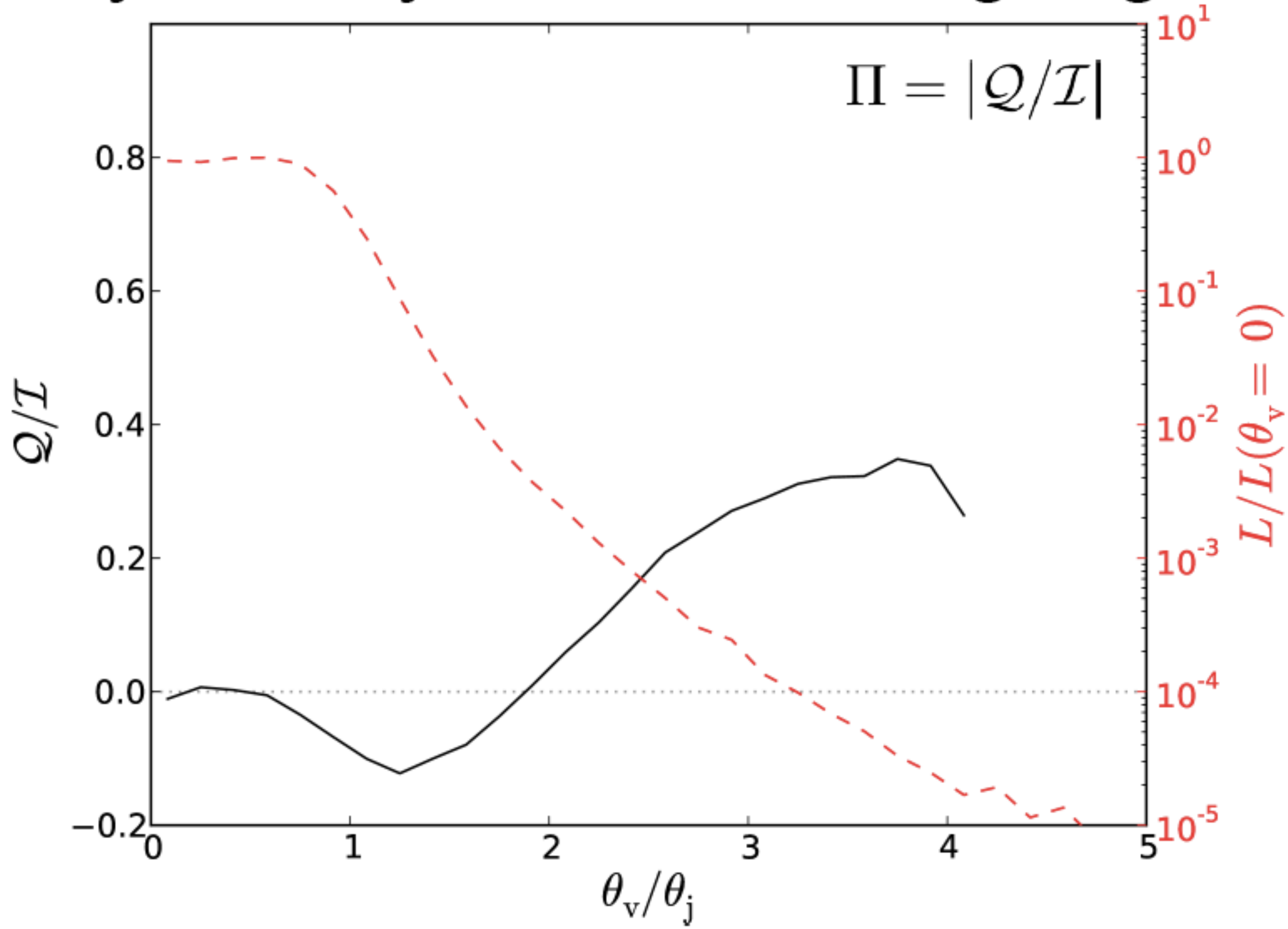

Polarisation from the photosphere

- Polarized emission in range **0-40% expected** (depending on viewing angle and jet structure)
- **Only** a change in pol. angle of **90º** is possible (due to jet axisymmetry)
- If jet is wide, most obs. see low polarization (few percent)
- Correlations expected between spectrum and polarization

Lundman, Pe'er, & Ryde 2014

Comparison with interesting GAP observations

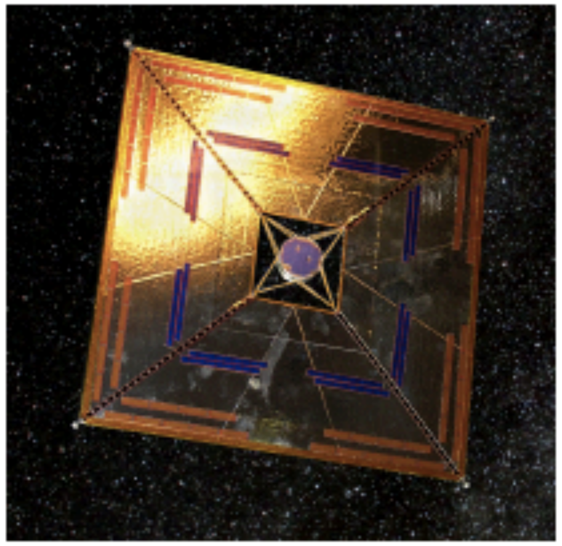

GAP observations of GRB100826A

- Polarization of prompt emission measured in two separate time bins
- First bin: $\Pi = 25\% \pm 15\%$
  $\phi = 159^\circ \pm 18^\circ$
- Second bin: $\Pi = 31\% \pm 21\%$
  $\phi = 75^\circ \pm 20^\circ$
- Consistent with a shift of $\Delta\phi \approx 90^\circ$

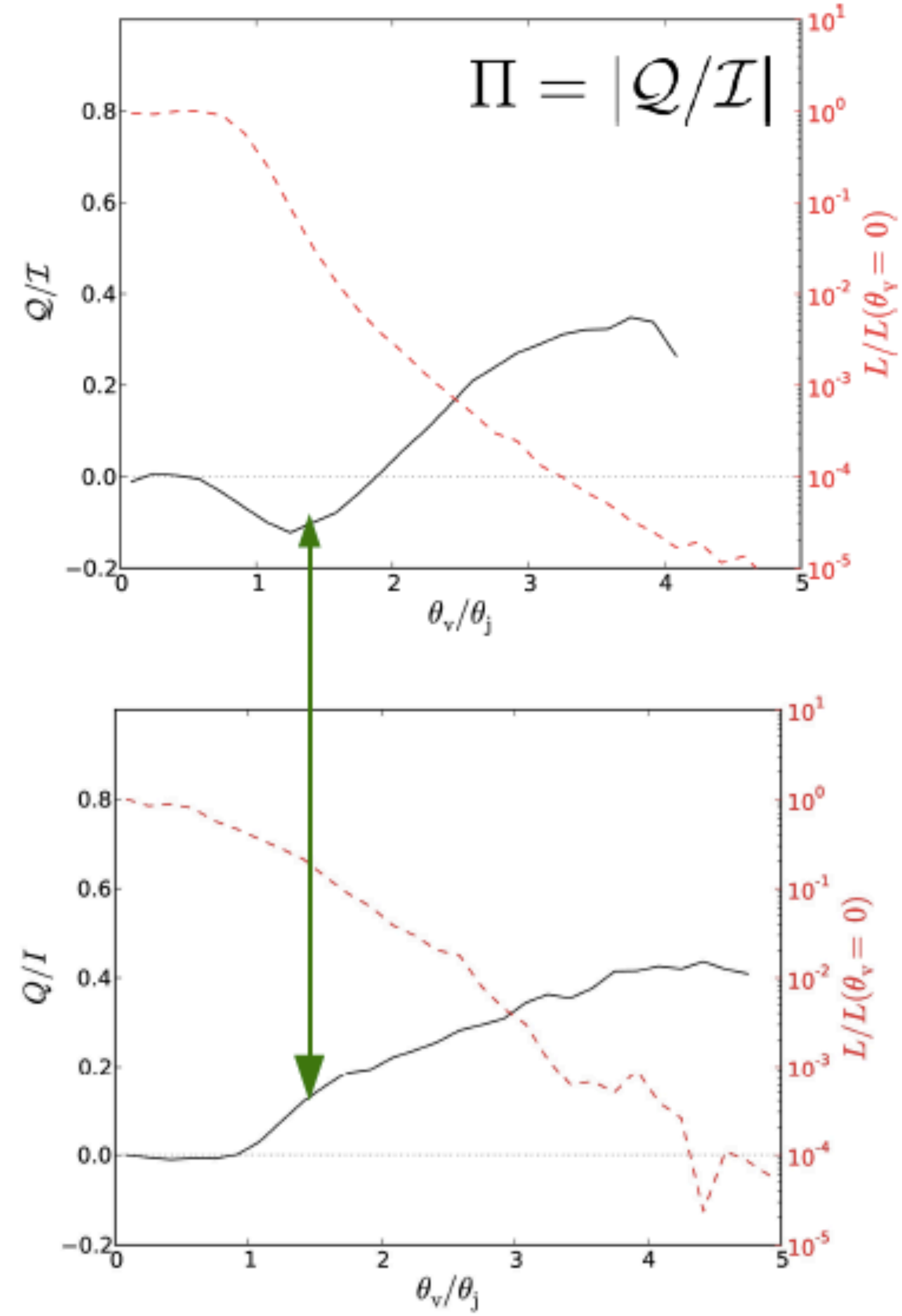

Sphinx small satellite proposal
Sweden Japan

Effective area ~95 cm2, ~ 100 GRBs per year
Field-of-view (~120°)
Energy range ~50 keV – ~300 keV
detect GRB polarisation ~25 GRBs per year

Localisation accuracy of 1 - 4°.

Plastic scintillator of hexagonal (Eljen Technologies EJ-204)
BGO scintillator slabs

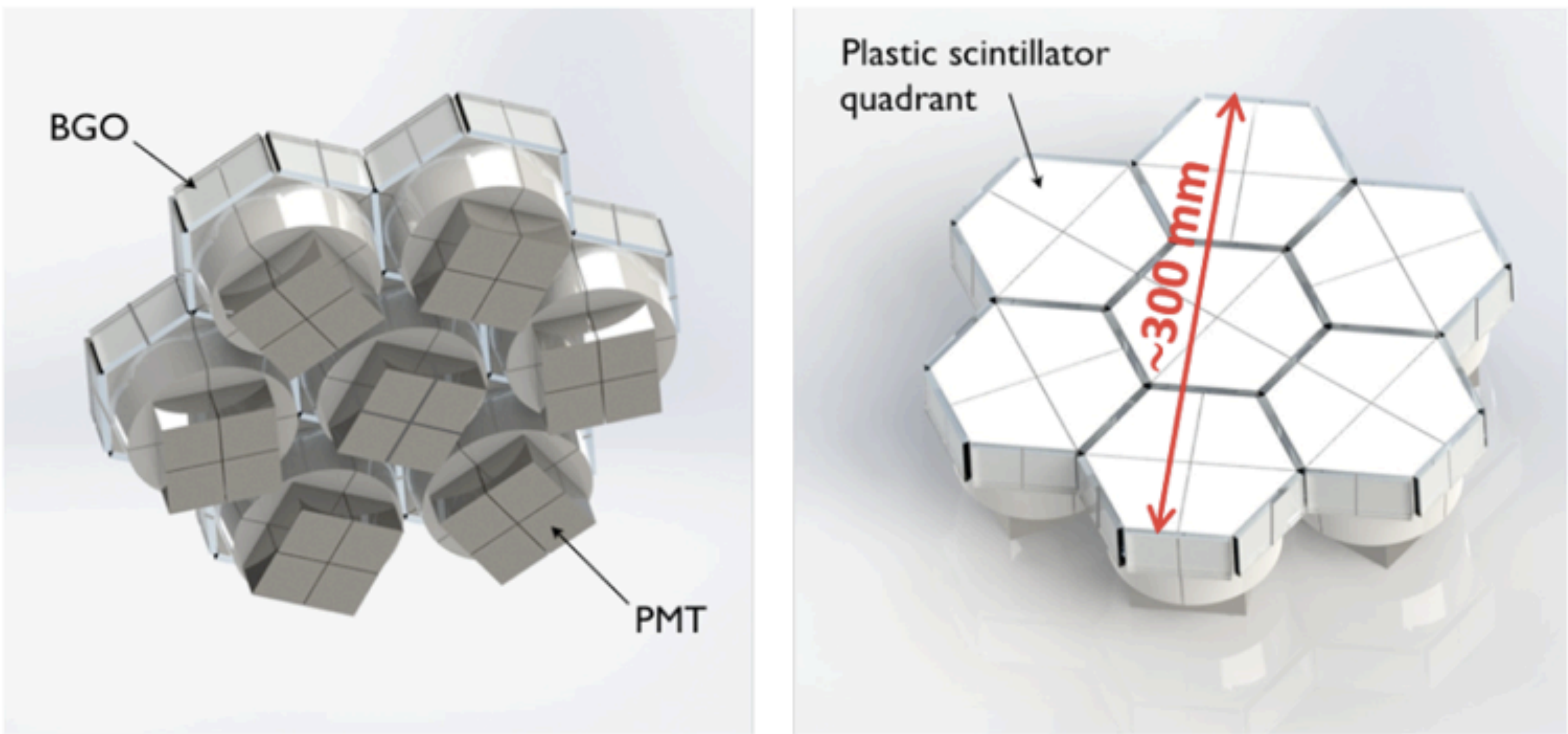

Figure 1: Overview of the SPHiNX detector. Avalanche photodiodes for reading out the BGO scintillators are not shown.

Sphinx small satellite proposal
Sweden Japan

Effective area ~95 cm2, ~ 100 GRBs per year
Field-of-view (~120°)
Energy range ~50 keV – ~300 keV
detect GRB polarisation ~25 GRBs per year

Localisation accuracy of 1 - 4°.

Plastic scintillator of hexagonal (Eljen Technologies EJ-204)
BGO scintillator slabs

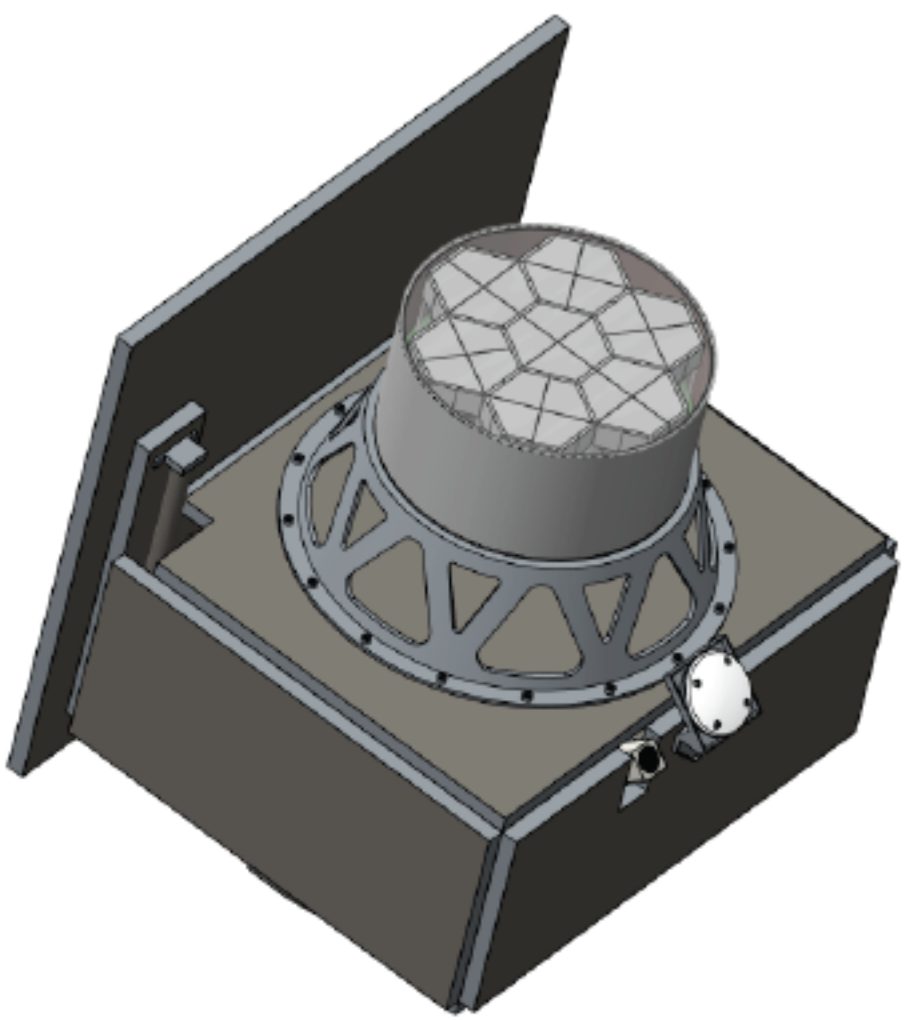

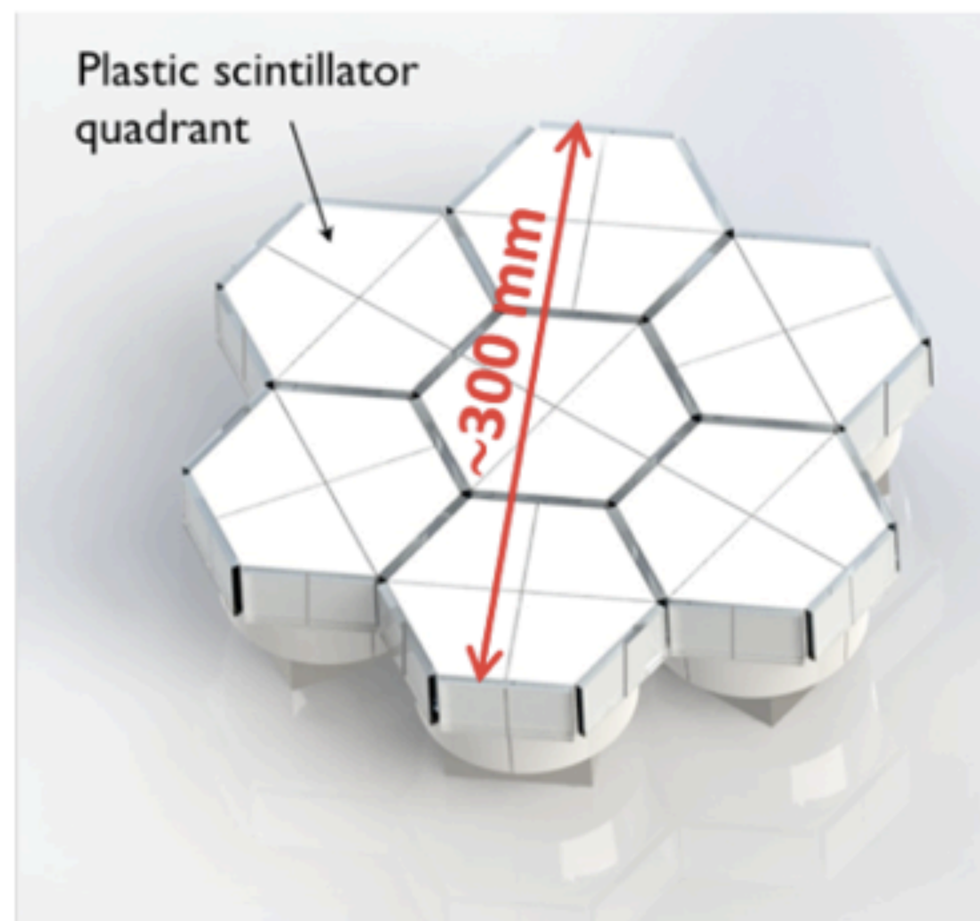

otodiodes for reading out the BGO scintillators are not shown.

Specifications

	SO	SR	PD	PG	CD
Maximum PD	~ 50 %	~ 40 %	~ 40 %	~ 40 %	~ 90 %
Peak of PD distribution	~ 40 %	~ 0%	~ 0%	~ 0%	~ 0%
Allowed α	≤ -2/3	≤ -2/3	≤ 1	≤ 1	≤ 0
PD - α correlation	Negative	Negative	No	Negative	No

Table 2: Predictions for five different emission models: Synchrotron emission in an ordered magnetic field (SO), synchrotron emission in a magnetic field with random directions on small scales (SR), Photospheric emission with spectral broadening due energy dissipation below the photosphere (PD), photospheric emission with broadening due to the geometric jet structure (PG) and Compton drag (CD).

Item	Unit mass (g)	Number	Total (g)
R7600U PMT	35	28	980
S8664-55 APD	3	60	180
Plastic scintillator	440	7	3080
BGO	47	60	2820
Pb/Sn/Cu shield	2068	1	2068
Other mechanics	2000	1	2000
CFRP scintillator array	43.5	7	304.5
CFRP shield	913	1	913
PCBs (3)	1022	1	1022
Electronics	3000	1	3000
Total			**14128**
Currently unreserved			872

Component	Power consumption (W)
VATA analogue front-end	2
Miscellaneous analogue	1
FPGA	5
Miscellaneous digital	2
PMT/APD high voltage	2.5
Subtotal	**12.5**
DC/DC inefficiency (15%)	1.9
Subtotal	14.4
Contingency (25%)	3.6
Total	**18.0**

Table 5: The SPHiNX power budget. Heaters are only expected to be used during the safe mode and are therefore not included here.

Specifications

	SO	SR	PD	PG	CD
Maximum PD	~ 50 %	~ 40 %	~ 40 %	~ 40 %	~ 90 %
Peak of PD distribution	~ 40 %	~ 0%	~ 0%	~ 0%	~ 0%
Allowed α	≤ -2/3	≤ -2/3	≤ 1	≤ 1	≤ 0
PD - α correlation	Negative	Negative	No	Negative	No

Table 2: Predictions for five different emission models: Synchrotron emission in an ordered magnetic field (SO), synchrotron emission in a magnetic field with random directions on small scales (SR), Photospheric emission with spectral broadening due energy dissipation below the photosphere (PD), photospheric emission with broadening due to the geometric jet structure (PG) and Compton drag (CD).

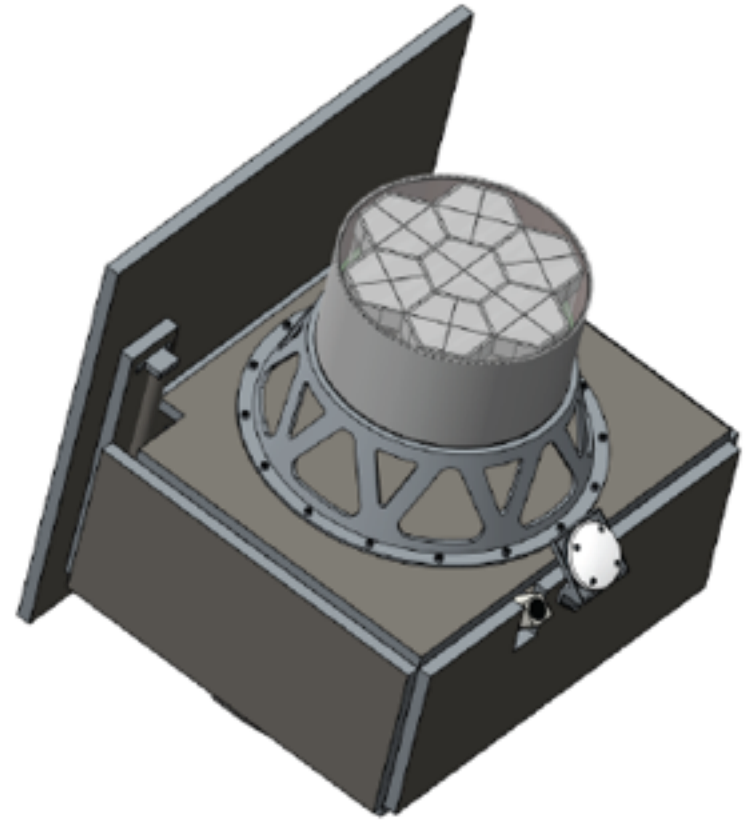

Item	Unit mass (g)	Number	Total (g)
R7600U PMT	35	28	980
S8664-55 APD	3	60	180
Plastic scintillator	440	7	3080
BGO	47	60	2820
Pb/Sn/Cu shield	2068	1	2068
Other mechanics	2000	1	2000
CFRP scintillator array	43.5	7	304.5
CFRP shield	913	1	913
PCBs (3)	1022	1	1022
Electronics	3000	1	3000
Total			**14128**
Currently unreserved			872

Component	Power consumption (W)
VATA analogue front-end	2
Miscellaneous analogue	1
FPGA	5
Miscellaneous digital	2
PMT/APD high voltage	2.5
Subtotal	**12.5**
DC/DC inefficiency (15%)	1.9
Subtotal	14.4
Contingency (25%)	3.6
Total	**18.0**

Table 5: The SPHiNX power budget. Heaters are only expected to be used during the safe mode and are therefore not included here.

Conclusions

The jet photosphere is important for the understanding of GRB emission

It dominates many bursts, maybe all!

Interpretations -multi zone emission -pure photospheric emission

Polarisations measurements are important!